CANADIAN THESES ON MICROFICHE

I.S.B.N.

THESES CANADIENNES SUR MICROFICHE

National Library of Canada
Collections Development Branch

Canadian Theses on
Microfiche Service

Ottawa, Canada
K1A 0N4

Bibliothèque nationale du Canada
Direction du développement des collections

Service des thèses canadiennes
sur microfiche

NOTICE

The quality of this microfiche is heavily dependent upon the quality of the original thesis submitted for microfilming. Every effort has been made to ensure the highest quality of reproduction possible.

If pages are missing, contact the university which granted the degree.

Some pages may have indistinct print especially if the original pages were typed with a poor typewriter ribbon or if the university sent us a poor photocopy.

Previously copyrighted materials (journal articles, published tests, etc.) are not filmed.

Reproduction in full or in part of this film is governed by the Canadian Copyright Act, R.S.C. 1970, c. C-30. Please read the authorization forms which accompany this thesis.

THIS DISSERTATION
HAS BEEN MICROFILMED
EXACTLY AS RECEIVED

AVIS

La qualité de cette microfiche dépend grandement de la qualité de la thèse soumise au microfilmage. Nous avons tout fait pour assurer une qualité supérieure de reproduction.

S'il manque des pages, veuillez communiquer avec l'université qui a conféré le grade.

La qualité d'impression de certaines pages peut laisser à désirer, surtout si les pages originales ont été dactylographiées à l'aide d'un ruban usé ou si l'université nous a fait parvenir une photocopie de mauvaise qualité.

Les documents qui font déjà l'objet d'un droit d'auteur (articles de revue, examens publiés, etc.) ne sont pas microfilmés.

La reproduction, même partielle, de ce microfilm est soumise à la Loi canadienne sur le droit d'auteur, SRC 1970, c. C-30. Veuillez prendre connaissance des formules d'autorisation qui accompagnent cette thèse.

LA THÈSE A ÉTÉ
MICROFILMÉE TELLE QUE
NOUS L'AVONS REÇUE

NL-339 (r. 82/08)

Canada

0-315-05922-2

National Library
of Canada

Canadian Theses Division

Ottawa, Canada
K1A 0N4

Bibliothèque nationale
du Canada

Division des thèses canadiennes

53842

PERMISSION TO MICROFILM — AUTORISATION DE MICROFILMER

- Please print or type — Écrire en lettres moulées ou dactylographier

Full Name of Author — Nom complet de l'auteur
ANDRES, DAVID DONALD

Date of Birth — Date de naissance
JAN. 18, 1952

Country of Birth — Lieu de naissance
CANADA.

Permanent Address — Résidence fixe
9011 - 91 ST.
EDMONTON, AB.
T6C 3N6

Title of Thesis — Titre de la thèse
THE EFFECTS OF TURBULENCE ON FRAZIL PRODUCTION

University — Université
UNIVERSITY OF ALBERTA.

Degree for which thesis was presented — Grade pour lequel cette thèse fut présentée
M. Sc. C.E.

Year this degree conferred — Année d'obtention de ce grade
1981

Name of Supervisor — Nom du directeur de thèse
R. GERARD

Permission is hereby granted to the NATIONAL LIBRARY OF CANADA to microfilm this thesis and to lend or sell copies of the film.

The author reserves other publication rights, and neither the thesis nor extensive extracts from it may be printed or otherwise reproduced without the author's written permission.

L'autorisation est, par la présente, accordée à la BIBLIOTHÈQUE NATIONALE DU CANADA de microfilmer cette thèse et de prêter ou de vendre des exemplaires du film.

L'auteur se réserve les autres droits de publication; ni la thèse ni de longs extraits de celle-ci ne doivent être imprimés ou autrement reproduits sans l'autorisation écrite de l'auteur.

Date
Oct. 16/81

Signature

NL-91 (4/77)

THE UNIVERSITY OF ALBERTA

THE EFFECTS OF TURBULENCE ON FRAZIL PRODUCTION

by

© DAVID D. ANDRES

A THESIS

SUBMITTED TO THE FACULTY OF GRADUATE STUDIES AND RESEARCH

IN PARTIAL FULFILMENT OF THE REQUIREMENTS FOR THE DEGREE

OF MASTER OF SCIENCE

DEPARTMENT OF CIVIL ENGINEERING

EDMONTON, ALBERTA

FALL, 1981

THE UNIVERSITY OF ALBERTA

RELEASE FORM

NAME OF AUTHOR DAVID D. ANDRES

TITLE OF THESIS THE EFFECTS OF TURBULENCE ON FRAZIL PRODUCTION

DEGREE FOR WHICH THESIS WAS PRESENTED MASTER OF SCIENCE

YEAR THIS DEGREE GRANTED FALL, 1981

Permission is hereby granted to THE UNIVERSITY OF ALBERTA LIBRARY to reproduce single copies of this thesis and to lend or sell such copies for private, scholarly or scientific research purposes only.

The author reserves other publication rights, and neither the thesis nor extensive extracts from it may be printed or otherwise reproduced without the author's written permission.

(SIGNED) ....

PERMANENT ADDRESS:

...9011...91 ST.......
EDMONTON...AB.....
.......T6C...3N6...

DATED ....October 15.....1981

THE UNIVERSITY OF ALBERTA

FACULTY OF GRADUATE STUDIES AND RESEARCH

The undersigned certify that they have read, and recommend to the Faculty of Graduate Studies and Research, for acceptance, a thesis entitled THE EFFECTS OF TURBULENCE ON FRAZIL PRODUCTION submitted by DAVID D. ANDRES in partial fulfilment of the requirements for the degree of MASTER OF SCIENCE.

R Gerard

Supervisor

....

....

Date October 15/81

Abstract

Frazil is produced in highly turbulent streams where a stable surface cover cannot form and the bulk of the flow is cooled to the nucleation temperature. The frazil particles are disc shaped ice crystals which have diameters between 1 and 5 mm and can exist in concentrations up to 10 particles per cm^3. These particles exhibit little buoyancy and can be transported great distances downstream from their origin. Their cohesiveness results in accumulations in low velocity areas, and in their active state, their adhesion allows an accumulation on objects projecting into the flow. This presents many difficulties in designing and managing water resources projects in cold regions.

The characteristics of nucleation and crystal growth in rivers have not been thoroughly investigated with respect to the effects of air temperature and stream turbulence. Therefore a laboratory model, simulating a highly turbulent natural stream, was instrumented to observe nucleation, surface cover development, frazil generation, and the growth of ice particles under varying air temperatures and turbulence intensity. A literature review of the thermodynamics of nucleation and crystal growth was also summarized.

Although nucleation theories have not progressed far enough to quantify the nucleation process, sufficient advancement has been made in crystal growth theories that generalized growth rates and frazil particle shapes can be

computed from water temperature and turbulence. The major difficulty is, however, adequately characterizing the turbulence.

The laboratory investigations showed that the development of a surface ice cover and frazil production are the same process. High intensity turbulence prevents the formation of a surface cover by entraining the small nucleating particles from the surface, instead causing nucleation to occur throughout the flow. A reduction in the required supercooling for nucleation was observed with a decrease in air temperature and an increase in turbulence. It was also deduced that nucleation is initiated by the nucleating particles produced or carried in the air and transported across the air-water interface.

The total amount of frazil generated can be computed from the supercooling curves. It was found that the number of frazil particles produced can be estimated by proportioning the total amount of ice produced into that produced by particle growth and by nucleation, if the growth rates of the ice particles are known. The deduced number of particles was between 0.2 and 300 particles per cm^3. This is within an order of magnitude of estimates by other investigators, but greater than estimated visually. For any given sub-zero air temperature it appears that the number of particles produced was maximized at a consistent optimum turbulence intensity - most probably determined by the supply of nucleating agents and the effects of turbulence on the ice production attributed to only crystal growth.

At this time the understanding of nucleation of frazil is still phenomenological and it is recommended that further work be done in developing experimental techniques to actually observe and quantify processes such as nuclei deposition on the water surface, nuclei entrainment, crystal growth in a turbulent flow field, and secondary nucleation.

Acknowledgements

Numerous individuals have contributed towards this investigation. Dr. N. Rajaratnam provided funding for the initial experimentation. Messrs. Lovell, Gitzel, McGowan, and Marshall assisted in the construction of the experimental apparatus and the data acquisition system. Dr. R. Gilpin, of the Department of Mechanical Engineering made available the cold rooms in which the experiments were conducted. Mr. P. Steffler gave his time to measure the turbulence with the laser anemometer.

The writer acknowledges the financial assistance provided by Alberta Environment and also thanks Dr. R. Harrington of the Alberta Research Council for his assistance.

A very special acknowledgement must go to Dr. R. Gerard for his stimulating discussions, advice, and hours spent in reviewing this report.

Nola Shaw also deserves recognition for her time spent in preparing the manuscript.

Finally, a special thank you is given to Wendy, for her patience, support, and understanding.

Table of Contents

Chapter Page

Abstract iv

Acknowledgements vii

List of Tables x

List of Figures xi

List of Symbols xiv

1. INTRODUCTION 1

  1.1 River Ice 4

  1.2 Frazil Problems in Rivers 8

  1.3 Mechanism of Frazil Ice Production 13

  1.4 Study Objectives 17

2. LITERATURE REVIEW 20

  2.1 The Characteristics of Water 20

    2.1.1 The Water Molecule 20

    2.1.2 The Structure of Water 23

  2.2 The Characteristics of Ice 25

    2.2.1 Structural Characteristics 25

    2.2.2 Thermodynamic Properties 28

  2.3 Nucleation 31

    2.3.1 Homogeneous Nucleation 32

    2.3.2 Heterogeneous Nucleation 35

    2.3.3 Observations of Nucleation and Other Theories 42

  2.4 Crystal Growth 51

  2.5 Morphology of Ice Crystals 58

  2.6 Summary 62

3. EXPERIMENTAL PROCEDURE AND DATA SUMMARY 65

3.1 Experimental Apparatus 66

3.1.1 The Insulated Tank 66

3.1.2 Temperature Data Aquisition System 73

3.1.3 The Generation and Measurement of Turbulence 76

3.2 Experimental Results 81

3.2.1 Turbulence Measurements 81

3.2.2 Frazil Observations and Temperature Measurements 84

4. ANALYSIS AND DISCUSSION OF EXPERIMENTAL RESULTS 92

4.1 Nucleation Temperatures 93

4.2 Volumes and Rates of Frazil Production 102

4.3 Nucleation and Growth of Frazil Particles 111

4.3.1 Growth of Frazil Particles 113

4.3.2 Nucleation Prior to Maximum Supercooling ...119

4.3.3 Nucleation Following Maximum Supercooling ..124

4.4 Comparison with Muller's Data 128

4.5 Residual Supercooling 135

5. CONCLUSIONS AND RECOMMENDATIONS 141

5.1 Conclusions 141

5.1.1 Surface Cover Development and Nucleation Temperatures 141

5.1.2 Ice Production During Supercooling 143

5.1.3 The Shape and Growth of Frazil Particles ...144

5.1.4 Nucleation of Frazil Particles 145

5.1.5 Residual Temperature 146

5.2 Recommendations 148

6. LIST OF REFERENCES 151

7. APPENDIX A 158

List of Tables

Table Page

2.1 Thermodynamic Properties of Ice and Liquid Water at Temperatures Near 0°C 30

2.2 Summary of Muller's (1978) Data 48

2.3 Summary of Available Data from Supercooling Experiments 48

2.4 Experimentally Determined Constants in the Crystal Growth Equation under Quiescent Conditions 52

2.5 Experimentally Determined Constants for Crystal Growth Parallel to the c-axis 52

2.6 Experimentally Determined Constant in the Crystal Growth Equation Under Forced Convection Conditions 54

2.7 Summary of Observed Sizes of Frazil Particles 61

3.1 Heat Transfer Characteristics of Tank Insulating Agents 66

3.2 Heat Loss Rates from Tank 66

3.3 Summary of Turbulence Characteristics 81

3.4 Summary of Frazil Observations 86

3.5 Summary of the Characteristics of the Supercooling Experiment 89

4.1 Computed Volumes and Rates of Frazil Generation 103

4.2 Computed Values of B From Estimates of Frazil Particle Sizes 116

4.3 Frazil Particle Sizes 116

4.4 Summary of Nucleation Rates 120

4.5 Summary of Muller''s (1975) Nucleation Data 129

4.6 Comparison of Measured and Calculated Residual Temperatures 138

List of Figures

Figure Page

1.1 Classification of River Ice (after Michel, 1971) 5

1.2 Development of a Dynamic Ice Cover (after Carstens, 1970) 7

1.3 Typical Supercooling Curve (after Carstens, 1966) 16

2.1 Structure of a Five Molecule Water-Cluster (after Walrafen, 1972) 22

2.2 Structure of Ice Ih (after Fletcher, 1970) 27

2.3 Nucleation Temperatures of Small Water Droplets (after Fletcher, 1970) 34

2.4 Nucleation Temperature Due to Spherical Particles Suspended in Supercooled Water (after Fletcher, 1963) 41

2.5 Linear Growth Rates of Ice Crystals in Supercooled Water 57

3.1 Insulated Tank in Cold Room 69

3.2 Top View of Insulated Tank 70

3.3 Side View of Tank Showing Location of Probes 71

3.4 Data Aquisition System 72

3.5 Typical Calibration Curve of the Temperature Probes 74

3.6 Data Aquisition Process 75

3.7 Typical Mixing Test Results 79

3.8 Typical Trace of Measured Velocity Fluctuations 80

3.9 Turbulence Characteristics 83

3.10 Typical Supercooling Curves 88

4.1 Nucleation Characteristics for the Observed Nucleation Temperatures 94

Figure Page

4.2 Effects of Turbulence and Air Temperature on the Formation of a Surface Ice Cover 98

4.3 Effects of Turbulence and Air Temperature on the Nucleation Temperature 99

4.4 Ratio of Mean Rate of Frazil Generation During the Supercooling Period to that Following Residual Supercooling as a Function of the Supercooling of Nucleation 106

4.5 Ratio of Frazil Generation Rates During Various Supercooling Periods as a Function of Turbulence Intensity 109

4.6 Effects of Turbulence on the Heat Transfer Coefficient 115

4.7 Effects of Turbulence on the Computed Frazil Particle Size 118

4.8 Effects of Turbulence on the Production of Frazil Particles 122

4.9 Effects of Turbulence on the Rate of Production of Frazil Particles 123

4.10 Variation of B_r/B_s with Turbulence Intensity 127

4.11 Results of a Typical Experiment by Muller (1978) 130

4.12 Effects of the Nucleation Temperature on the Number of Frazil Particles Produced 134

4.13 The Effects of the Nucleation Temperature on the Nucleation Rate of Frazil Particles 136

4.14 Comparison of Measured and Calculated Residual Supercooling 140

List of Symbols

a - coefficient relating the potential growth of frazil nuclei prior to and following maximum supercooling.

$a_i i^{2/3}$ - number of water molecules in contact with an ice particle

A - constant in the equation for crystal growth under forced convection.

A^* - constant in Carstens' crystal growth equation

B, B_s, B_r - coefficients relating the crystal growth rates to the supercooling temperature at any time, prior to maximum supercooling, and following maximum supercooling, respectively.

b, c - coefficients in the equation for kinetically controlled crystal growth rates.

C - constant relating the crystal Reynolds number to the crystal Nusselt number in Carstens' crystal growth rate equation.

C_p - heat capacity of water.

Δg^* - least maximum free energy difference for the nucleation process (activated complex).

ΔG - free energy difference.

ΔG_v - free energy difference between ice and water per unit volume of ice

ΔG^* - critical difference in the free energy of formation of an ice particle during nucleation.

h - Planck's constant.

H - hydrogen atom.

H_o - rate of heat loss from a water body.

i - number of molecules in an ice-like structure.

$J+$ - rate at which water molecules are attached to an ice crystal.

$J-$ - rate at which ice molecules are dettached from an ice crystal.

J_e - net rate of molecular attachment to an ice crystal.

k - thermal conductivity of water

- Boltzmann Constant

K - constant in Carstens' equation for crystal growth rates.

L - latent heat of fusion of water.

- water molecule.

m - variable indicating the compatability between the structure of ice and the structure of the nucleating particle.

- exponent in relationship between crystal Nusselt number and Reynolds number.

M_i - mass of ice.

M_w - mass of water.

n - exponent in the equation of crystal growth in still water.

n_i - steady state concentration of ice nuclei containing i molecules.

n_s - number of water molecules near the unit surface area of a nucleating agent.

N, N_s, N_r - number of frazil particles created during supercooling at any time, at maximum supercooling, and at residual supercooling, respectively.

N_u - Nusselt Number of an ice particle.

$\dot{N}$ - nucleation rate

$\dot{N}_{ns}$ - average nucleation prior to maximum supercooling

$\dot{N}_{sr}$ - average nucleation rate following maximum supercooling

O - Oxygen atom.

p - coefficient in equation of crystal growth in still water.

r, r_s, r_r - radius of ice particle at any time, at maximum supercooling, and at residual supercooling, respectively.

r_o, $r*$ - critical radius of nucleated ice particle.

R_e - radius of nucleating agent.

R - Reynold's number of ice crystal.

S - entropy.

S_{sl} - surface area of the interface between ice and water.

S_{sn} - surface area of the interface between ice and the nucleating particle.

ΔS_v - change in entropy during freezing of water.

t - time.

t_o, t_n, t_s, t_r - time at which supercooling curve achieves the melting temperature, nucleation temperature, maximum supercooling temperature, and residual temperature, respectively.

t_m - mixing time.

T - water temperature.

T_a - air temperature.

T_n, T_s, T_r - absolute value of the nucleation temperature, maximum supercooling temperature, and residual temperature, respectively.

ΔT - degree of supercooling.

u' - root-mean-square velocity fluctuations.

u'_s - root-mean-square surface velocity fluctuations.

v - flow velocity near a stationary ice crystal.

v_a - growth velocity along the a-axis.

v_c - growth velocity along the c-axis.

V - volume of ice.

V, V_s, V_r - volume of frazil generated at any time, at time of maximum supercooling, and at time of residual supercooling, respectively.

$\dot{V}_{ns}$ - frazil generation rate prior to maximum supercooling.

$\dot{V}_{nr}$ - frazil generation rate averaged over the total supercooling period.

$\dot{V}_{sr}$ - frazil generation rate following maximum supercooling.

x - ratio of radius of nucleating particle to the radius of the nucleated ice particle.

ρ_i - density of ice.

ρ_w - density of water.

σ_{ln} - free energy of the interface between water and the nucleating particle.

σ_{sl}, σ_{12} - free energy of the interface between ice and water.

σ_{sn} - free energy of the interface between ice and the nucleating particle.

1. INTRODUCTION

Ice can be found in regions on earth where the latitude or elevation is high enough to allow prolonged periods of subzero temperatures. The ice produced can take many forms and has a major impact on the state and the utilization of the natural environment. For example, ice plays a major role in determining local climatic patterns, transportation systems, resource utilization schemes, and recreation.

Mellor (1964) identifies eight types of ice. Snow occurs through the freezing in air of highly supercooled water droplets which remain in the liquid state at temperatures as low as -40°C. Glacial ice results from thermal and pressure metamorphosis of snow accumulation. Frost, rime and glaze all occur by the condensation and freezing of water vapour in highly supersaturated air or by rapid freezing of small supercooled water droplets on surfaces with subzero temperatures. Sea ice results from the freezing at the surface of ocean waters and develops into pack ice when these sheets of sea ice are broken by wind and tidal currents. Contribution to pack ice is also made by the advancement of glaciers into the ocean and their subsequent deterioration into large broken ice masses. Ground ice can be found in subsurface areas where ground water can be frozen. Permafrost is one example of ground ice; aufeis, which forms if groundwater freezes when it discharges onto the earth's surface, is another. Lake ice forms on the surface of a quiet water body by the supercooling and freezing of a thin surface layer. Additional growth then occurs in a downward direction parallel to the surface layer. River ice, on the other hand can exist in various forms. Quiescent flows result in ice formed in the same manner as that of quiet lakes. Turbulent flows result in the formation of frazil.

Mellor (1964) indicates that about 2% of all known surface water is in the form of ice. Of this portion, a majority is in a permanent glacial form of which 99% is located in Anarctica and Greenland, and 1% is contained in mountain glaciers. All other forms of ice, aside from permafrost, occur in transient forms and in relatively small quantities.

Apart from the obvious effects of glaciers on climate, water supply, and recreation; the effects of sea ice on ocean transportation; the effects of rime, glaze, and frost on aircraft, ships, power transmission and road safety; river and lake ice are the most significant types of ice in Canada. Lake and river ice play a major role in the design of transportation systems, hydro power generation, the design of flood control schemes, dispersion and assimilation of pollutants, and the design of water distribution systems. These effects are becoming more important with the development occurring in the Canadian north.

Lake ice is relatively easy to analyse, compared to river ice, because its growth is primarily a function of temperature. It tends to react slowly to changes in temperature and its structural stability makes it easier to observe and measure. River ice can be the opposite. Although in some instances its characteristics resemble lake ice, the addition of a second variable, turbulence, which results in frazil production, makes its study and understanding considerably more difficult. This has resulted in a reluctance or an inability to deal with the additional problems associated with river ice. Considering that most Canadian rivers are ice covered for a period ranging between five and ten months of the year, this lack of attention often proves disastrous, or at least uneconomical.

The production of frazil ice in turbulent streams is one of the least understood aspects of river ice. Difficulty has been encountered in isolating the mechanisms of nucleation, the subsequent growth of the frazil particles, and their behavior while transported by the turbulent flow. In this light, this study will attempt to discern the effects of turbulence and air temperature on the nucleation process; the development of a surface ice cover; and, by considering the growth of ice particles, deduce the number of frazil particles produced during the period of measured supercooling.

1.1 River Ice

River ice forms when any portion of the water in a river is cooled below its freezing point for a period long enough to allow for sustained ice crystal growth. Michel (1971) proposed the classification illustrated in Figure 1.1, which categorizes the types of river ice which can be produced. The major distinction is between static ice and dynamic ice.

Static ice formation occurs where the local turbulence is sufficiently low to allow the surface of the water to be undisturbed enough for supercooling to occur in a very thin layer. Ice will form in this layer and, if the turbulence intensity is low enough, the ice will not be transported below the surface and a thin ice cover will be produced (Devik, 1948). Following the formation of this initial ice cover, a temperature gradient is established in the ice and growth proceeds in the direction of maximum heat transfer. This type of ice can be seen on the surfaces of calm lakes and low velocity streams, and as border ice on higher velocity streams.

In highly turbulent streams that are not too deep the mixing induced by turbulence does not allow a temperature gradient to be established in the flow and the whole mass of water cools at the same rate. This rate is proportional to the rate of heat loss from the boundaries of the water body. When the mass of water is cooled to a temperature slightly below the normal freezing point of water, a large quantity

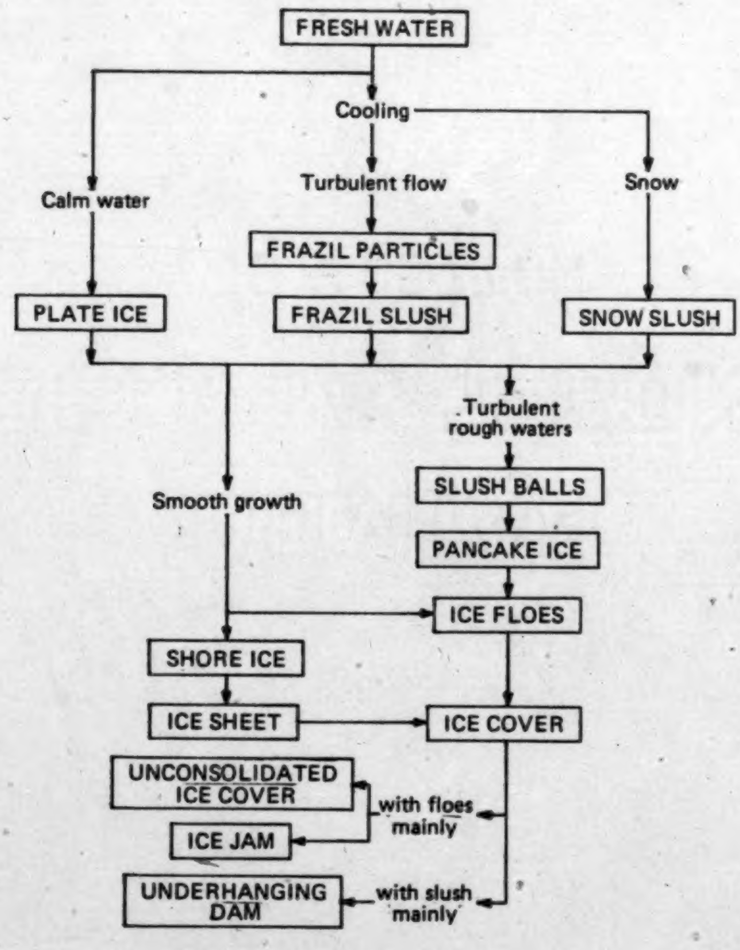
FRESH WATER
Cooling
Calm water
Turbulent flow
Snow
FRAZIL PARTICLES
PLATE ICE
FRAZIL SLUSH
SNOW SLUSH
Turbulent rough waters
SLUSH BALLS
Smooth growth
PANCAKE ICE
ICE FLOES
SHORE ICE
ICE SHEET
ICE COVER
UNCONSOLIDATED ICE COVER
with floes mainly
ICE JAM
UNDERHANGING DAM
with slush mainly

Figure 1.1 Classification of River Ice (after Michel, 1971)

of small ice crystals is produced thoughout the flow. This is known as frazil, a French Canadian term for fine spicular ice (Barnes, 1928). During its formation and while the water is supercooled, frazil is in its active state and tends to adhere to objects in the flow or to itself, thus floculating into more buoyant, loose accumulations. After these masses float to the water surface a crust forms on contact with the cold air. These masses then take on a pancake-like appearance, with a solid flat surface and a mass of porous frazil slush underneath. If conditions are appropriate, the downstream movement of this pancake ice can be arrested and a very rough and porous initial ice cover can form. Because of the dynamics involved in the creation of this type of ice cover, this manner of ice formation has been labelled as dynamic ice formation. The general processes involved are illustrated in Figure 1.2.

During frazil formation, when the frazil is active, anchor ice can also form. This anchor ice is produced by either the nucleation of supercooled water which is in contact with crystalline objects or by active frazil ice adhering to heat-conductive objects. Williams (1967) indicates, however, that anchor ice will only form on certain types of materials, depending on their composition. For example, metallic materials appear to have a high affinity for frazil adhesion, while frazil seldom sticks to plastic, glass, and silicone. Regardless of the mechanism and location of anchor ice formation, frazil and anchor ice

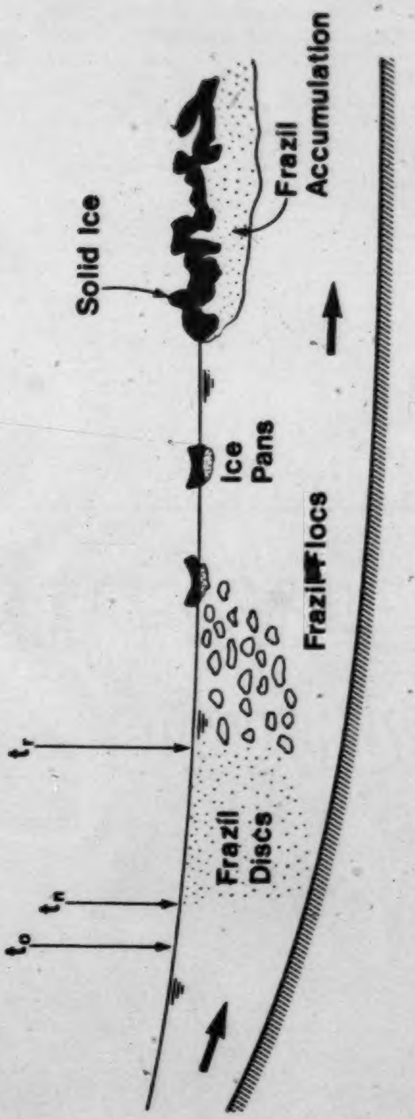
Solid Ice
Frazil Accumulation
Ice Pans
Frazil Flocs
Frazil Discs
t_r
t_n
t_o

Figure 1.2 Development of a Dynamic Ice Cover (after Carstens, 1970)

appear to form by similar processes (Arden and Wigle, 1972).

In the dynamic ice formation process, the most important phenomenon is the generation of frazil. It is this frazil, during and shortly after the period of time when it is in its active state, which presents most of the problems and difficulties effecting the efficient management of rivers in cold regions of the world.

1.2 Frazil Problems in Rivers

The existence of frazil is most noteworthy, not because of the complexity of its formation, but because of the difficulties which this ice phenomena presents in the development of rivers and their floodplains. Its characteristic adhesiveness, cohesivity, negligible buoyancy, and transportability while in suspension make frazil very difficult to deal with.

One of the most remarkable facets of frazil is the tremendous vo which can be created in a relatively short time. Because it does not stay on the surface and inhibit further heat transfer, as in the growth of surface ice, the ultimate volume of frazil produced can be an order of magnitude larger than for static ice growth. For example Stakle (1936) reported that the 150 m wide Daugava River in Latvia contained 476,000 m^3 of frazil ice for each kilometre of its length. This results in an average depth of ice of 3 m compared to a total flow depth of only 7 m. Schaefer

(1950) observed frazil particle concentrations approaching $10^6/m^3$ ($1/cm^3$) and Ardin and Wigle (1972) indicated that frazil formation on the Upper Niagara River below Lake Erie consumed up to 25% of the flow. The writer has observed frazil accumulations having a thickness of 5 m on the Peace River near Taylor, while on the same river at the Town of Peace River frazil floes or frazil slush accumulated to depths of 4 m. All this ice can be produced over a period of a few weeks in a climate where static ice can grow to a thickness of only 1 m during the entire winter.

The production, transportation, and deposition of frazil has a major influence on the conveyance capabilities of streams and can often lead to flooding. Numerous examples of this are evident. While the frazil is in suspension, Tsang (1970) reported a reduction in the velocity gradients and the average velocity, but not necessarily the maximum velocity. As a result an increase in stage can occur. Osterkamp, Gilfilian, and Benson (1975) observed similar behavior in very small streams.

The deposition of frazil slush can produce large hanging dams. Beltaos and Dean (1981) report a hanging dam 700 m long extending 16 m below the ice surface on the Smoky River in Alberta. During breakup such a large mass of ice can cause broken ice sheets to accumulate upstream of the hanging dam to such an extent that serious flooding can occur. Similar hanging dams have been reported by Sampson (1973) on the Peace River near Hudson Hope, and by Gold and

Williams (1963), who observed a 450 m to 600 m long hanging dam which extended to a depth of 90 m in a 150 m wide section of the Ottawa River. Kuuskoski (1972) observed frazil slush accumulations on the Kemi River in the north of Finland where 60% to 90% of the flow area was taken up by frazil deposition to depths of 5 m while the total depth was increased by 75% to 100%. The writer has observed similar conditions on the Bow River, North Saskatchewan River and Peace River in Alberta where the accumulation of frazil ice floes has resulted in bankfull stages during extremely low flow conditions. Calkins (1979) has reported such conditions on the Ottauquechee River in Vermont. Henshaw (1887) attributed most of the flooding problems on the St. Lawrence River to frazil production.

Frazil ice production also has a significant influence on hydro power production. The reduction of the conveyance of channels downstream of dams (Tsang, 1980) can be such that the tailwater increase is sufficiently large to markedly reduce the head and power generating capacity of hydro power installations. In most instances, the flow releases, and hence power production, must be reduced during the period of ice cover formation to minimize the increase in ice thickness and stage related to the formation of a stable cover. On both the Brazeau and Bighorn Dams on the North Saskatchewan River, and the Ghost Dam on the Bow River, where the head is not reduced by the presence of an accumulation of frazil, a reduction in power generation must still be made in order to prevent flooding downstream of the dams.

If frazil ice is being produced upstream of an intake, it has a tremendous affinity to adhere to the trash racks and inlet gates. Willey (1970) describes the large expenditure of effort in dealing with these problems on the Burfell hydro-electric project on the Thjorsa River in Iceland. The upstream channel was deepened, the rapids and waterfalls were drowned out, and even snow fences were constructed in attempts to reduce the quantity of snow blowing into the channel - all in an effort to limit the production of frazil and to prevent it from reaching the intakes. Acres Ltd. (1971) reported that the annual costs of maintaining ice-free trash racks on the Churchill Falls power development was about $60,000 in 1971.

Similar problems exist for other water intakes. The writer has observed a number of industrial water intakes which have become inoperative on the Bow and South Saskatchewan Rivers. In all instances the causes are similar. Either the intake is located in a reach of the river where large masses of frazil ice are deposited, and no flow can reach the intake, or the intake withdraws a large quantity of ice with the water so that the pumps become clogged. In most instances a relocation of the intake is necessary, or off-site storage must be developed to store sufficient water to last the duration of freeze-up. Tesaker (1975) reported the same type of conditions at the

Gamlebrofoss power plant in Norway, where frazil ice deposited in a delta-like formation upstream of the water intake and prevented flow from entering the intake. Williams (1972) observed such phenomena even during spring breakup on the Ottawa River, when a cold spell initiated frazil production.

The formation of frazil ice in the pipes of water distribution systems is described by Gilpin (1977). He indicates that if supercooling of the water in a pipe is allowed to progress below -3°C, and nucleation occurs, the quantity of frazil ice produced is such that almost complete blockage of the flow results. In fact, this very phenomena occurred in the Leningrad water supply in 1914. This ultimately led to the intensive investigation by Altberg (1936) of the characteristics of frazil ice production

Considering the above discussion there is little doubt frazil is a very significant factor to be dealt with in rivers. An understanding of how to deal with it efficiently can only come from a thorough understanding of how frazil is produced. Unfortunately, the formation of frazil is transient in nature and difficult to observe, measure and study.

1.3 Mechanism of Frazil Ice Production

The results of frazil production in natural streams are obvious. However, as mentioned, the mechanisms of this production are difficult to observe and measure. For example, considering that frazil was a known problem as early as 1887 (Henshaw, 1887) it was not until 1972 that Gilfilian, Kline, Osterkamp, and Benson reported actual measurements of a variety of changes that occurred during frazil formaton in a small stream in Alaska. Numerous theories have been advanced about the origin of frazil. Henshaw (1887) suggested that frazil is produced in "cold currents" which have their origin at the surface and preserve their characteristics as they are transported throughout the flow. He postulated that an independent nucleus is required to initiate frazil production and that these nuclei are apparently produced by the freezing of vapour above the water surface, which then falls into the water and initiates frazil production.

Other theories were also reported by Henshaw. One was that frazil is formed as small needles on the water surface and, if the surface is agitated, is transported throughout the flow. Another theory was that the disintegration of anchor ice leads to the appearance of frazil. Yet others were that frazil forms from small masses of water thrown into the air as foam or spray which subsequently freeze, or that frazil forms in rapids where air can be mixed into the flow. All these theories were based on qualitative field observations and it appears that little thought was given to the fundamental mechanisms. For instance, Barnes (1928) still firmly believed that frazil was only produced during periods when long wave radiation emitted from the surface of the water was a maximum, presumably because this is the only time he could observe frazil.

Fortunately investigators such as Altberg (1936), Michel (1963), Carstens (1966), and Muller (1978) produced and observed frazil under laboratory conditions. This laboratory research did much to clarify the mechanisms of frazil formation, even though these investigators only provided temperature measurements and qualitative estimates of the type of ice produced during frazil production. All the experiments indicated that if a body of water is well mixed, so that a temperature gradient cannot exist, and this water body is supercooled, ice nucleates at a temperature slightly below the melting point of the water. Following nucleation, which probably results from the transport of ice nuclei across the air-water interface, small discoidal shaped ice particles appear, grow in size, and cause additional particles to be formed by secondary nucleation. Prior to maximum supercooling, new frazil particles can be generated from those transported from the air into the water. Following maximum supercooling, when secondary nucleation is the major process by which new particles are formed, the rate of ice production by crystal growth and secondary nuclation is greater than can be sustained by heat loss across the boundaries of the water and the water temperature returns to near the melting point, when additional nucleation is minimal. Altberg and Carstens indicated that this residual temperature, or equilibrium temperature, is always slightly less than the melting temperature, but Michel suggested that it is exactly the melting temperature.

Regardless of the differences of opinion between these three principle investigators, there was general agreement on the frazil generation process. The temperature curve and the ice production curves for a typical frazil generation experiment are shown in Figure 1.3. Four distinct phases were identified:

1. the cooling of a water body;
2. the creation of small ice crystals or nuclei at time t_n and nucleation temperature T_n;
3. the growth of these nuclei and the production of additional nuclei as the water temperature achieves the maximum supercooling temperature T_s at time t_s and then returns to residual temperature T_r at time t_r; and
4. the period of steady residual supercooling during which the process of crystal growth appears to be the predominant factor.

The cooling rate is purely a function of the rate of heat transfer across the boundaries and the intensity of turbulence in the water body. Nucleation is a function of the temperature and the presence of suitable nucleating

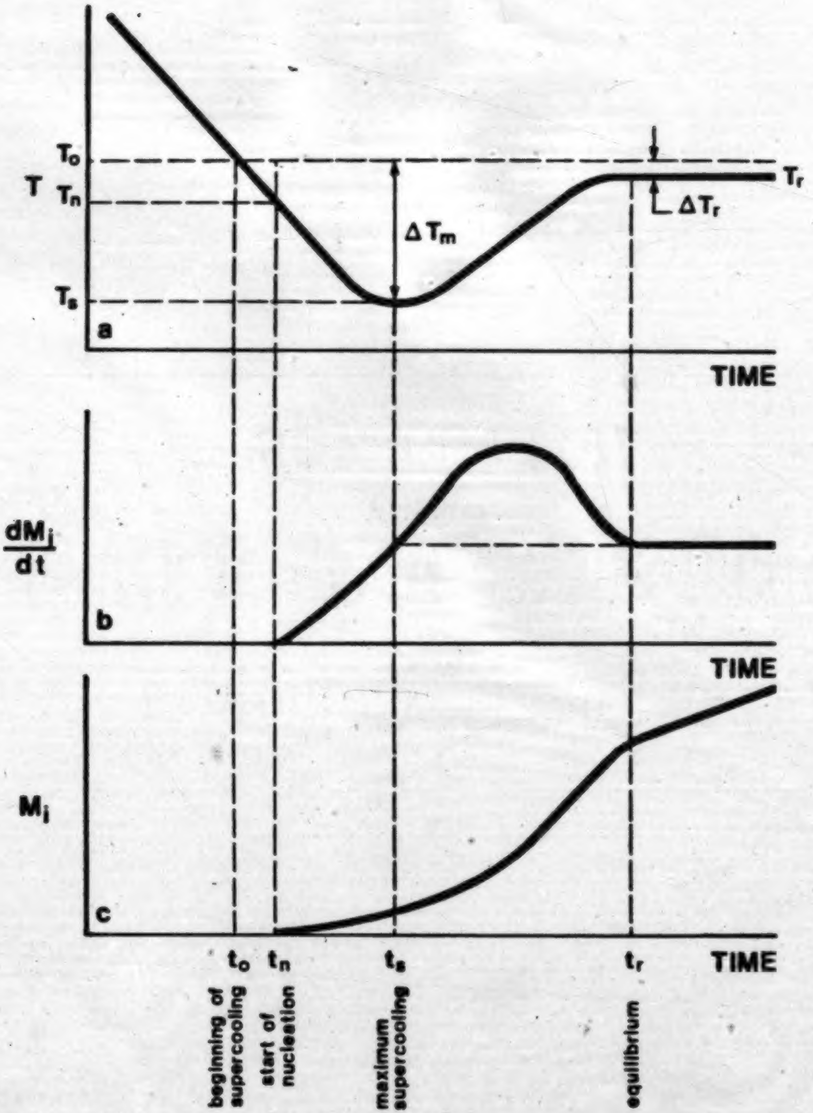

Figure 1.3 Typical Supercooling Curve (after Carstens, 1966)

solids. Following nucleation the rate of ice production is a function of nucleating characteristics, crystal growth, and the rate of heat loss. Carstens (1966) indicated that the rate of ice production is given by:

$$dM_i/dt = 1/L \, [C_p M_w (dT/dt) + H_o] \tag{1.1}$$

where M_i is the mass of ice, M_w the mass of water, L the latent heat of fusion, C_p the specific heat of water, t time, T water temperature, and H_o the rate of heat loss from the water.

Carstens (1966) also showed that the cooling rate had a marked effect on the supercooling curve. If the cooling rate was increased the maximum supercooling increased, the residual supercooling increased and the duration of supercooling was reduced. With respect to turbulence, a high turbulence intensity reduced the maximum supercooling and the duration of supercooling. Because the turbulence and the temperature affect the rate of crystal growth, Carstens reasoned that the measured supercooling curves could be explained on the basis of crystal growth rates.

1.4 Study Objectives

From the results of the controlled laboratory experiments by previous investigators a good idea of the process of frazil production in rivers was obtained. This information, along with field observations by Devik (1948), who measured surface supercoolings and surface ice growth on small quiescent streams, and by Schaefer (1950), who observed small frazil particles in turbulent streams, removed much of the mystery of how frazil ice is produced.

Unfortunately, many of the processes which were inferred from the experimental results discussed in the previous section are very complex. However, many of these processes are also important in other fields of science. Especially important are the processes of nucleation and crystal growth. Numerous theories regarding nucleation have been developed by Turnbull and Fisher (1948) and Fletcher (1958). Crystal growth has also been investigated by many individuals, from Van Hook (1961) to Kallungal (1975). Many of these results can be applied to the frazil production problem in order to quantify some of the inferred processes. However, none of this work has been brought into one singular discussion. Up to now, publication of a complete set of supercooling curves that cover the appropriate 5 variation in the fundamental variables - rate of heat loss or air temperature and turbulence intensity is lacking. Muller (1978), in his experiments, did not model a typical highly turbulent stream where nucleation occurs at limited supercoolings.

Similarly, although all experimentors observed the discoidal shape of the frazil particle and also deviations from that shape, the theory of crystal growth has not been used to explain these observations.

At present, there are numerous theories about the characteristic nucleation temperatures of natural streams, all of which indicate that turbulence plays an important role. Although Carstens' equation can be used to compute the total mass of ice produced, only Muller (1978) attempted to differentiate the amount of ice produced due to crystal growth and that produced by the formation of new nuclei.

As a contribution to answering some of the remaining questions about frazil production, the objectives of this investigation were to:

1. Review the properties of ice and water as they pertain to the ice formation phenomena;
2. Discuss some of the existing theories of nucleation and how observations of frazil nucleation relate to these theories;
3. Review the physics of crystal growth and how it relates to the observed shapes of frazil particles;
4. Experimentally investigate the effects of turbulence and the rate of heat loss on the nucleation temperature, the supercooling curves, and the nature of ice production in a reasonable model of a natural stream; and
5. Deduce frazil nucleation mechanisms and rates of nucleation and particle growth from the supercooling curves.

2. LITERATURE REVIEW

The phenomena of frazil production in rivers and streams is a complex change-of-phase problem. This change of phase is a process of nucleation applied to both the initial nuclei production and the growth of these nuclei.

The nucleation temperature, the size of the newly formed crystal, and the growth rate of this crystal (frazil particle) are all functions of the properties of both ice and water and of the environment in which the nucleation and crystal growth is occurring. These processes involve aspects of physics, thermodynamics, and fluid mechanics.

2.1 The Characteristics of Water

Water is composed of two elements - hydrogen and oxygen. The bonding of these two elements results in a water molecule which, with other molecules arranged in a liquid structure, behaves in a fashion that produces the unique bulk characteristics of water.

2.1.1 The Water Molecule

The water molecule is composed of one oxygen atom and two hydrogen atoms. Oxygen has two vacant electron positions in its valence shell. Because each hydrogen atom has only one electron, one hydrogen atom must bond to each of the vacant p-orbitals in this outer shell. The three p-orbitals are 90° apart so the initial H-O-H bond angle must be 90°.

However, the two O-H bonds are not electrically neutral (Fletcher, 1970) and thus the hydrogen atoms repell each other and create a bond angle greater than 90°. The final equilibrium configuration is tetrahedral with an oxygen nucleus at the centre, hydrogen nuclei at two vertices and an electron distribution such that the unbonded electrons tend to exist at the two remaining vertices. Hobbs (1974) shows that if one assigns the appropriate masses to the oxygen and hydrogen atoms and forms an expression for the principle moments on the basis of the length and angle of the O-H bond, then the O-H bond length and angle can be computed to be $9.57\text{x}10^{-11}$ m and 104.52° respectively. This structure is illustrated in Figure 2.1.

Both oxygen and hydrogen have a relatively high ionization energy, which makes it difficult to remove an electron from their atoms. Also, both have a low electron affinity which makes it difficult for either atom to accept another electron. Therefore, the O-H bond is covalent. That is, there is a mutual sharing of electrons. Although there is a substantial charge differential which creates a dipole effect between the negatively charged oxygen atom and the two positively charged hydrogen atoms, the polarity of the bond is insufficient to exhibit any ionic bonding characteristics. The dipole effect is important, however, because it provides sufficient polarity to influence the manner in which water molecules react with each other.

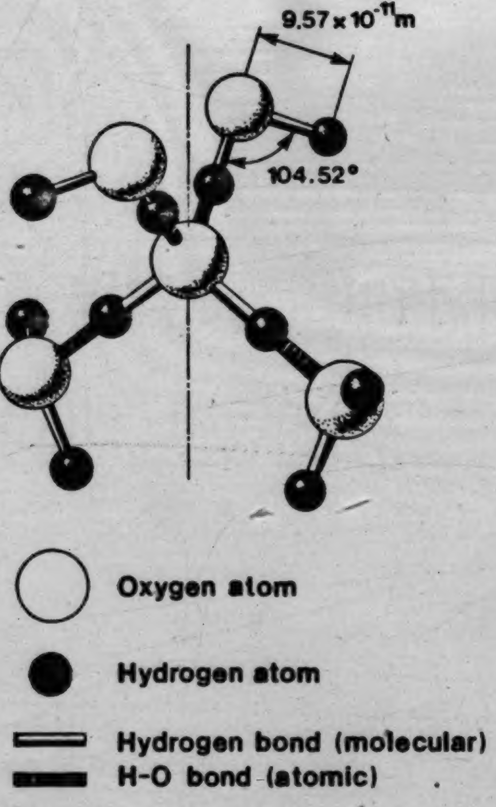
9.57×10^{-11}m
104.52°
Oxygen atom
Hydrogen atom
Hydrogen bond (molecular)
H-O bond (atomic)

Figure 2.1 Structure of a Five Molecule Water-Cluster (after Walrafen, 1972)

2.1.2 The Structure of Water

The individual water molecules form what is known as an associated liquid. This is because of the strong electrostatic attraction between the hydrogen atoms of one molecule and the oxygen atoms of another molecule. This intermolecular bond is known as a hydrogen bond and most of its strength arises out of attractive forces between the dipole effects within each of the molecules (Rao, 1972).

The exact molecular structure of water is open to speculation. On the basis of x-ray spectrography, Nanten and Levy (1972) indicate that the distance between two oxygen atoms ranged between $2.84x10^{-10}$ m at 4°C and $2.94x10^{-10}$ m at 200°C, while the O-H bond length was $1x10^{-10}$ m (similar to Hobbs, 1974). Their observations indicated that a large portion of the structure had a tetrahedral arrangement, which agreed with observations made by Walrafen (1972), who documented the Raman and infrared spectral properties. These observations suggest that tetrahedral 4-bonded units (similar to the form of ice at atmospheric pressure and near freezing temperature) are a common occurrence for water temperatures near 0°C. As the water temperature was increased the tetrahedral structure became less common and more broken bonds became apparant.

On the basis of these types of observations and calculations based on the principles of wave mechanics, numerous structural models of liquid water have been developed. Fletcher (1970) characterizes them into homogeneous models, such as Pople's, which suggests that one structure only is found throughout, and mixture models, where water is presumed to be a mixture of many types of structures which exist as clusters of similarly bonded molecules. Frank (1972) suggests the experimental evidence of unbonded molecules discounts the homogeneous models. He indicates that the most likely form of water is that described by mixture models, with interstitial molecules taking up residence within the tetrahedral structures.

Nemethy and Scheraga (1962) suggest that liquid water is composed of clusters of tetrahedrally bonded molecules in positions similar to those in ice. Their model suggests that at 0°C the clusters are composed of about 90 molecules and have a size in the order of 2.5×10^{-9} m.

As a point of interest, Frank (1972) documents some of the theories of density changes in water. Bernard and Fowler, with their homogeneous model, suggest that density decreases due to the bending, but not breaking, of the hydrogen bond. Samoilev, using a multi-bond approach consistent with mixture models, suggests that when ice melts, individual molecules become loose and assume interstitial positions, hence increasing the density.

There is no doubt that the amount of information about the molecular structure of water is increasing. However, a thorough understanding of this structure does not yet exist. At this time it is believed that hydrogen bonding and near-neighbour tetrahedral co-ordination clusters are dominant features of liquid water, and that such a structure involves about 10 to 100 molecules, with a lifetime in the order of the molecular vibration period. When one considers the similarity between this structure and that of ice there appears to be a logical transition between water and ice, based on an increase in the number of ice-like tetrahedral structures as the water temperature is lowered.

2.2 The Characteristics of Ice

The phase change between liquid water and solid water involves nucleation (three dimensional ice growth) and the growth of ice crystals (planar or two dimensional ice growth). In this section the structural and relevant thermodynamic properties of ice which effect the rates of these processes will be discussed.

2.2.1 Structural Characteristics

The structure of water in its solid state, as in its liquid state, is a function of the configuration of the molecules. Whalley (1969) indicated that ice can exist in a number of stable or metastable forms, depending on the temperature and pressure. In all these forms the structure is dominated by the fact that each oxygen molecule is surrounded by four other oxygen molecules.

Of the ten forms of ice described by Whalley (1969) only Ice Ih, where the intermolecular hydrogen bonds form a hexagonal structure, is stable at temperatures and pressure common at the earth's surface. Therefore, only the characteristics of Ice Ih will be discussed, although consideration of the nine other forms can shed some light on the characteristics of Ice Ih.

The relative positions of the oxygen atoms in the Ice Ih have been determined by the technique of x-ray diffraction. These studies are summarized by Fletcher (1970). In all instances the structure was found to be tetrahedral with the O···O bond length being 2.75x10^{-10} m. This is about 4% shorter than for liquid water and seems to contradict the fact that ice is less dense than water. However, as mentioned previously, it is argued that in water the density is increased by the presence of interstitial molecules, which more than compensate for the shorter bond length.

The measured length of the c-axis shown in Figure 2.2 varies between 7.31 and 7.38x10^{-10} m and the length of the a-axis varies between 4.48 and 4.52x10^{-10} m at temperatures of -200°C and 0°C respectively. Regardless of the temperature, the ratio of the length of the a-axis to the c-axis ranges between 1.627 and 1.632. This is lower than the perfect tetrahedral value of 1.633 which confirms measurements indicating that the O···O bond length parallel to the c-axis is 0.01x10^{-10} m shorter than the other O···O bonds, which implies a distortion in the tetrahedral bond angles.

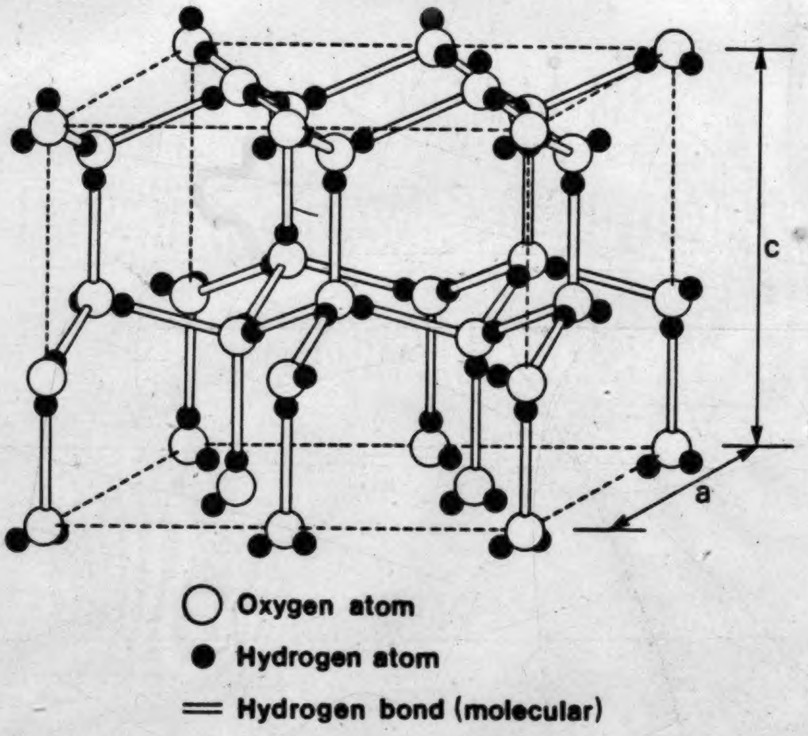
c
a
Oxygen atom
Hydrogen atom
Hydrogen bond (molecular)

Figure 2.2 Structure of Ice Ih (after Fletcher, 1970)

The positions of the hydrogen atoms are difficult to determine because they have minor effects on the electron concentrations and therefore cannot be observed in spectrographic studies. Hobbs (1974) briefly summarizes the work carried out to determine the location of the hydrogen atoms. Bernal and Fowler reasoned that the O-H bond angle is the same as the O···O bond angle. This means that the hydrogen atom is located 1x10^{-10} m from one oxygen atom and 1.76x10^{-10} m from the other. Fletcher (1970) suggests that if one assumes that there is only one hydrogen atom along each O···O bond and that there are only two hydrogen atoms close to each oxygen atom the hydrogen atom can fluctuate back and forth between its two most favoured locations.

2.2.2 Thermodynamic Properties

Many of the thermodynamic characteristics of ice which are important in the calculations of phase changes can be determined from molecular considerations. However, these thermodynamic characteristics can also be determined from bulk properties, on the basis of experimental evidence.

For example, the transfer of heat through ice is accomplished by lattice vibrations which travel through the crystal in waves. This determines the coefficient of thermal conductivity, which is defined as the ratio of the heat energy transmitted across a unit area of solid per unit time to the temperature gradient normal to the unit area. The value of the thermal conductivity has been measured to be about 2.2 W/m°C at 0°C. This is about four times that of water. When considering heat transfer across an ice-water interface this fact becomes important. As a matter of interest, the heat transfer rate along the c-axis is 5 to 8% greater than along the a-axis (Hobbs, 1974).

The heat capacity, C_p, of ice is considered to be the energy of a set of vibrating molecules. That is, as the temperature of ice is increased, the kinetic energy of the molecules increases. From experimental work the value of C_p is about 2.1 J/g°C. This is about one half that of water.

The latent heat of fusion, L, is defined as the change in enthalpy when a unit mass of liquid water is isothermally converted into ice. The accepted value of L is 333.6 J/g at 0°C (Hobbs, 1974).

The entropy, S, is a measure of the randomness of the molecular configuration. For the process of phase changes ΔS_v is the change in entropy and enters into the free energy budget. Fletcher (1970) indicates that the average entropy of fusion over the usual range of supercooling, ΔT, is given by

$$\Delta S_v = (1.13 - 0.004\Delta T)\ \mathrm{J/cm^3\,°C}$$

During the processes of nucleation and crystal growth, the most important variable which must be evaluated "a priori" is the surface free energy between ice and water, σ_{sl}. Hobbs (1974) defines it as the amount of energy required to create a unit area of interface. The value is difficult to evaluate theoretically and can only be determined from the number of bonds which must be cut to create an ice surface. Estimates for the value of σ_{sl} have ranged between 7.7 mJ/m² and 122 mJ/m² at temperatures between -40°C and 0°C.

Based on the homogeneous nucleation theory described in section 2.3.1, Fletcher (1970) suggests that a value of 22 mJ/m² is appropriate for a temperature of -40°C. Hobbs (1974) described his experiments which measured liquid-solid grain angles and suggested that σ_{sl} had a value of 33 mJ/m² at 0°C and that its value changes with temperature at a rate of 0.1 to 0.35 mJ/m²°C. Suzuki and Kuroiwa (1972) indicate that the experiments to which Hobbs referred incorrectly determined the grain angle and that a better value for σ_{sl} is about 45 mJ/m². Kallungal (1975) reviews the calculated value of σ_{sl} on the basis of the crystal growth velocity experiments addressed in section 2.4 and suggests that the most likely range should be between 34 and 54 mJ/m². He also indicates that although σ_{sl} has always been assumed to be isotropic, the prefered growth rates of crystals along the a-axis suggest that σ_{sl} associated with the basal face may be different. For example, he quotes values of σ_{sl} for growth along the c-axis to be only 6.2 mJ/m².

A summary of all the relevant properties is made in Table 2.1. For comparison, the properties of water are also tabulated.

Table 2.1

Thermodynamic Properties of Ice and Liquid Water at Temperatures Near 0°C

Property	Water	Ice
Density (g/cm^3)	0.999	0.917
Thermal Conductivity (W/m-°C)	0.57	2.2
Specific Heat (J/g-°C)	4.22	2.09
Latent Heat of Fusion (J/g)	333.6	333.6
Entropy of Fusion (J/g)	1.224	1.224
Surface Free Energy (mJ/m^2)	-	40
Viscosity (g/cm-sec)	0.0018	-
Kinematic viscosity (cm^2/sec)	0.0018	-

2.3 Nucleation

In a liquid the molecules are in constant motion, both in vibrational and translational modes. A reduction in temperature reduces the tendency for translation and this allows stronger intermolecular forces to be established. At 4°C the maximum density is achieved as the intermolecular forces become strong enough to maintain dense clusters of water molecules in the ice-like form, with some single water molecules dispersed interstitially. Below 4°C the structure becomes more open with the density decreasing as the interstitial water molecules are forced out. Finally, when freezing or crystalization occurs, the molecules assume a fixed position within the crystal lattice where they are free to vibrate, so maintaining some kinetic energy which is a function of the absolute temperature of the ice crystal.

The manner in which the transformation between liquid and solid actually occurs is not a well known process. However, it has been agreed (Van Hook, 1961) that the adjustment of any metastable state - supercooled liquid, for example - involves the surmounting of an energy barrier which defines the condition and the subsequent passage to a state of lower energy and greater stability. That is, for the ice-like water clusters to become true ice clusters the configuration of the water molecules must be such that it becomes energetically advantageous to maintain the ice configuration and to increase the size of the ice cluster. On the basis of the possible configuration of water molecules this process is probably a random event with the probability of occurrence increasing as the water temperature decreases (Mason, 1958).

A number of nucleation theories have been developed to explain these processes.

2.3.1 Homogeneous Nucleation

The homogeneous nucleation theory holds for pure water and suggests that ice crystals are formed by multiple collisions that result in the formation of an ice-like water cluster. That is, a very small volume of liquid must first crystalize and this volume must grow in size to become a viable ice crystal. If the water temperature is not favourable, the small newly formed ice crystal will dissolve. If, however, the random association of molecules produces a structure of sufficient size such that its representative radius maximizes the sum of the entropy of fusion (which is a function of the structure volume) and the free energy of the ice-water interface (function of the surface area of the structure) a stable ice crystal will be produced and will grow in size (Fletcher, 1970).

For true homogeneous nucleation Hobbs (1974) indicates that the creation and growth of an ice crystal from pure water can only occur at temperatures in a range between -20°C and -50°C and that this nucleation temperature should not vary with the size of the water sample. However numerous experimenters, in their study of the freezing temperatures of minute water droplets in the atmosphere, have found the nucleation temperature to be strongly dependent on the sample volume. This phenomenon is illustrated in Figure 2.3. Mason (1958) suggests that this variation is due to the difficulty of isolating a truly pure sample of water, where no boundary conditions can cause contamination. He suggests that the lower nucleation temperatures of small samples simply reflect the fact that fewer impurities exist in the smaller samples.

Therefore, it appears that the nucleation of frazil ice observed in rivers and laboratory experiments cannot be explained by the homogeneous nucleation theory.

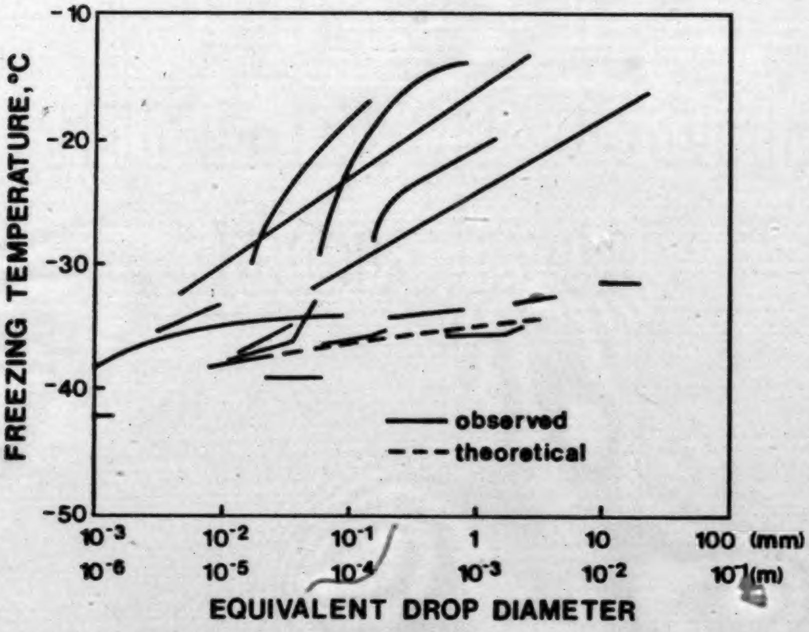

Figure 2.3 Nucleation Temperatures of Small Water Droplets (after Fletcher, 1970)

2.3.2 Heterogeneous Nucleation

The heterogeneous nucleation theory has been developed to explain the discrepancies observed in the appplication of the homogeneous theory. Whereas the homogeneous theory is essentially three dimensional nucleation, the heterogeneous theory assumes a two dimensional ice growth on surfaces of foreign substances within supercooled water. Fletcher (1970) indicates that these substances may be dissolved molecules or suspended particles. However, because dissolved materials tend to reduce the nucleation temperature by breaking up the ice-like clusters of water molecules it appears that suspended particles exert the most influence.

The basis of the theory of heterogeneous nucleation (as for homogeneous nucleation) is the Clausius-Clapeyron equation which is essentially the derivative of the Gibbs free energy equation and can be written as:

$$\Delta G_v = -\Delta S_v \bullet T \text{ J/cm}^3\text{°C} \tag{2.1}$$

if pressure and volume are constant. In this equation ΔG_v is the free energy difference per unit volume of ice between matter in the liquid state and matter in the solid state; ΔS_v is the average entropy of fusion over the supercooling range; and T is the amount of supercooling.

Fletcher (1958, 1959, 1962) indicates that for heterogeneous nucleation the total energy difference of a nucleating particle (and an ice crystal growing on that particle) surrounded by supercooled water is composed of the sum of the energy difference between solid and liquid states of the ice crystal, the difference in the surface free energy of the interface between the ice crystal and the nucleating particle, and the difference in surface energy of the interface between the ice crystal and the supercooled water. That is:

$$\Delta G = \Delta G_v V + \sigma_{sl} S_{sl} + (\sigma_{sn} - \sigma_{ln}) S_{sn} \text{ J/cm}^3 \qquad (2.2)$$

where V is the volume of ice, σ_{sl} the free energy of the ice-water interface which Hobbs (1974) defines as being the amount of energy required to create a unit area of that interface, σ_{sn} the free energy of the interface between ice and the nucleating particle, σ_{ln} the free energy of interface between water and the nucleating particle, S_{sl} the surface area of the ice water interface, and S_{sn} the surface area of the interface between ice and the nucleating particle.

Fletcher (1958) indicated that if a spherical ice crystal of radius, r, is growing on a spherical nucleating particle with a radius, R, equation 2.2 can be differentiated to determine the critical radius of a stable and growing volume of ice, r*, by setting the derivative to zero. Subsequently, with the reinsertion of r* into equation 2.2, ΔG*, the height of the thermodynamic barrier of nucleation, can be determined. These equations are given as:

$$r^* = -2\sigma_{sl}/\Delta G_v \text{ cm} \qquad (2.3)$$

and

$$\Delta G^* = 8\pi\sigma_{sl}^3 f(m,x)/3(\Delta G_v)^2 \qquad (2.4)$$

where

$$f(m,x) = 1 + (1-mx^2/g) + x^2[2-3(x-m/g) + (x-m/g)^3] + 3mx^2[(x-m/g)-1] \quad (2.5)$$

$$g = (1 + x^2 - 2mx)^{1/2} \quad (2.6)$$

$$x = R/r* \quad (2.7)$$

and

$$m = (\sigma_{ln} - \sigma_{sn})/\sigma_{sl} \quad (2.8)$$

The parameter m is a function of the surface energies of the ice embryo and the nucleating agent. It can vary between -1 and +1. A value of m near +1 indicates a high degree of compatibility. For example, m would equal +1 for ice particles acting as nucleating agents.

The parameter x is an indicator of the curvature of the ice embryo compared to the nucleating particle. If R >> r then the nucleating particle would be a plane surface and x would approach infinity. If R << r then essentially homogeneous nucleation would occur.

The effects of m and x on the parameter f(m,x) are illustrated by Fletcher (1958) for a spherical nucleating particle. For a minimum value of m the function f(m,x) is independent of x and has a value of 2.0. For a maximum value of m the function f(m,x) is also independent of x as long as x < 0.6. In this instance the value of f(m,x) again takes on a value of 2.0. For x > 0.6 and m = 1.0 the value of f(m,x) appears to vary tremendously between zero and 1.0. If m < 1.0 the value of f(m,x) ranges between 0.004 and 1.0.

Because the function f(m,x) determines the free energy of formation, ΔG*, of a critical embryo, it plays a major role in determining the nucleating temperature. Unfortunately it is not well defined within the range of most observed nucleation temperatures, and small variations in either m or x can lead to tremendous error in estimating f(m,x), ΔG^*, and, ultimately, the nucleation temperature.

Hobbs (1974), further to Fletcher's earlier work, suggests that lattice misfits between ice and a nucleating particle can reduce the effectiveness of the nucleating particle. That is, there will exist a certain concentration of dislocations across the interface and some elastic strain will occur in the ice. In general, an increase in the concentration of dislocations will result in a larger value of σ_{sn} which results in a decrease in the value of m. The increased strain in the ice will also result in a higher value of ΔG_v.

Fletcher (1959) also considers the effects of imperfections on the surface of the nucleating particle. These conical pits cause the nucleation to first occur within them because it is energetically advantageous. The nucleation rate then becomes a function of the surface area of these pits and the reduced free energy due to their existence. On the basis of Fletcher's model the existence of these pits is not significant when the nucleating particle is less than 10^{-8} m in radius.

With the definition of the critical size of the ice embryo and the level of the energy barrier which must be crossed, the potential for growth can be determined.

Turnbull and Fisher (1948) suggest that if a volume of ice, described by the characteristic radius r, exists within a volume of supercooled water the transformation of water molecules into ice molecules can be written as:

$$I_i + L_1 \rightleftharpoons I_{i+1} \tag{2.9}$$

where I_i is an ice-like structure containing i molecules and L_1 is a water molecule. The free energy of $I_i + L_1$ is ΔG_i and the free energy of I_{i+1} is ΔG_{i+1}. As in all chemical reactions or phase changes, there is some free energy change greater than either of the two and the activated complex is the configuration of the path of the least maximum free energy. The theory of absolute reaction rates gives the rate of the forward reaction to be:

$$J^{+} = n_i a_1 i^{2/3} (kT/h) \exp(-\Delta g_1^{*}/kT) \tag{2.10}$$

where n_i is the steady state concentration of I_i nuclei, $a_1 i^{2/3}$ is the number of liquid molecules in contact with the ice nucleus and $n_i a_1 i^{2/3}$ is the total concentration of liquid molecules available for the reaction. The specific reaction rate for the formation of the activated complex with a free energy increment is given by:

$$(kT/h) \exp(-\Delta g_1^{*}/kT) \tag{2.11}$$

Using the same reasoning, Turnbull and Fisher (1948) write the reverse reaction rate to be

$$J^{-} = n_{i+1} a_2 i^{2/3} (kT/h) \exp(-\Delta g_2^{*}/kT) \tag{2.12}$$

and the net forward rate of the attachment of molecules is the difference between the two rates. The difference between the activated complex and the mean of ΔG_i and ΔG_{i+1} is Δg^{*}.

By assuming there is an insignificant difference in the number of water molecules in contact with the ice surface and the number of ice molecules in contact with the water surface, that $\Delta G_i(n_i)$ is a smooth function, and that the second derivatives of ΔG_i with respect to i are small, both Turnbull and Fisher (1948) and Fletcher (1970) show that the rate of attachment of water molecules to the unit surface area of an ice crystal is:

$$J_e = n_s\, kT/h \exp(-\Delta g/kT) \exp(-\Delta G^*/kT) \qquad (2.13)$$

Fletcher (1970) goes on to suggest that $n_s kT/h$ has a value of 10^{28}/cm²sec, where n_s is the number of molecules per square centimetre of surface area of the nucleating agent and $\Delta g/kT$ has a value of about 10 in the vicinity of 0°C. He also indicates that if one considers a nucleating sphere with a surface area of $4 R^2$ the rate at which molecules would attach themselves to one square centimetre of surface in one second is given by:

$$J_e = 10^{24} R^2 \exp(-\Delta G^*/kT) \qquad (2.14)$$

With $J > 1$ the potential for growth is positive and the ice crystal should increase in size.

Fletcher (1962), with the substitution of equations 2.1, 2.3 and 2.4 into equation 2.14, derived an implicit equation to determine the nucleation temperature for ice in supercooled water when the value of J_e is equal to unity. The temperature of nucleation is a function of only the representative diameter of the nucleating particle and m. The relationships are illustrated in Figure 2.4. From the

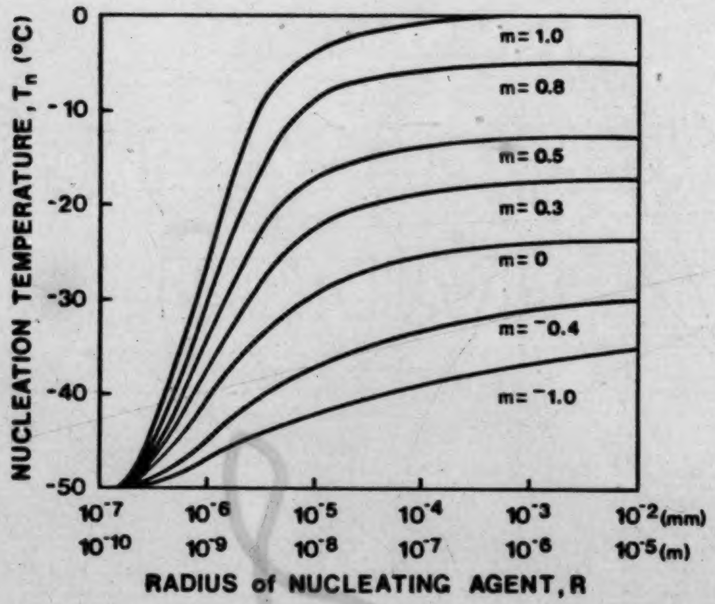

Figure 2.4 Nucleation Temperature Due to Spherical Particles Suspended in Supercooled Water (after Fletcher, 1963)

plot it is evident that on the basis of the small amounts of supercooling observed in natural streams, m, which gives the degree of compatibility between the structure of ice and the structure of the nucleating agent, must be near unity. This would indicate that an injection of ice from some external source must initiate nucleation. It is also evident that this ice must have a spherical radius greater than 10^{-7} m.

2.3.3 Observations of Nucleation and Other Theories

In conjunction with the classic theories of homogeneous and heterogeneous nucleation, numerous observations of the nucleation process were made under varying conditions. Most of these observations discredited the homogeneous theory and many showed that heterogeneous nucleation would require modification to explain the observations.

Altberg (1936) performed a series of experiments in an outdoor tank where he observed nucleation of frazil at a supercooling of 0.18°C. Devik (1948) observed nucleation on the surface of a small stream at temperatures between -0.10 and -0.12 °C. Both individuals suggested that nucleation was produced by the presence of nucleating agents on the boundary of, or within, the water body. Altberg suggested that these nucleating particles could be small dust particles and that nucleation was produced only if there was sufficient turbulence to maintain these small particles in motion. He also found that the greater the turbulence, the higher the nucleation temperature.

Dorsey (1948) performed numerous experiments to determine the nucleation temperatures of various types of water under different cooling conditions. His interest was aroused out of conflicting reports of nucleation temperatures ranging between -6 and -20°C. His primary purpose was to determine the effects of agitation, thermal shock, and length of cooling time on the nucleation temperature. In general, he found that the nucleation temperatures were independent of most of these factors and that for any given samples of similar water all the nucleation occurred at temperatures that fell within narrow bands between -3 and -20°C. Dorsey considered all nucleation to occur due to the presence of foreign particles, hence he supported the concept of heterogeneous nucleation, and that nucleation could be enhanced by the introduction of foreign materials by turbulence, agitation, or mechanical friction along the walls of the containers. However, regardless of the intensity of the disturbances, no nucleation could be produced above a temperature of -2°C. Gilpin (1978) observed a similar phenomenon in the supercooling of water in pipes. He found that shock could cause nucleation at almost any supercooled temperature, but without such a disturbance the nucleation temperature would range between -6.1°C in winter and only -4.8°C in summer (lower concentrations of suspended sediment occur in winter).

Dorsey (1948) had one problem with heterogeneous nucleation. He believed that since only a finite number of foreign objects are available in any one sample, nucleation should not proceed at the high rates he observed in his experiments. On this basis he suggested a new theory, where an absorbed layer of liquid water exists on each foreign particle. These absorbed layers can be detached by bombardment with moving water molecules at rates depending on the water temperature and the quality of the foreign particles. These detached layers can then form viable ice crystals. It should be noted that this theory was not too different from the heterogeneous theory already in existence. However, the heterogeneous theory does not contain the possibility of the ice crystal being detached from the nucleating agent.

Michel (1963, 1967) measured nucleation temperatures in the order of -0.045°C in an outdoor flume. He suggested that nucleation occurs heterogeneously in the thin layer of highly supercooled water near the surface and that the nucleating agents are small particles whose characteristic nucleating temperatures are less than -2°C.

Carstens (1966) produced frazil in a circular flume and observed nucleation at supercoolings of 0.025 to 0.12°C. He observed new nuclei being formed during the entire supercooling period following inital supercooling. This length of supercooling, and therefore the length of nucleation time, was reduced under more turbulent conditions, other variables being held constant.

Chalmers and Williamson (1965) observed the formation of new ice crystals following initial nucleation as did Carstens (1966) and Michel (1963). They called it a crystal multiplication process, whereby a single crystal placed in turbulent supercooled water would cause discoidal-shaped crystals to grow on its surface. These discs maintained their circularity up to a diameter of 1 cm and a thickness of 0.07 cm and eventually broke off to allow other crystals to grow in their places, and to also produce new crystals themselves. This is possibly the phenomenon observed by Dorsey, except in Chalmers' and Williamson's observations it occurred at a slower rate and produced considerably larger crystals.

Hanley and Michel (1977) produced frazil in a large insulated tank where turbulence was generated by paddle stirrers and the heat loss was confined to the surface. They observed nucleation temperatures at supercoolings of 0.015 to 0.050°C. They were the only investigators to attempt to measure the quantity of ice produced rather than infer the quantity from the cooling curves. Unfortunately they could not isolate the nucleation period and simply measured the volume of ice at large time intervals following the return to the residual temperature.

Osterkamp (1977) observed frazil generation in a small stream in Alaska. The recorded nucleation temperature was about -0.02°C in the stream. However, when the water was supercooled under laboratory conditions nucleation occurred at water temperatures between -4 and -14°C. Therefore, given the fact that the nucleating temperatures of foreign substances range between -15 and -4°C and that the coldest surface temperature observed on a normally cooled body of water was always in the order of -1°C, Osterkamp believed that the heterogeneous nucleation theory applied to foreign nucleating agents could not possibly explain the small amounts of supercooling required to cause nucleation in natural streams.

Osterkamp devised another theory. Quoting research that showed that air above a stream surface can contain ice particles ranging in sizes between $6\text{-}35\text{x}10^{-5}$ m at concentrations between 10^2 and 10^5 particles per cubic metre, Osterkamp suggested that these tiny ice crystals, whose origin is freezing water vapor, come in contact with the water and initiate nucleation. This nucleation must be heterogeneous in a fashion, except that because the nucleating material is ice, the temperature of nucleation is determined only by the sizes of the water vapor ice crystals.

In his paper, Osterkamp also acknowledges the fact that secondary nucleation by mechanical fragmentation of the thermally detached dendritic ice crystals can also add to the nucleation process following the initial nucleation point. This may have been observed by Muller (1978) who started nucleation by inserting one ice crystal into a small ($4.13\text{x}10^{-3}$ m^3) body of turbulent supercooled water. Muller counted the rate of secondary nucleation using a Schlieren light system and generally he found that this rate increased with an increase in turbulence or supercooling. He measured nucleation rates which varied between 6.2×10^{-4} and 4.3×10^{-2} particles per second per cubic centimetre, with maximum concentrations following the nucleation period ranging between 0.11 and 3.7 particles per cubic centimetre.

Muller's data is tabulated in Table 2.2. The less complete data of the other experimenters referred to previously is tabulated in Table 2.3. This data reflects both highly turbulent and quiescent flow conditions in natural streams, and also laboratory experiments where mass transfer across the water-air interface was both prevented and allowed.

For natural streams, Devik's data indicate that in a quiescent stream, surface nucleation occurs at surface supercoolings between 0.10 and 1.0°C. The fact that no ice is transported below the water surface allows a surface cover to form. The tremendous variation in the nucleation temperatures noted is probably due to the random appearance of nucleating agents such as organic debris and atmospheric ice crystals. Osterkamp, who studied highly turbulent streams, even observed nucleation temperatures above the computed ice point (which he suggested was less than 0°C because of the impurities in the water), although he was measuring the bulk water temperature. Again, surface nucleation of some unmeasured supercooled temperature was probably occurring, except in this instance the newly generated frazil ice was being transported below the cover to facilitate a general appearance of frazil. It should be noted that Osterkamp's measurements must be considered with a some reservations. One of his major difficulties was the measurement of a transient process with stationary probes, hence he could not follow the frazil generation process downstream.

In the laboratory experiments where mass transfer across the water surface is not allowed, nucleation did not occur for water temperatures as low as -1.33°C (Table 2.2), although the actual nucleation temperatures were never observed because nucleation was initiated by seeding the water sample with ice crystals. When mass transfer across the air-water interface was allowed, nucleation occured at water temperatures between -0.025°C and -0.13°C (Table 2.3). Again, the variation is probably due to the presence of nucleating agents, although some of Carstens' data seems to suggest that if the cooling rate is reduced the nucleation temperature is increased.

Therefore, it appears there is agreement that nucleation in natural streams in initiated by the transport of small ice particles from the air into the water. These small ice nuclei then contribute to a secondary nucleation process by which ice particles breed new ice particles. Growth of all these particles also occurs because the particles are located in supercooled water.

Table 2.2

Summary of Muller's (1978) Data

Experiment Number	Reynold's[3] Number	Maximum Supercooling (°C)	Maximum Nuclei Produced (/cm^3)	Nucleation[1] Rate (/cm^3•min)	Heat Gain (cal/min•cm^3)	Maximum[2] Radius (mm)	Growth[2] Rate (mm/min)	Average Nu
E3	2300	0.127	2.64	0.127	0.127	0.29	0.05	12
E5	2300	0.137	2.83	0.94	0.221	0.75	0.14	20
E6	2300	0.108	0.54	0.06	0.040	0.60	0.06	7
E7	1500	0.200	2.70	1.80	0.401	0.62	0.28	15
E8	1500	0.180	2.55	1.02	0.596	0.67	0.20	20
E9	1500	0.136	1.33	0.33	0.347	0.60	0.14	21
E11	1500	0.168	2.08	0.70	0.184	0.39	0.02	8
E12	1500	0.092	0.11	0.037	0.031	0.98	0.04	31
E13	2300	0.148	3.72	2.48	0.254	0.30	0.02	12
E14	2300	0.067	0.34	0.076	0.030	0.47	0.05	7
E15	2300	0.105	1.79	0.36	0.075	-	-	5
E16	2300	0.099	1.98	0.50	0.080	0.33	0.04	7

[1] assumed constant over the time period.

[2] the ice particles were assumed to be spherical.

[3] based on grid-rod diameter.

Table 2.3

Summary of Available Data from Supercooling Experiments

Investigator	Ta (°C)	dT/dt x 10**4 (°C/sec)	tn (sec)	Tn (°C)	ts (sec)	Ts (°C)	tr (sec)	Tr (°C)	Comments
Altberg (1936)	-	11.0	162	0.18	330	0.22	900	0.01	stirred tank
Devik (1948)	-2.0 to -18.5	-	-	0.10 to 1.06	-	-	-	-	surface temperature in a natural stream, low wind velocity
Kumai & Kazuhiko (1954)	-7.0	5.7	-	-	-	0.14	-	0.05	nucleation produced by seeding with ice particles
	-9.0	4.2	-	-	-	1.33	-	-	
Williams (1959)	-	1.3	410	0.05	410	0.05	800	0.00	stirred tank
Michel (1963)	-	2.8	168	0.045	318	0.052	444	0.00	open air flume
Carstens (1966)	-10	3.0	96	0.034	330	0.077	630	0.018	flume
	-10	10.4	120	0.125	150	0.140	240	0.005	stirred tank
	-10	5.2	180	0.095	210	0.100	300	0.01	stirred tank
	-10	3.9	180	0.070	300	0.080	480	0.001	stirred tank
	-10	2.1	300	0.063	360	0.070	480	0.00	stirred tank
	-10	1.0	300	0.030	390	0.035	690	0.00	stirred tank
	-10	1.4	180	0.025	420	0.040	660	0.03	stirred tank
	-10	2.7	150	0.040	180	0.045	540	0.020	stirred tank
	-10	0.95	420	0.040	540	0.045	720	0.00	stirred tank
	-10	0.83	480	0.045	3360	0.100	-	0.00	vibrated tank
	-	3.6	140	0.050	240	0.060	350	0.001	vibrated tank
	-	1.2	300	0.040	420	0.040	780	0.00	vibrated tank
Osterkamp et.al., (1975)	-	-	-	>0.00	-	0.003	-	0.00	natural stream, temperatures adjusted for ice point
	-	-	-	>0.00	-	0.036	-	0.00	
Hanley & Michel (1977)	-2	0.20	-	-	-	0.026	-	-	stirred tank
	-5	0.44	-	-	-	0.037	-	-	stirred tank
	-10	0.68	-	-	-	0.037	-	-	stirred tank
	-20	1.5	-	-	-	0.038	-	-	stirred tank

2.4 Crystal Growth

The nucleation process described in section 2.3 results in the formation of a stable ice crystal. This crystal has some unknown shape but its size can be characterized by a critical radius. The internal structure of the crystal is consistent with the ice characteristics described in section 2.2.1. That is, the water molecules (in the ice phase) would be structured with a consistent c-axis alignment. If one considers a three dimensional image of such a crystal (Figure 2.2) the basal plane parallel to the a-axis and a crystal plane parallel to the c-axis can be defined.

The growth of the crystal occurs along both axes at different rates, and the shape of the crystal is a function of these growth rates. Fletcher (1970) indicates that the rate and form of growth depends on the transport of liquid molecules to the ice surface, the accommodation of these crystals on the interface, and the transport of latent heat away from the surface.

In quiescent water, it appears that the rate of heat removal from the crystal surface limits the growth rate. If the crystal surface is "rough" (the solid-liquid interface extends over several inter-molecular distances) the water molecules can be attached at random sites. The surface then advances in a continuous manner, in a direction normal to itself, at a rate proportional to the supercooling. Kallangal (1975) summarized the experimental evidence which suggests that the fastest growing crystal face (which is in the plane parallel to the c-axis) grows at a velocity

$$v = p\,\Delta T^{n} \qquad (2.15)$$

Table 2.4 lists the values of p and n from various experiments. Most of the variation can be attributed to experimental techniques since a majority of the ice crystals were grown in capillary tubes, which affect the heat transfer rates. Kallungal (1975), who has produced the latest and probably most reliable data, suggests that the velocity of growth is given by:

$$v = 0.023\,\Delta T^{2.17}\ \text{cm/sec} \qquad (2.16)$$

If the solid-liquid interface is "smooth", the transition from liquid to solid occurs over many intermolecular distances and attachment can occur at kinks where unfinished growth layers are found. The rate of advance of the interface is then a process similar to homogeneous nucleation. The velocity of growth can be written as:

$$v = b\,\exp\,(-c/\Delta T) \qquad (2.17)$$

In these instances the growth rate is kinetically controlled. That is, the growth rate is a function of the ability of molecules to attach themselves to the ice particle and not of the rate of heat transfer from the ice-water interface.

Experimenters have found that growth along the c-axis is kinetically controlled and therefore can be determined by equation 2.17. The constants in equation 2.17 were documented by Kallungal (1975) and are shown in Table 2.5.

Table 2.4

Experimentally Determined Constants in the Crystal Growth Equation under Quiescent Conditions

Investigator[1]	n	p
James (1967)	1.30	0.10
Hallett (1964)	1.90	0.08
Farrar and Hamilton (1965)	2.04	0.0096
Pruppacher (1967)	2.22	0.035
Huige and Thijssen (1969)	2.22	0.030
Boiling and Tiller (1961)	2.62	0.017
Kallungal (1975)	2.17	0.012

Table 2.5

Experimentally Determined Constants for Crystal Growth Parallel to the c-axis

Investigator[2]	b	c
Simpson et. al. (1974)	0.00017	0.234
Hillig (1958)[3]	0.0030	0.35

Table 2.6

Experimentally Determined Constant in the Crystal Growth Equation Under Forced Convection Conditions

Investigator	A
Fernandez and Barduhn (1967)	0.0466
Poisot (1968)	0.0374
Simpson et. al. (1974)	0.038
Kallungal (1975)	0.037

---

[1] see Kallungal (1975) for reference

[2] see Kallungal(1975) for reference

[3] experiments conducted in confined state with supercooling less than 0.65°C.

Comparing equations 2.16, equation 2.17, and Table 2.5, the growth rate perpendicular to the c-axis can be 12 to 23 times as large as the growth rate along the c-axis at supercoolings of 0.05°C.

Jackson quoted by Kallungal (1975) suggests that the difference in growth rates can be explained on the basis of "smooth" and "rough" surfaces. For growth to occur along the c-axis ("smooth" surface), three molecules, each making a single bond to the layer below, must be present on three neighbouring sites before a molecule can be added. This requires the coherent existence of a four-molecule cluster. For growth normal to the c-axis ("rough" surface), one molecule making a single bond to the adjacent layer can be joined by a second molecule to make one bond to each. This requires only a two-molecule cluster and hence is easier to form.

If an ice crystal is located within a velocity field heat is removed by forced convection and the growth rate of the rough surface can be accelerated. Various models for crystal growth under this condition have been developed and all have the form:

$$v_a = A\ V^{1/2}\ \Delta T^{3/2} \tag{2.18}$$

where A can vary between 0.037 and 0.047. Kallungal (1975) provides the best data and suggests that A should have a value of 0.037. A summary of the experimentally determined values of A is presented in Table 2.6.

Most crystal growth rates have been measured while a single crystal has been held stationary and supercooled water was moved past the crystal. However, Carstens (1966), putting aside differential growth rates, indicated that the growth of the mass of an ice crystal is proportional to the surface area of the crystal and the supercooling. The constant of proportionality is given by the product of the ratio of the thermal conductivity of the water to a characteristic length scale of the crystal and the crystal Nusselt number. Thus for one crystal:

$$L\, dM_i/dt = k\, N_u A*(\Delta T)/r \qquad (2.19)$$

Carstens also assumed that

$$N_u = C\, R_e^m \qquad (2.20)$$

where C is a constant, m is about 0.8, and R_e is the Reynolds number of the crystal.

If the crystal is assumed to have a characteristic radius r then equation 2.19 reduces to

$$dr/dt = K\, v^{0.8} \Delta T/r^{0.2} \qquad (2.20)$$

where K is a constant, v is a mean flow velocity, and dr/dt is the growth rate. Comparing this equation to the earlier ones, one can see that the velocity is a slightly more important variable while the dependence on temperature is reduced. In this instance, the increased radius tends to reduce the rate of heat loss which does not appear consistent with the fact that as crystal size becomes larger the effects of turbulence should be more apparant. Unfortunately Carstens had no way to determine the validity of this equation because he did not document the growth rate or the flow velocity.

Muller (1978) considered the effects of velocity on a crystal situated within a turbulent flow field. The turbulence was generated by a moving grid and was characterized by the Reynolds number based on the grid-rod diameter. The larger the Reynolds number, the greater was the turbulence. He suggests that the turbulent heat exchange depends on the ratio of the microscale of turbulence to the size of the crystal. If the crystal is small compared to the turbulence scale the crystal will be convected with the flow and heat loss will be by conduction only. Convected heat loss only becomes apparant when the turbulence scale is smaller than the crystal. Velocity differences will occur at the crystal face and the rate of heat loss could be up to ten times as large as by pure conduction. This is somewhat born out in Figure 2.5, which illustrates the comparison of growth rates at various supercoolings and velocities. The growth rates normal to the c-axis are 2 to 3 order of magnitudes larger than the growth rate along the c-axis, regardless of the strength of the velocity field. In addition, the estimates made by Muller (1978) for turbulent flow conditions are only slightly larger than the measured values of Kallungal (1975), for quiescent flow conditions. This suggests that for the relative length scales of turbulence and frazil particles in Muller's experiment, the rate of heat transfer from the particle surface does not

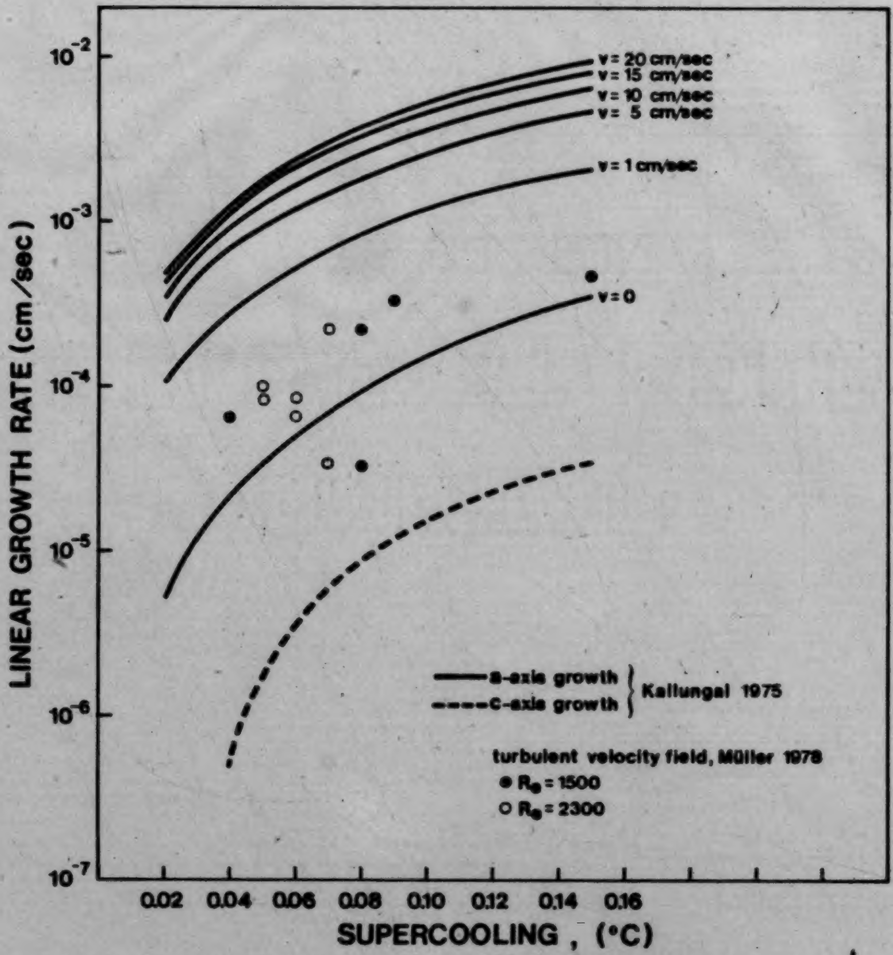

Figure 2.5 Linear Growth Rates of Ice Crystals in Supercooled Water

depend strongly on the turbulence. It should be noted however, that Muller estimated the size of the particle on the basis of the volume of ice generated and the number of ice particles he counted, with the assumption the particles were spheres. This would tend to underestimate the growth rates because he did not distinguish between the difference in growth rates along the c-axis and a-axis.

2.5 Morphology of Ice Crystals

In the previous section theoretical and experimental growth rates of ice crystals along the two major axes were discussed. Inherent in those growth experiments was some evaluation or observation of the crystal shape. Prior to a discussion of findings by the various experimenters, it should be noted that various types of ice growth can occur. Hobbs (1974) indicated that ice crystals can grow in a supercooled environment where a majority of heat is transferred by the fluid. This can occur under both slightly supercooled conditions or strongly supercooled conditions. If ice is being grown in a situation were the heat is conducted away from the interface through the ice, then planar growth occurs and the water need not be supercooled. This type of ice growth is typical of lake or river surface ice growth, occurs very slowly, and is easily observed.

For ice growth in supercooled water the crystal will grow along the two principle axes by the various growth modes discussed in section 2.4 and the ultimate shape of the crystal will be a function of the differential growth rates along the two axes.

Numerous observations of the shape and sizes of ice crystals formed in supercooled turbulent water have been made. In all cases, for supercoolings less than 0.5°C, the ice crystals were discoidal in shape. Altberg (1936) reported observing round, smooth sided discoids with diameters between 1 to 8 mm and thicknesses of 0.1 mm. Schaefer (1950), who like Altberg, made his observations in natural streams, reported discs with diameters ranging in size between 1 and 5 mm and thicknesses in the order of 0.03 to 0.10 mm.

Arakawa (1954) suggested that, following nucleation, the ice crystals grew into discoids during the early stages of growth. In these experiments nucleation was produced on a brass rod maintained at -20°C and immersed in about 100 cm^3 of water. Tiny ice crystals, initially dendrites, were produced on the brass rod, detached themselves, and took on a discoidal shape as they floated to the surface. These crystals grew quickly to a diameter of 1 mm and maintained their discoidal shape. Their fall velocity was about -0.002 m/sec.

Kumai and Itagaki (1954) used cinematography to observe the growth of ice crystals in supercooled water. Approximately 3 cm^3 of water with a depth of 0.3 cm was seeded with various nuclei. Of the various substances, such as silver iodide, kaolin, and carbon, only ice crystals facilitated crystal growth. In supercooled water between 0°C and -0.3°C only discoid ice crystals resulted from seeding. At -0.05°C, the diameter of the discoids increased from about 1 mm to 3 mm in a time of 140 sec. This is a growth rate about 46 times larger than predicted by Kallungal (1975). As the discoid grew larger with time it slowly became hexagonal in shape and developed dendritic arms. It was also determined that for supercooling between -0.3°C and -0.6°C a mixture of discoids, semicircular discoids, and spicules formed. Spicules were observed to predominate in the supercooling range of -0.06°C to -0.9°C. Below -1.0°C most of the crystals had a stellar or dendritic shape similar to that of snowflakes.

Recent observations of frazil ice in natural streams by Gilfilian et. al. (1972) and Ardin and Wigle (1972) confirmed the discoidal shape of newly formed frazil particles. Gilfilian et. al. (1972) indicate that the ice crystals were first observed at diameters of 0.1 to 0.5 mm and these crystals grew as large as 5 mm in diameter. Scalloped edges on these discs were observed when the diameter exceeded 1 mm. Arden and Wigle (1972) reported discoidal frazil particles with diameters up to 8 mm being produced on the Upper Niagara River.

Chalmers and Williamson (1965) observed crystal shapes in turbulent supercooled water under laboratory conditions. They noted discoidal shaped crystals with diameters of 10 mm and thicknesses of 0.7 mm growing on bulk ice.

Lindemeyer and Chalmers (1966) indicated that when ice crystals are grown under free growth conditions, where the supercooling is less than 0.2°C, thin discs will form and grow to a diameter of about 3 mm with a thickness of 0.25 mm. At supercooling greater than 0.2°C the discs become unstable and protuberences appear on the edge of the discs. With supercooling nearing about 1°C dendritic shapes predominate.

Kallungal (1975), in his review of ice crystal morphology, quoted works by Pruppacher, Macklin and Ryan, and Hallet. It appears to be generally accepted that at supercooling below 1°C crystals are essentially discoidal and the c-axis is always normal to the fastest growth direction. However, as the supercooling temperature is increased, the ratio of the growth velocities, v_a/v_c, decreases from about 100 at -1°C to 1.3 at -16°C. Jackson (1958) suggests that the reduction in the ratio is due to the "roughening" of the basal plane as the supercooling is increased. This allows the growth along to the c-axis change modes and become a function of the rate at which latent heat is removed from the interface rather than being dependent on the ability of the molecules to attach themselves to the face of the crystal.

Table 2.7 summarizes the observed dimensions of the discoids. It should be noted that the ratio of thickness to diameter varies between 10 and 80, well within the ratios of

Table 2.7

Summary of Observed Sizes of Frazil Particles

Investigator	Diameter (mm)	Thickness (mm)	Diameter/ Thickness
Altberg (1928)	1-8	0.1	10-80
Schaefer (1950)	1-5	0.03-0.10	33-50
Kumai and Itagaki (1954)	1-3	-	-
Chalmers and Williamson (1965)	10	0.7	14
Lindemey and Chalmers (1966)	3	0.25	12
Gilfilian, et.al. (1972)	5	-	-
Arden and Wigle (1972)	8	-	-

the rates of growth of the two crystal planes.

2.6 Summary

A brief explanation of the structural differences between liquid water and ice makes apparant the physical changes which must occur during freezing. On the basis of the nucleation theories, especially the quantitative approach summarized in much of Fletcher's work, it is possible to predict the temperature at which nucleation and hence a change in phase will occur.

Unfortunately, the difficulty of observing the nucleation process has resulted in a considerable variation of opinions as to what causes nucleation, although some theories are more plausible than others. However, once nucleation has occurred there are many theories and techniques which allow the computation of the rate of growth and the shape of the resulting frazil particles. Numerous observations in both the field and the laboratory have confirmed the predictions of theory. Knowledge of the growth characteristics and the shapes of the frazil particles is important because the ultimate shape and growth of the ice particles effects the amount of ice produced at any typical supercooled temperature. Improper assessment of the shape can lead to considerable error in estimating the number or size of the frazil particles.

In ice engineering it is very important to understand the nucleation process as it applies to natural streams. Similarly, it is also necessary to estimate the number, the rate of production, and the rate of growth of the frazil particles produced during the supercooling period. Although not always possible in natural streams, laboratory experiments can illustrate the relative importance of air temperature and turbulence on the nucleation temperature. With careful observations it is possible to infer how nucleation occurs in natural streams and by measuring the water temperature during the frazil generation period (supercooling period) and applying the better known fundamentals of crystal growth it is possible to understand or at least quantify the lesser known processes of nucleation and the rate of production of new nuclei. To this end, the experiments described in the following chapter were carried out.

3. EXPERIMENTAL PROCEDURE AND DATA SUMMARY

The observation and measurement of frazil production in natural streams is very difficult. Therefore, it must be recognized that to produce meaningful data, measurements in laboratory models, where there is good control of the important variables, provide a good alternative.

The use of a laboratory model requires that the natural situation be duplicated as closely as possible. A reasonable volume of water must be observed so that boundary effects can be neglected. The water body should have a depth/width ratio greater than unity, which is typical of a column of water extending from the bed to the surface of a turbulent stream; and the majority of the heat loss should be from the surface. Also, it is important to allow natural phenomena such as air flow, condensation, and air temperature gradients to exist at the water surface. Turbulence must be created in the water body, such that the vertical and lateral transport process of natural streams can be duplicated. Finally, the water quality should be maintained reasonably constant so that only the effects of heat loss rates and turbulence can be studied.

In this investigation frazil production was observed and the water temperatures measured in a relatively large insulated tank, filled with water, with only the water surface exposed to the air. Turbulence was generated by means of a paddle stirrer with inclined blades. The water was cooled by placing the tank in a large cold room and the cooling rates were altered by changing the air temperature in the cold room.

Experiments were carried out at various rates of cooling for different turbulence intensities. For each experiment, the water temperature at various depths was measured, the turbulence characterized, and a qualitative description of the ice formation processes made.

3.1 Experimental Apparatus

3.1.1 The Insulated Tank

All experiments were performed in an eight-sided plexiglass tank which had an inscribed diameter of 0.38 m and a height of 0.52 m. The tank was filled to within 0.05 m of the top, resulting in a water volume of 54 L. The water surface area was 0.12 m^2.

The sides of the tank were insulated by 0.010 m of plexiglass, 0.033 m of zonolite insulation, and 0.013 m of plywood. The insulating properties of these materials are tabulated in Table 3.1 and the rates of heat loss for various air temperatures are shown in Table 3.2. The rate of cooling for the water as a whole was determined from the measured water temperatures, while the relative contributions from the top and sides were computed using heat transfer theory. It is apparant that a majority of heat transfer is across the water surface. Heat transfer across

Table 3.1

Heat Transfer Characteristics of Tank Insulating Agents

Material	Thickness (m)	Area (m)	Thermal[3] Conductivity (W/m °C)
Side plexiglass	0.010	0.60	0.138
Side insulation[1]	0.033	0.60	0.062
Side plywood	0.013	0.60	0.138
Bottom plexiglass	0.015	0.12	0.195
Bottom insulation[2]	0.10	0.12	0.038
Bottom plywood	0.010	0.12	0.138

---

[1] zonolite (vermiculite)
[2] fibreglass
[3] data from "The Insulation Handbook"

Table 3.2

Heat Loss Rates from Tank

Temperature Difference (°C)	Heat Loss Rate (W)			
	Total[1]	Side[2]	Bottom[2]	Top[3]
15	67	13	0.6	55
20	82	17	0.8	64
30	112	26	1.2	85
35	128	30	1.4	97

---

[1] measured
[2] computed
[3] residual

the sides and bottom constitute about 20% of the total.

The paddles used to generate turbulence were located in the centre and at a distance of 0.11 m above the bottom of the tank. Swirl in the tank was prevented by a 0.05 m wide baffle located on one of the sides of the tank.

Temperature probes were positioned 0.10 m in from the side of tank and 90° away from the baffle. The five probes were located at depths of 0.35 m, 0.15 m, 0.02m, 0.015 m, and as near to the surface as possible (without causing exposure because of the surface turbulence). Temperature probes were also located above the water surface at heights of 0.065 cm, 0.015 cm, and again, as close to the water surface as possible.

In addition to the temperature probes, two conduction probes were placed on the side of the tank directly opposite the temperature probes. Their original intent was to measure the quantity of ice being produced on the basis of concentration changes. Unfortunately this proved fruitless and these probes were only used in an attempt to evaluate the turbulence.

Figure 3.1 shows the insulated tank in the Mechanical Engineering Cold Room at the University of Alberta. Figure 3.2 shows the top view of the insulated tank and Figure 3.3 shows a side view, which illustrates the arrangement of the various probes.

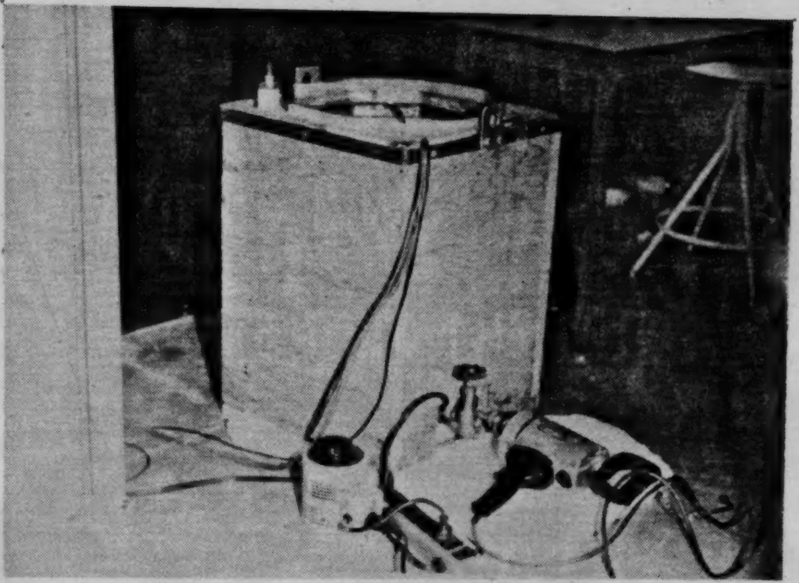

Figure 3.1 Insulated Tank in Cold Room

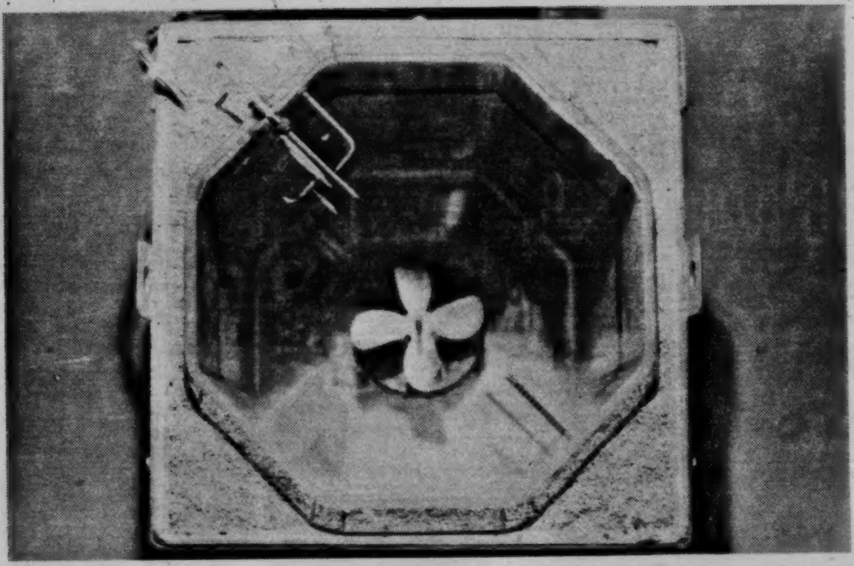

Figure 3.2 Top View of Insulated Tank

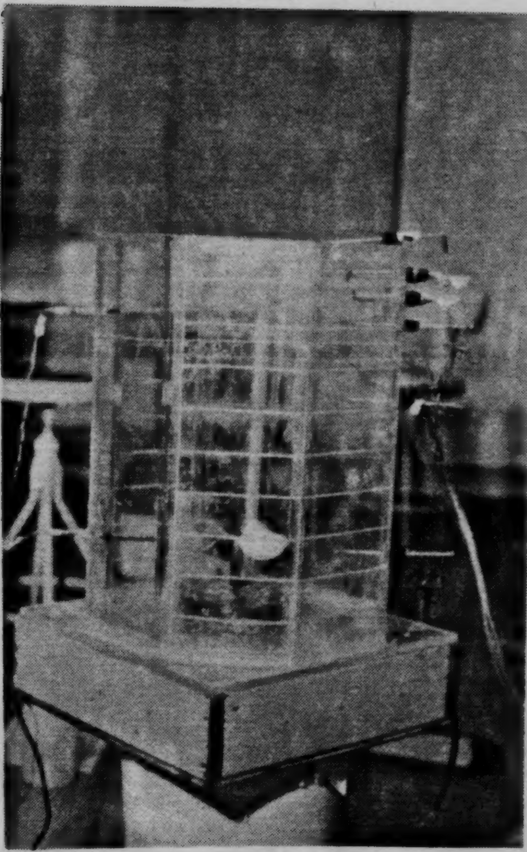

Figure 3.3 Side View of Tank Showing Location of Probes

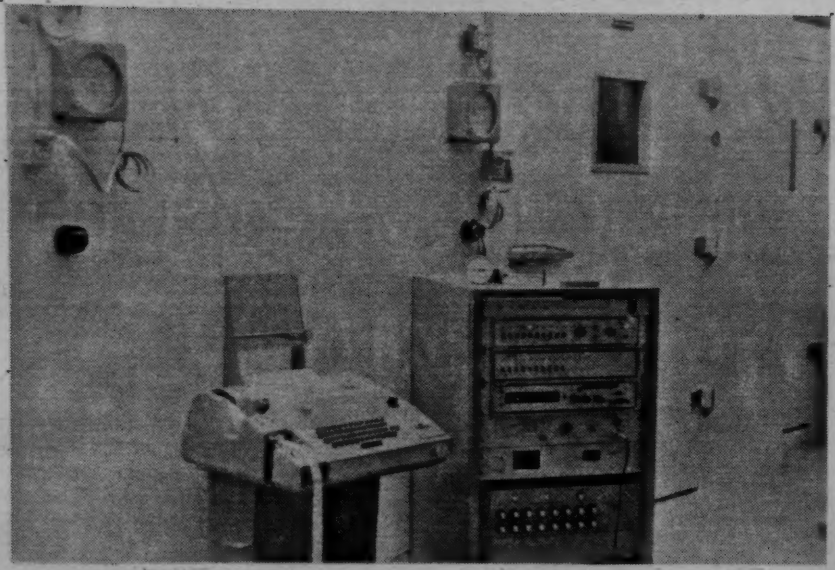

Figure 3.4 Data Aquisition System

3.1.2 Temperature Data Aquisition System

The data aquisition system for measuring the air and water temperatures is shown in Figure 3.4 and consisted of the following components:

1. glass thermister probes (code number GB 32P2),
2. VIDAR 500 ten channel scanner,
3. lapse timer and scan counter, and
4. Teletype Model ASR33 teleprinter.

The thermistors used to measure the water temperatures were calibrated in a glycol bath with an HP-2801A quartz thermometer for temperatures between -5°C and +5°C. A typical calibration curve is shown in Figure 3.5. It should be noted that the design of the Wheatstone bridge resulted in a minimum voltage differential of 0.001 volts which corresponds to a temperature resolution of 0.01°C.

The air temperature probes were calibrated over a temperature range between 0°C and -40°C in air, to an accuracy of 0.50°C.

The line chart for data handling is shown in Figure 3.6. The VIDAR 500 ten channel scanner was prompted by a lapse timer. At a specified interval the scanner would be activated and automatically sense the voltage drop across each of the thermistors. The scan counter set the number of readings to be integrated over a specified time length for each of the channels. This integrated signal was then routed to the digital voltmeter where it was converted to binary form. It should be noted that only a single scan was used in

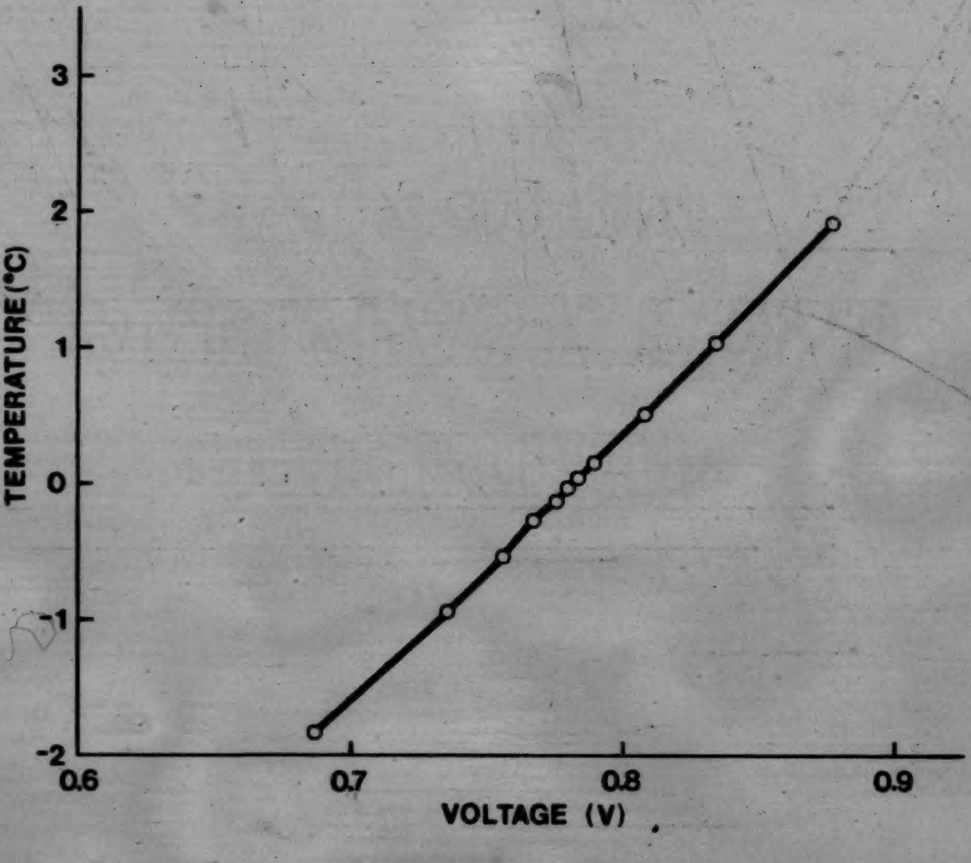

Figure 3.5 Typical Calibration Curve of the Temperature Probes

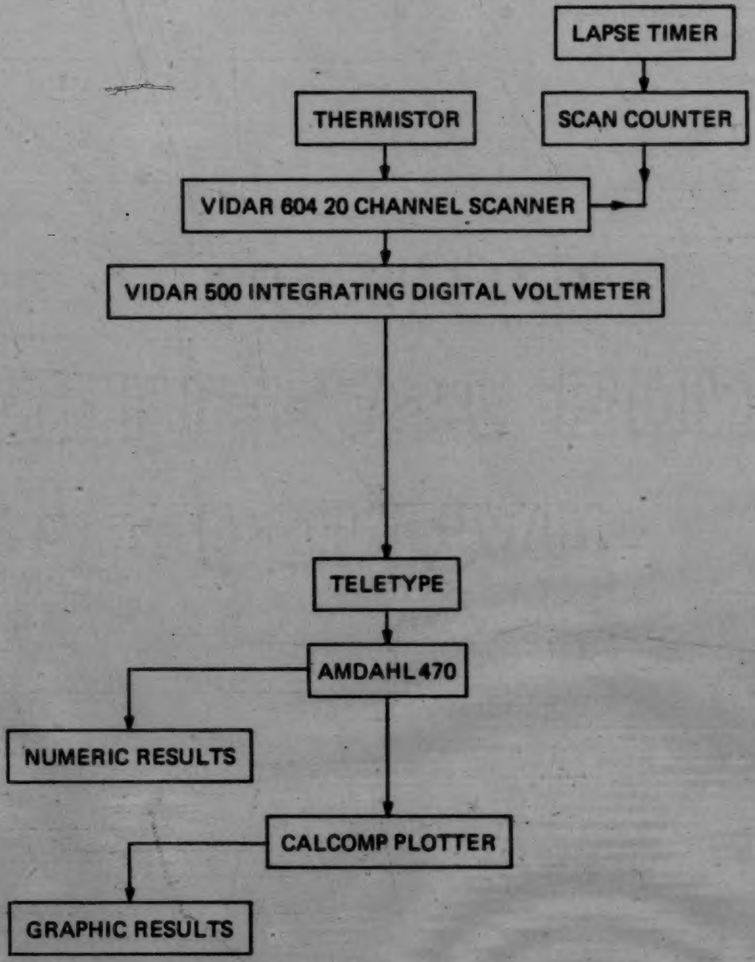
LAPSE TIMER
THERMISTOR
SCAN COUNTER
VIDAR 604 20 CHANNEL SCANNER
VIDAR 500 INTEGRATING DIGITAL VOLTMETER
TELETYPE
AMDAHL 470
NUMERIC RESULTS
CALCOMP PLOTTER
GRAPHIC RESULTS

Figure 3.6 Data Aquisition Process

the temperature measurements because in many instances the lapse time between readings was very short.

The output from the digital voltimeter was transmitted to the teleprinter which printed the data on paper tape. This tape was decoded by the AMDOL 470 computer, fed into a computer program written to fit a spline function (Peterson and Howell, 1972) to specified points on the calibration curve, and then the voltages were transformed into temperatures. Finally, the time vs. temperature curves were plotted by the Calcomp plotting routine.

3.1.3 The Generation and Measurement of Turbulence

Ideally, the best way to model the transport process in a stream is by generating turbulence in flow over a rough boundary in a flume. To produce frazil under these conditions, the flume must be constructed in a cold room. Such a system was not available at the time of the experimental investigation.

The approach used instead was to produce a pseudo-turbulence by the mixing of a stationary body of water. That is, although the turbulent flow field produced could not be readily characterized, all sizes of eddies were in existence. As in a natural stream, the large energy producing eddies, which can be scaled by the depth of flow, were evident and could be measured by the laser anemometer. However, the small energy dissipating eddies, which have the most effect on the transport of heat away from the frazil particle could not be identified because of the poor resolution of the laser system. Therefore, an explicit estimate of the effects of the turbulence generated in any particular experiment could not be made. It was felt that the effect of the flow field on a small particle would be similar to that of turbulence in a flowing stream but it becomes difficult to generalize the observations to rivers, where the turbulence is generated by shear flow. However, the technique is sufficient to judge the influence of turbulence on nucleation and crystal growth in a very general way.

The effects of turbulence were established by agitating the water body with a 0.15 m diameter, four blade, aluminum paddle. Each blade of the paddle was approximately rectangular in shape, was inclined at an angle of 30° to the plane of its rotation, and had a surface area of 0.0023 m^2 normal to its axis. The sum of the areas of all the blades was 50% of the total area swept out by the paddle.

The paddles were driven by an electric drill, the speed of which could be adjusted by a rheostat. The drill was connected to the paddle by a shaft running under and up through the bottom of the tank. Both the paddle and any portion of the steel shaft exposed to the water in the tank were coated with teflon to prevent frazil adhering to their surfaces.

The flow patterns produced in the tank were similar for all agitation speeds. A circular convection cell with an upflow in the centre above the paddle and a downflow along the sides of the tank was produced. The baffle prevented any noticeable swirl and the dispersion of injected dye showed that although the dye was initially convected within the cell, transport perpendicular to the direction of motion within the cells was great enough to produce complete mixing in a very short time.

The flow field and the mixing process in the tank were characterized by two parameters. The first, being the time required for the mixing of a tracer, was measured and correlated with the speed of the paddles. A highly conductive salt solution was injected on the water surface and the variation in voltage across the two concentration probes was recorded (Figure 3.7). The mixing time was taken as the length of time between the time of injection and the time when the difference in voltage between the probes was zero.

The vertical velocity component was measured by a laser anemometer. Measurements were made over a time period of 10 seconds at each of the temperature probe locations. A trace of the velocity fluctuations was recorded on a chart recorder (Figure 3.8), digitized, and the root mean square of the velocity fluctuations computed. A weighted average root mean square velocity was then determined on the basis of the volume that each measuring point typified.

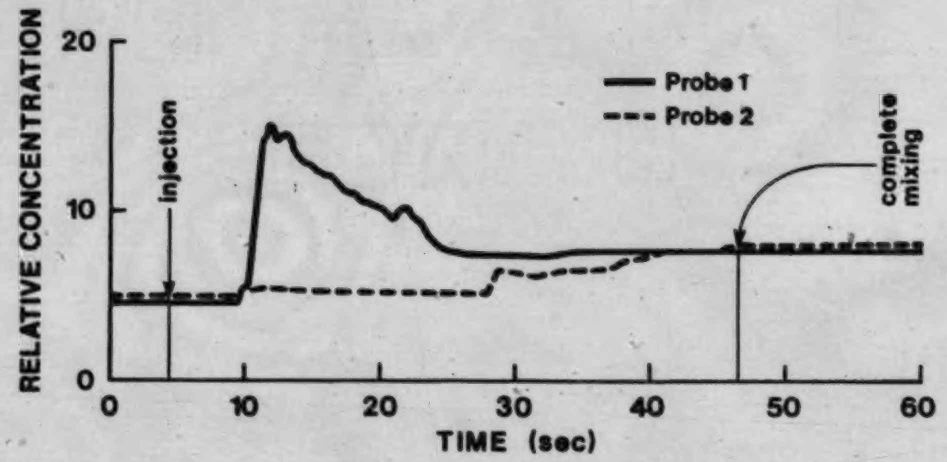

Figure 3.7 Typical Mixing Test Results

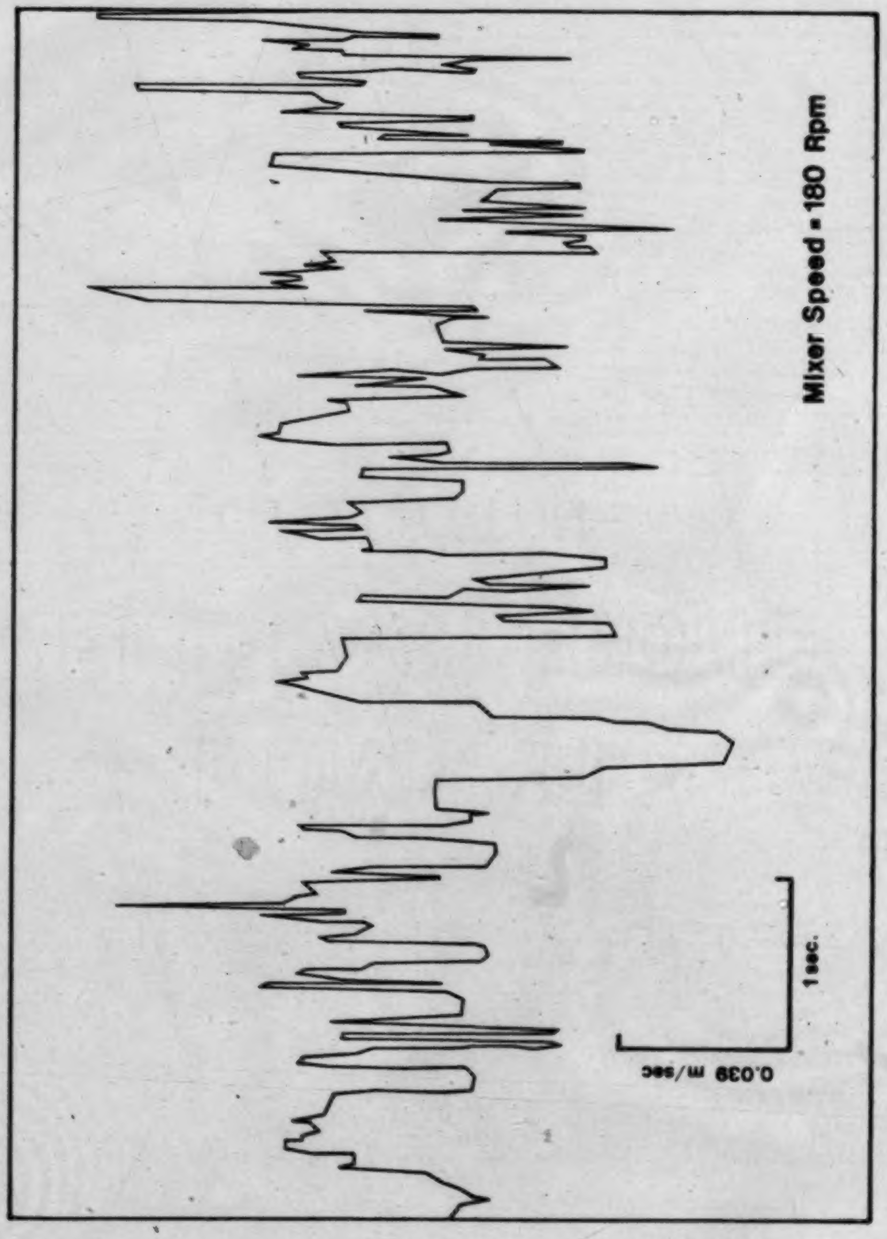

Figure 3.8 Typical Trace of Measured Velocity Fluctuations

3.2 Experimental Results

The experiments were carried out for ambient air temperatures ranging between -13°C and -36°C, and paddle speeds varying between 65 rpm and 210 rpm.

3.2.1 Turbulence Measurements

During each frazil-generation run the speed of the paddle, and hence the turbulence intensity, was kept constant. Although this turbulence can be quantified simply on the basis of the speed of the stirrer, physically more meaningful variables would be more useful. These variables were chosen to be the root-mean-square value of the velocity fluctuations, u', and the time required for complete mixing, t_m. These quantities are tabulated in Table 3.3 and illustrated in Figure 3.9.

The root-mean-square value of the velocity fluctuations varies almost linearly with the mixer speed, although u', the root-mean-square surface velocity fluctuation, tends to increase faster as the mixer speed increases. The mixing time, on the other hand, is reduced very rapidly as the mixer speed increases at speeds below 100 rev/min. However, at speeds in excess of 150 rev/min the variation in mixing time is not sensitive to change in the mixer speed.

Table 3.3

Summary of Turbulence Characteristics

Mixer Speed (rev/min)	tm (sec)	u' (m/sec)	u'_s (m/sec)
29	42.3	-	-
41	33.3	-	-
55	30.4	-	-
65	26.1	0.027	0.005
75	23.0	-	-
80	-	0.034	0.006
86	20.5	-	-
90	-	0.044	0.004
100	18.8	0.048	0.010
114	17.2	-	-
120	-	0.054	0.008
145	-	0.055	0.014
162	13.3	0.064	0.020
180	-	0.066	0.036
200	10.5	0.079	0.023
210	-	0.081	0.029
230	-	0.083	0.033
250	-	0.089	0.042

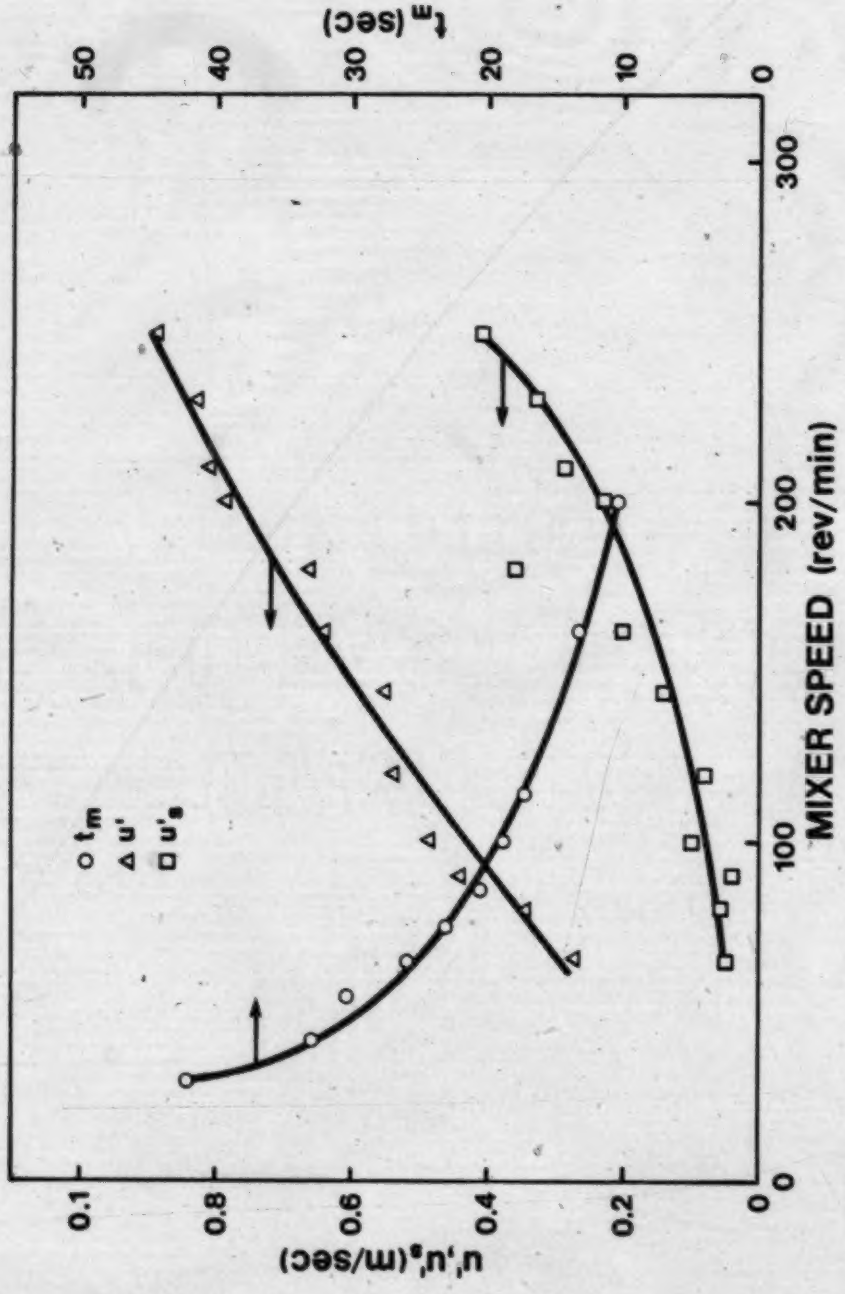

Figure 3.9 Turbulence Characteristics

3.2.2 Frazil Observations and Temperature Measurements

The observation and quantification of the frazil generation process was the major goal of the experiments. The principal method by which this was achieved was the simultaneous measurement of the water temperature at specified time intervals at each of the five probes located in the water. From this data, time-temperature plots were compiled. These graphs are shown in Appendix A. From these plots, it was possible to determine the time and temperature at which nucleation occurred, the time and temperature of maximum supercooling, and the time when the residual temperature was achieved. These characteristic times and temperatures completely define the supercooling curve. Although maximum supercooling has no particular significance in terms of general frazil production it does indicate the point at which latent heat produced by nucleation and crystal growth is equal to the heat loss across the boundaries of the water body. Also, it crudely differentiates between the times when heterogeneous and secondary nucleation predominate.

It should be noted that because the nucleation temperature was determined from the temperature plots, its existence was only apparant when the supercooling curve deviated from its normal downward trend. It is possible that the amount of supercooling required for nucleation was overestimated (nucleation temperature underestimated) because during the very early stages of nucleation there may have been insufficient latent heat produced to alter the supercooling curve.

In addition to the temperature measurements, various other observations were also made. The growth of the border ice was characterized for each experiment. The extent of the surface ice cover was described as being either complete, partial, or negligible prior of the onset of nucleation. Visual estimates of frazil production were categorized into three components. With respect to the location of the first obvious frazil particles, they were either labelled as originating at or near the surface or the particles existed throughout the bulk of the water body. The time and temperature of the first siting of frazil, was characterized as occurring either prior to, or at, maximum supercooling.

An estimate of the time and temperature at which no additional nucleation was occurring was also attempted. However because the small ice particles were in constant motion it was difficult to estimate exactly when nucleation ceased. In the experiments with low turbulence, the estimate was easier because as the new frazil particles became apparent they floated to the surface. Nevertheless an attempt was made to determine whether frazil production ceased prior to, at, or after the attainment of the residual supercooling.

Following the cessation of nucleation the buoyancy of the frazil was also documented. If the turbulence was of a relatively low intensity the frazil particles floated to the top and either created a surface cover or attached themselves to the existing ice cover. With higher turbulence the frazil particles remained in suspension.

The final parameters observed were the size and shape of the frazil particles. In all instances the frazil particles were discoidal in shape, with diameters between 1 and 2 mm. The thickness could not be determined, but it was estimated to be an order of magnitude smaller than the diameter. It should be noted that no direct measurement of the size or the concentration of the frazil particles was attempted. Firstly, the photographic means were not available, and secondly, mechanical measurement by removing the particles from their surroundings would have interfered with the process which was being observed.

The measured temperature curves for the experiments are given in Appendix A. Table 3.4 summarizes the qualitative observations for each of the experimental runs and Figure 3.10 illustrates three typical supercooling curves.

Figure 3.10a illustrates the relative ease in determining t_n, t_s, t_r, and H_o when the temperature curve is not being affected by the growth of a surface cover. The time of nucleation, t_n is chosen as the time when the temperature curve departs from its downward trend. The time of maximum supercooling is distinct, as is the time when the residual temperature is achieved and equilibrium conditions begin.

Table 3.4

Summary of Frazil Observations

Run Number	Surface Cover Growth	Initial Frazil Location	Appearance Temperature	Temperature at Cessation of Frazil Production	Frazil Deposition on Surface
11	negligible	-[1]	-	-	yes
12	moderate	-	-	-	no
13	complete	-	-	-	yes
14[2]	-	-	-	-	-
15	complete	widespread	Ts	Tr	yes
21	complete	widespread	Ts	Tr	yes
22	negligible	surface	<Ts	>Tr	no
23	negligible	-	-	Tr	yes
24	negligible	surface	Ts	Tr	yes
25	complete	-	-	-	yes
31[2]	-	-	-	-	-
32	complete	widespread	Ts	>Tr	yes
33	moderate	surface	Ts	>Tr	yes
34	negligible	widespread	Ts	>Tr	no
35	negligible	-	Ts	>Tr	no
41	complete	widespread	Ts	Tr	yes
42	complete	widespread	Ts	>Tr	yes
43	moderate	widespread	Ts	Tr	yes
44	negligible	-	<Ts	>Tr	no
45	negligible	surface	<Ts	>Tr	no
50	complete	widespread	<Ts	>Tr	yes
51	negligible	surface	Ts	>Tr	no
52	complete	widespread	<Ts	>Tr	yes
53	negligible	surface	Ts	>Tr	no

[1] indicates no observation
[2] experiment unsuccessful

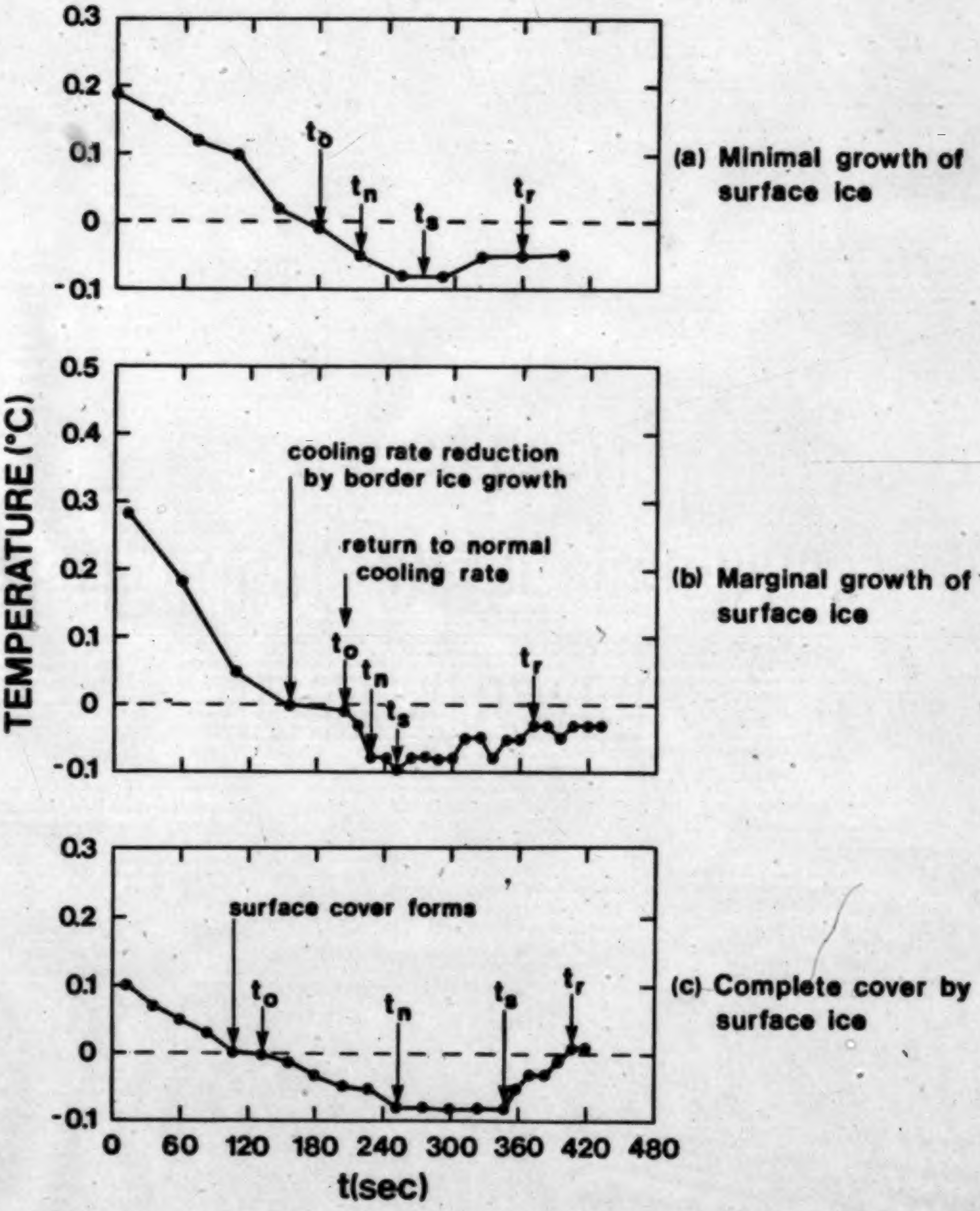

Figure 3.10 Typical Supercooling Curves

Figure 3.10b illustrates the effects of the growth of border ice on the temperature variation. When the water temperature reaches 0°C, border ice growth begins to occur and there is a lag time during which the temperature remains constant at 0°C until the border ice growth is stopped by the turbulence. The temperature trend then continues and the relevant characteristic times and temperatures can be determined.

Figure 3.10c shows a typical case where a surface cover forms prior to nucleation. In this instance there is a reduction in the rate of heat loss due to this cover and some subjectivity is introduced in determining the net heat loss available for frazil production. Generally, however, the reduced heat loss rate can be determined with little difficulty. It should be noted that when a surface cover exists the supercooling curves tend to exhibit much less distinct characteristic times and temperatures. For example, in Figure 3.10c, the nucleation temperature is near the maximum supercooling temperature and there is a considerable length of time during which the maximum supercooling is maintained. In these instances the time of maximum supercooling was chosen as the time when the temperature began its upward trend.

A summary of the relevant data is tabulated in Table 3.5. It should be noted that the rate of heat loss (characterized by the change in water temperature with time) was computed at water temperatures of 1°C when no surface

Table 3.5

Summary of the Characteristics of the Supercooling Experiments

RUN	U' (m/sec)	U's (m/sec)	Ta (°C)	$(dT/dt \times 10^{4})$ (°C/sec) 1°C	0°C	tn (sec)	Tn (°C)	ts (sec)	Ts (°C)	tr (sec)	Tr (°C)
11	0.050	0.008	-13	2.6	2.6	192	0.05	624	0.10	1416	0.02
12	0.058	0.011	-14	2.5	2.3	384	0.09	510	0.11	924	0.03
13	0.42	0.006	-13	3.0	0.71	1095	0.07	1905	0.08	2580	0.03
14'	-	-	-	-	-	-	-	-	-	-	-
15	0.027	0.004	-13	2.5	0.52	1890′	0.10	3315	0.11	3480	0.01
21	0.050	0.008	-19	3.3	1.5	360′	0.06	960	0.06	1110	0.01
22	0.077	0.024	-19	3.5	3.5	252	0.08	420	0.11	828	0.02
23	0.064	0.014	-19	3.3	3.4	302	0.08	372	0.10	624	0.03
24	0.056	0.010	-19	3.7	3.4	248	0.07	382	0.09	683	0.03
25	0.041	0.006	-18	3.3	1.3	510	0.07	1680	0.07	2070	0.01
31'	-	-	-	-	-	-	-	-	-	-	-
32	0.044	0.007	-24	4.5	1.3	420	0.05	1020	0.05	1335	0.02
33	0.058	0.011	-26	4.5	3.9	270	0.07	360	0.10	792	0.03
34	0.070	0.019	-24	4.3	4.4	180	0.08	294	0.09	564	0.03
35	0.077	0.024	-24	4.5	4.4	156	0.06	312	0.09	660	0.02
41	0.036	0.005	-29	5.2	1.2	735	0.09	1275	0.13	2250	0.03
42	0.041	0.007	-28	4.4	1.3	765	0.10	1290	0.12	1815	0.04
43	0.057	0.010	-28	5.0	2.7	144	0.04	432	0.08	936	0.02
44	0.070	0.019	-29	5.5	4.8	84	0.03	516	0.08	984	0.03
45	0.080	0.028	-28	5.2	4.6	192	0.08	204	0.09	408	0.03
50	0.052	0.008	-32	4.8	4.3	420	0.05	1660	0.08	2035	0.04
51	0.077	0.024	-32	5.7	5.6	36	0.01	228	0.06	792	0.02
52	0.049	0.008	-36	5.2	2.6	105	0.03	360	0.07	840	0.01
53	0.077	0.024	-36	7.0	5.2	36	0.02	324	0.05	564	0.01

' data recording system failed

′ ice cover broken to initiate nucleation ice was evident and at 0°C when there was a possibility of surface ice growth. The difference in the two illustrates the magnitude of surface ice growth.

4. ANALYSIS AND DISCUSSION OF EXPERIMENTAL RESULTS

Information on the formation of a surface ice cover, the process by which nucleation is initiated, the growth of the frazil particles, and secondary nucleation can be drawn from the experimental results detailed in Chapter 3. Although the development of a surface ice cover could be observed and the growth of frazil particles documented visually, the time and temperature at the beginning of nucleation had to be inferred from interpretation of the supercooling curves. The process of secondary nucleation could not be identified because of the microscopic nature of the phenomenon.

However, the overall nucleation process can be examined by dividing the total measured volume of ice produced into either ice produced by the growth of the existing particles or by the nucleation of new ice particles. The investigations described in Chapter 2 have determined the rates of ice crystal growth in supercooled water. This information, coupled with the rate of ice production which can be determined from the supercooling curves, allows the evaluation of the rate of change in the number of new ice particles. This nucleation rate, for various segments of the supercooling curve, is related to the two fundamental independent variables - air temperature and turbulence intensity.

4.1 Nucleation Temperatures

Fletcher (1972) and others have indicated that heterogeneous nucleation is the process by which water normally freezes and that the supercooling required for this nucleation can be computed from equations 2.3, 2.4, 2.5, and 2.14. When combined, these equations yield an expression for the supercooling required for nucleation. That is

$$\Delta T^2/f(m,x) = 2126 \tag{4.1}$$

if it is assumed that σ_{sl} has a value of 40 mJ/m² and the critical radius of a nucleated ice particle is of the same order of magnitude as the radius of nucleating particle. The function f(m,x) designates the compatibility of the nucleating particle and normally has a value between 0 and 2.0. If the size and the molecular characteristics of the nucleating particle is known the nucleation temperature can be calculated. Unfortunately, in most situations the characteristics of the nucleating particles are unknown. They cannot be isolated because of "pollution" from numerous environmental factors. For example, under controlled conditions where air was not allowed to touch the water sample, Gilpin (1978) found that the nucleation temperature of tap water was in the range of -4 to -6°C, whereas in the present experiments the nucleation temperature for similar water was never lower than -0.12°C.

If the measured nucleation temperatures in Table 3.5 are used to compute values of f(m,x), they are in the order of 10^{-6} (Figure 4.1). This indicates that both m and x have

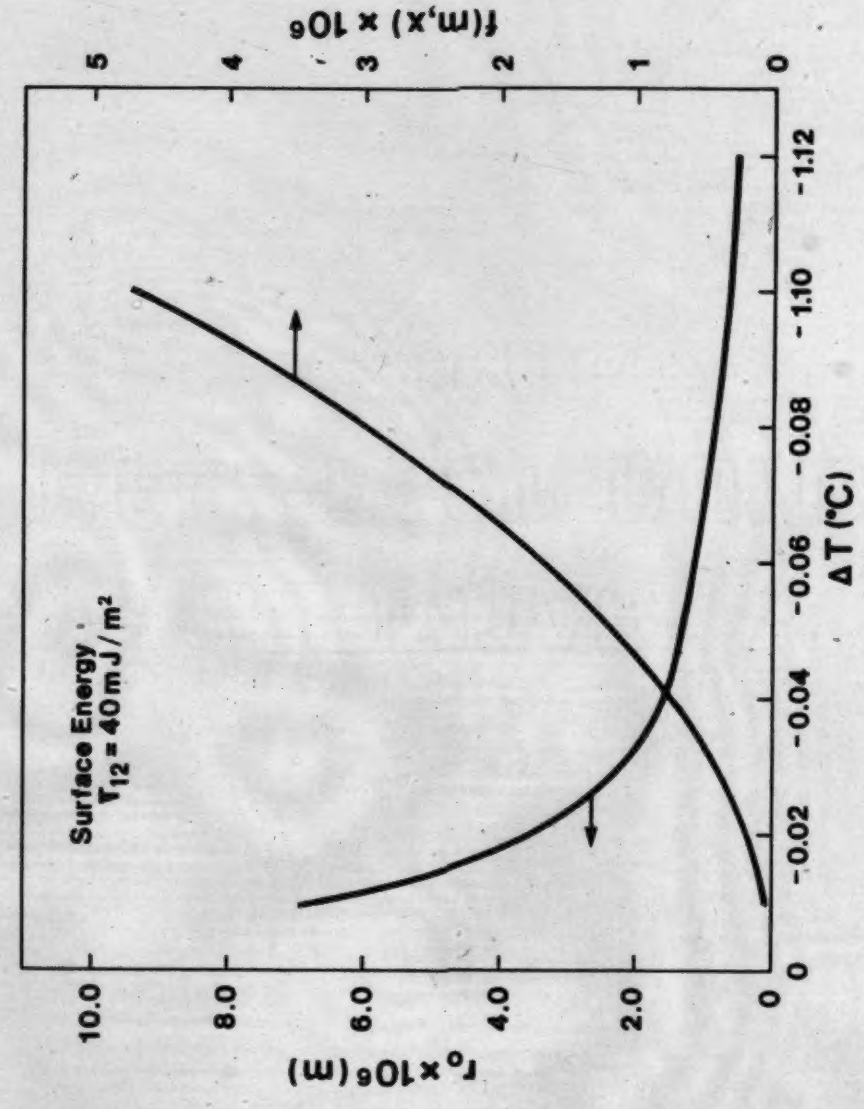

Figure 4.1 Nucleation Characteristics for the Observed Nucleation Temperatures

values near unity and indeed the nucleating particles should consist of ice crystals with characteristic diameters of the same order as the diameters of newly formed ice particles. For comparison, f(m,x) of the suspended nucleation particles active in Gilpin's experiments was about 0.011.

Equation 2.3, 2.4, 2.5 and 2.14 can also be used to compute the radius of the newly formed ice particles. For the nucleation temperatures observed, this radius must vary between 0.5 and 7.0×10^{-3} mm (Figure 4.1), decreasing as the supercooling at nucleation increases. Obviously such ice particles would not be discernable to the naked eye at the time of nucleation.

As discussed in Section 2.3.3, the origin of the active nucleating particles is open to speculation. Michel suggests that a thin layer of highly supercooled water exists on the surface and heterogeneous nucleation occurs at that location. The newly formed ice particles are then mixed into the bulk of the water by turbulence to then trigger widespread nucleation. Attempts were made to measure the water surface temperature but the size of the probe prevented a proper reading. Nevertheless, in all experiments, regardless of the air temperature or the turbulence intensity, no temperature gradient was ever recorded. Yet, visual observations indicated that small ice particles were always visible on the surface prior to nucleation in the bulk of water, so that nucleation did indeed occur first on the surface.

However, such an observation is also consistent with the sequence of events suggested by Osterkamp and others: the nucleating particles are produced by the condensation and freezing of water vapour above the air-water interface and are subsequently deposited on the water surface. It is very likely that the deposition of these ice particles causes the surface nucleation described by Michel.

Therefore nucleation occurs first at the surface and this occurrence strongly depends on the air temperature. For both the processes identified by Michel and Osterkamp, a certain turbulence intensity is also required to transport the effects of this process below the water surface to initiate nucleation in the bulk of the water. Therefore, the two fundamental variables affecting the nucleation temperature would be the air temperature and the turbulence intensity. The air temperature dictates the rate of production of ice particles (above or on the water surface) and turbulence effects the rate of transport of these ice particles from the air-water interface.

The variation of these two parameters, relative to each other, not only determines the nucleation temperature, but also the development of a surface ice cover. In general terms, if the air temperature is low, numerous large ice particles would be either deposited or grown on the surface. If the turbulence intensity is low, a majority of these particles would not be entrained. Instead, they would be integrated into a stable, solid, surface cover. The availability of nucleating particles within the bulk of the water would then be reduced and a lower nucleation temperature required.

On the other hand, if the turbulence intensity is high, the transport of the ice particles formed or deposited on the surface occurs easily, precluding a stable surface cover and providing a surfeit of nucleating particles which will lower the supercooling necessary for nucleation.

If the air temperature is high, but below freezing, the number and size of the ice particles growing or deposited on the surface is small. The surface cover takes longer to form if the turbulence intensity is low. Even if the turbulence intensity is high, there is a lack of nucleating particles, cooling occurs for a longer period of time, and hence more supercooling at nucleation results.

The measured effects of air temperature, T_a, and the turbulence intensity near the surface, u'_s, on the development of a surface ice cover are illustrated in Figure 4.2. The line shown approximately distinguishes between the zone where a solid surface cover can form and cannot form. At air temperatures of -10 to -20°C, u'_s must be about 0.008 m/sec to prevent a surface cover from forming. At air temperatures of -30°C the required values of u'_s is increased to about 0.02 m/sec.

The variation of the nucleation temperature with air temperature and turbulence intensity is shown in Figure 4.3. The data shows considerable scatter. Because of the

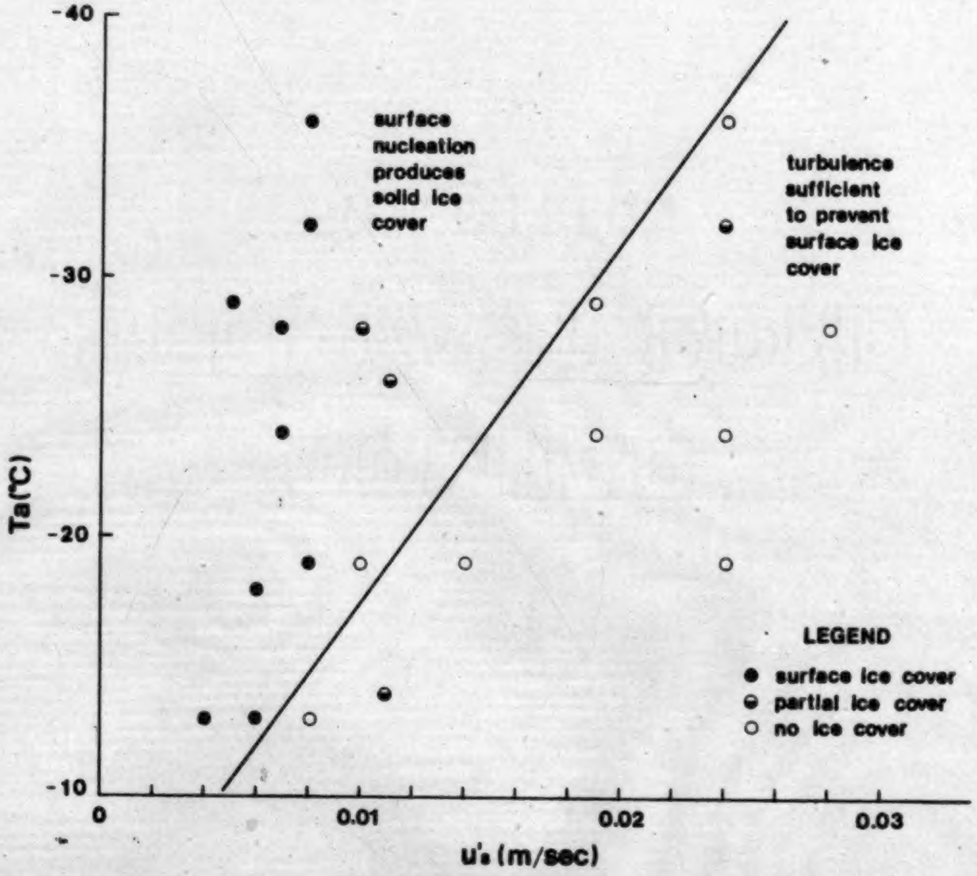

Figure 4.2 Effects of Turbulence and Air Temperature on the Formation of a Surface Ice Cover

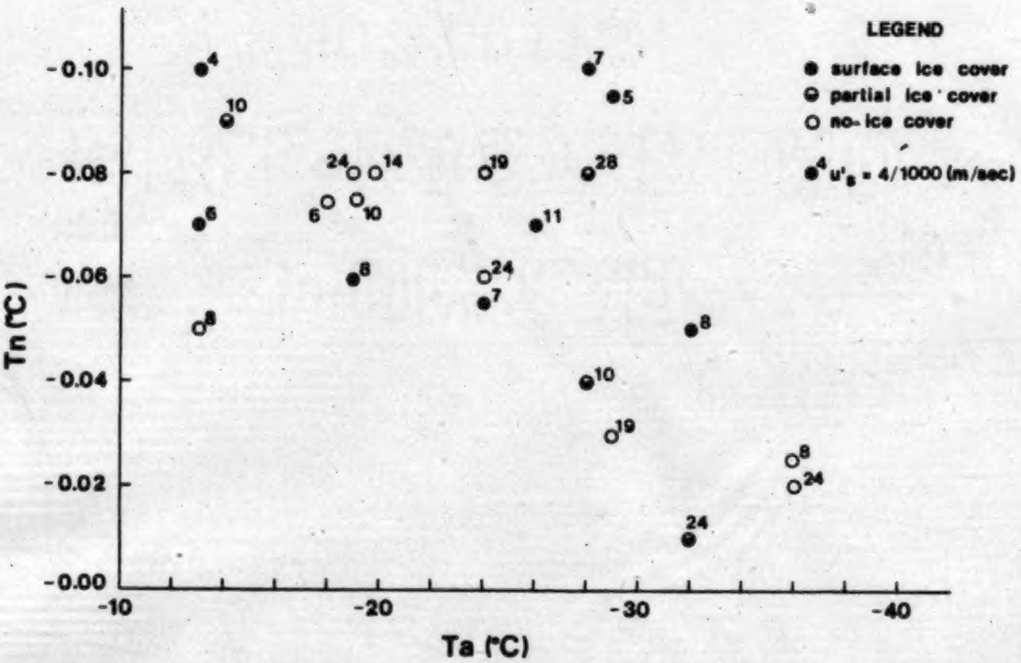

Figure 4.3 Effects of Turbulence and Air Temperature on the Nucleation Temperature

randomness of the size distribution of the nucleating particles and of the nucleation process itself, this is not unexpected. However, there is a trend which indicates that the supercooling required for nucleation is reduced with a reduction in air temperature. An influence of the surface turbulence intensity is more difficult to perceive but there is some indication that as the turbulence increases, the supercooling required for nucleation is reduced. If a surface cover is evident prior to nucleation, the supercooling required for nucleation is also greater, although there is considerable variation.

The maximum supercooling is related to the nucleation temperature. If the turbulence intensity is large the increased growth rate of an increased number of frazil particles should decrease the maximum supercooling. This is somewhat born out in Table 3.5 and appears to contradict Carstens' (1966) suggestion that the larger the cooling rate the greater the maximum supercooling.

The data shown in Figures 4.2 and 4.3 therefore provide some support for the postulate of deposition of ice particles from the air above the water surface, although it by no means discounts heterogeneous nucleation occurring within a strongly supercooled surface layer. However, in Muller's (1978) experiments in which a strongly supercooled layer existed on boundaries other than at the surface, the required supercooling for nucleation was considerably greater than measured in this study. This suggests that the deposition of small ice particles on the surface is the primary process responsible for the higher nucleation temperatures. There is no doubt, though, that additional supercooling does exist near the surface and nucleation is initiated earlier in this region after the deposition of ice crystals produced above the air-water interface. Turbulence then transports these nuclei below the surface and nucleation occurs throughout the whole water body.

One particularly unique situation was produced in experiments 15 and 21. The turbulence intensity was low and a surface cover formed following supercooling in the bulk of the water. This supercooling continued to exist even as the surface cover thickened by heat loss through the surface ice and through the sides. After 10 to 20 minutes (600 to 1200 seconds), during which the water temperature remained constant and no ice particles were visible, the ice cover was mechanically broken. Immediately, ice crystals of sufficient size to be visible (1 to 2 mm in diameter) appeared and the temperature returned to near the melting point of ice. The ice particles formed throughout the bulk of the water in a very short time - somewhat less than 30 seconds - compared to the growth time in the other experiments. These particles were discoidal in shape and appeared in concentrations of about 1 to 10 particles/cm^3. It should be noted that similar observations in natural streams have been reported.

The interesting point about this phenomena is that upon sudden disturbance, ice particles many times larger than the expected nucleation size were produced. In addition, the time between the inferred nucleation time based on the behavior and shape of the supercooling curve (see Section 3.2.2) and the disturbance was sufficient to produce ice particles of the size observed if typical growth rates were applied. Yet, their growth was not visible until the ice cover was broken. It is difficult to speculate what might have occurred had the ice cover not been disturbed.

It would seem that this sequence of events can only be explained if, following nucleation, the newly formed ice nuclei exist in some meta-stable, ice-like form without exhibiting any surface characteristics which are visible to the naked eye. Then, when disturbed, these nuclei alter their surface characteristics such that they become visible.

4.2 Volumes and Rates of Frazil Production

The rate of frazil mass production is given by equation 1.1 (Carstens, 1966). This equation relates the amount of ice generated to the release of latent heat of fusion as indicated by changes in the water temperature and to the heat loss across the boundaries of the water mass. If this equation is integrated with respect to time between t_o and t, the mass of ice produced before time, t, is given by:

$$M_i = (H_o t + T(t)\ C_p \rho_w)/L \qquad (4.2)$$

for a unit volume of water subjected to a heat loss of H_o, where

$$H_o = (dT/dt)_o \; C_p \; \rho_w \tag{4.3}$$

In the present experiments $(dT/dt)_o$ was determined from the net change in temperature near 0°C that was available for frazil generation after an allowance was made for the heat released by the growth of border or surface ice. This temperature change was a constant during each experiment.

From equations 4.2 and 4.3, using the appropriate numerical values of C_p, ρ_w, ρ_i, and L (section 2.2.2), the frazil volume generated per unit volume of water is given by

$$V = 0.01389 \; [T - (dT/dt)_o \; t] \tag{4.4}$$

where t is measured in seconds from the time the supercooling curve crosses the melting temperature, T is the water temperature (negative) in °C and $(dT/dt)_o < 0$. From the measured temperature curves the volume of ice produced at any given time can be determined. As a first approximation, and to simplify the analysis, the changes in temperature were represented by straight line approximations between the characteristic times t_o, t_n, t_s, t_r, and t_r+t.

Table 4.1 summarizes the computed volume of frazil produced at times t_s and t_r. It also shows the rate of frazil generation $\dot{V}_{ns}$, $\dot{V}_{sr}$, $\dot{V}_{nr}$, and H_o (the rate of heat loss written in terms of equivalent volume of ice produced) for the time periods t_s-t_n, t_r-t_s, t_r-t_n, and following t_r, respectively. In all experiments, regardless of the nucleating temperature and the turbulence intensity, the

Table 4.1

Computed Volumes and Rates of Frazil Generation

Run No.	V_s mm³/cm²	$\dot{V}_{ns} \times 10^{+3}$ (mm³/cm²•sec)	V_r mm³/cm²	$\dot{V}_{nr} \times 10^{+3}$ (mm³/cm²•sec)	$\dot{V}_{sr} \times 10^{+3}$ (mm³/cm²•sec)	$H_o \times 10^{+3}$ (mm³/cm²•sec)
11	0.87	2.01	4.83	3.95	5.00	3.61
12	0.10	0.79	2.54	4.70	5.89	3.20
13	0.77	0.95	2.13	1.43	2.05	0.98
15	0.87	0.61	2.37	1.49	9.09	0.72
21	1.16	1.93	2.17	2.89	6.73	2.08
22	0.51	3.03	3.74	6.49	7.92	4.86
23	0.37	5.28	2.53	7.86	8.57	4.72
24	0.55	4.10	2.81	6.46	8.37	4.72
25	2.06	1.76	3.60	2.31	3.95	1.81
32	1.14	1.90	2.13	2.33	3.14	1.81
33	0.56	6.22	4.01	7.68	7.99	5.42
34	0.55	4.82	3.03	7.89	9.19	6.11
35	0.66	4.23	3.76	7.46	10.2	6.11
41	0.32	0.59	3.33	2.20	3.09	1.67
42	0.66	1.26	3.65	3.48	5.70	1.81
43	0.51	1.77	3.23	4.08	5.40	3.75
44	2.33	5.39	6.14	6.82	8.14	6.67
45	0.05	4.17	2.19	10.1	10.5	6.39
50	1.89	1.52	3.09	1.93	3.33	1.81
51	0.94	4.90	5.88	7.78	8.76	7.78
52	0.33	1.29	2.90	3.95	5.35	3.61
53	1.65	5.73	3.93	7.44	9.50	7.22

maximum rate of ice production occurred following maximum supercooling and the frazil production rate following residual supercooling was always greater than the production rate prior to maximum supercooling.

Some general characteristics of the frazil production process are illustrated in Figures 4.4 and 4.5. In Figure 4.4 the ratio of the rate of ice production prior to residual supercooling to that following residual supercooling is plotted against the nucleation temperature for various turbulence intensities. From equation 4.2, the ratio of the ice production rates at any time to the rate following residual supercooling must have a lower bound of 1.0 and should increase as the nucleation temperature decreases. The data in Figure 4.4 conform with this and it is evident that at relatively high nucleation temperatures (low supercooling) the average rate of ice production during the supercooling period is not much larger than if only residual supercooling was evident during the entire process. Not until the nucleation temperature is reduced to below -0.05°C is there an accelerated ice production rate prior to residual supercooling. This increased production rate is primarily a function of the nucleation temperature because no stratification of the data on the basis of turbulence is apparent. At lower nucleation temperatures (-0.10°C) the average production rate in the supercooling period is twice the production rate following residual supercooling.

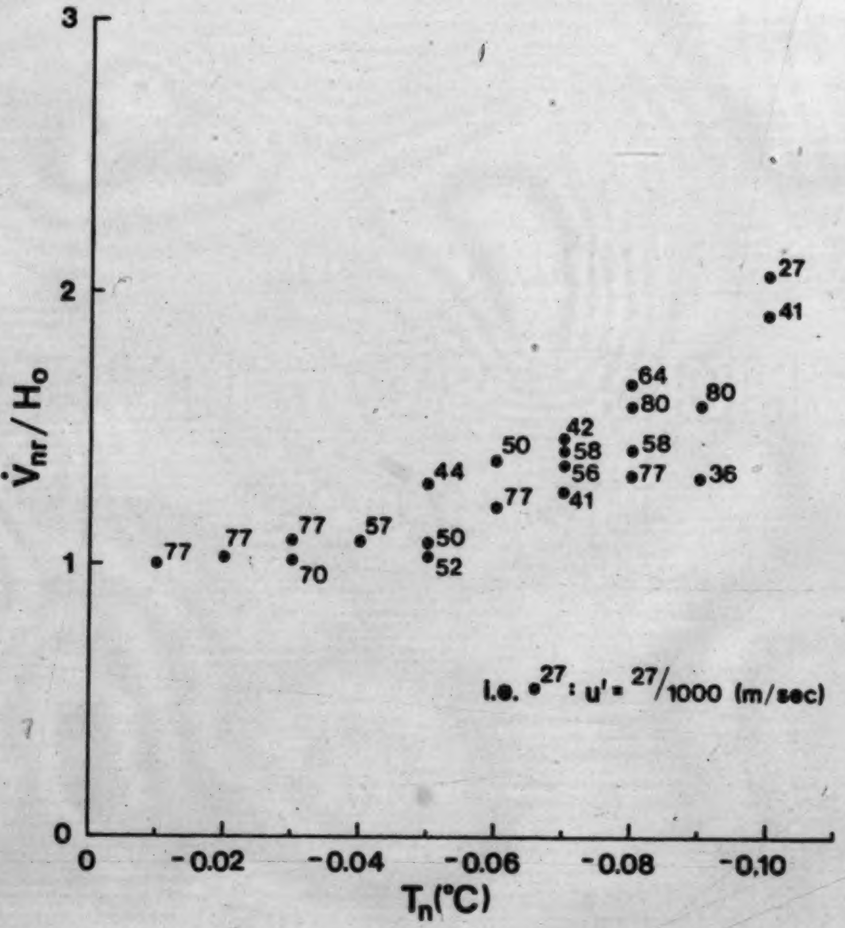

Figure 4.4 Ratio of Mean Rate of Frazil Generation During the Supercooling Period to that Following Residual Supercooling as a Function of the Supercooling of Nucleation

However, from Figure 4.3, it appears that the turbulence intensity has an effect on the nucleation temperature for any particular air temperature. This mechanism is explained in Section 4.1. If the turbulence intensity for any particular air temperature is large less supercooling is required to cause nucleation. From Figure 4.4, this higher nucleation temperature then results in a lower rate of frazil production during the supercooling period. This suggests that there is some optimum turbulence intensity which is high enough that a stable surface ice cover does not form and yet low enough to allow a considerable amount of supercooling to occur before nucleation is initiated.

It should be noted that the maximum rate of ice production during the supercooling period was only twice that expected following residual supercooling. Considering the fact that the period of equilibrium following supercooling can be in the order of days, while the duration of supercooling is only a matter of minutes, the actual contribution of the supercooling period to the total volume of ice generated during freeze up is very small. The supercooling period is important, however, because it is the process by which nucleation occurs and hence the heat loss from the water boundaries can be utilized to form ice.

Undoubtedly, the major influence on the production rate of frazil during the supercooling period is the water temperature. The greater the supercooling, the greater the growth rate of ice particles, although the production of additional particles by nucleation cannot be discounted. However, the general approach, as exemplified by the preceding analysis, cannot separate the effects of additional nucleation following the time of first nucleation.

Figure 4.5 illustrates the effects of turbulence intensity on the rates of frazil production during various phases of supercooling. It appears that the ratio of ice production following maximum supercooling (when the production rate is greatest) to that following residual supercooling varies between 1.2 and 3.2 and is seemingly independent of the turbulence intensity. Because the rate of ice production is a function of the size and growth rate of the frazil particle, it appears that the greater supercooling during the time period $t_r - t_s$ more than compensates for what could be an increased rate of ice production following residual supercooling when the size of the ice particle is larger.

There is considerably more variation in the ratio of frazil production rates between the time periods following maximum supercooling and prior to maximum supercooling. At high turbulence intensities the ratio is about 2.0 (Figure 4.5) but as the rms value of the turbulence is reduced below

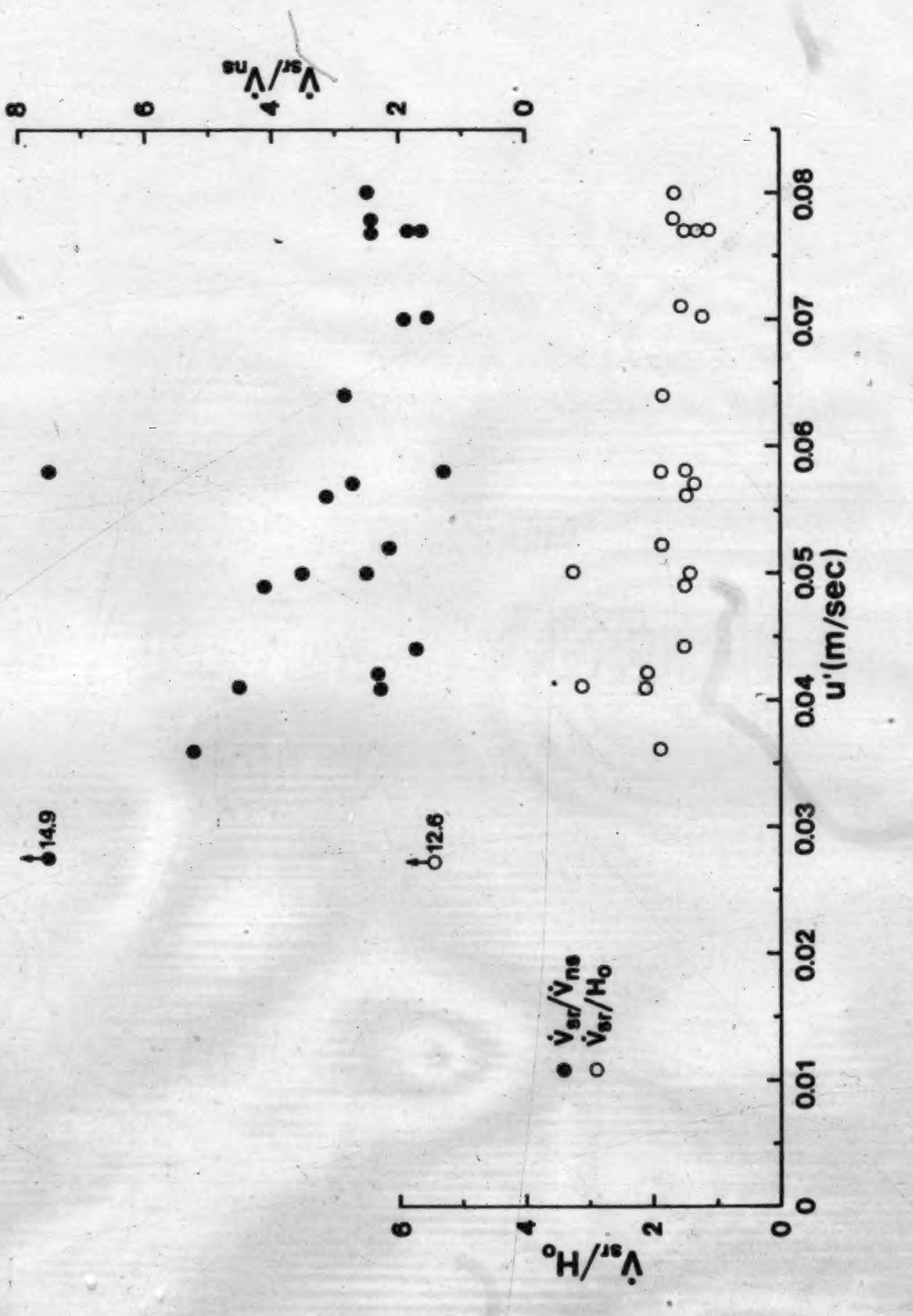

Figure 4.5 Ratio of Frazil Generation Rates During Various Supercooling Periods as a Function of Turbulence Intensity

0.05 m/sec, the ratio tends to increase. This suggests that turbulence has an influence on the growth rates. One explanation of this may be that when the frazil particles are small (prior to maximum supercooling) they are insensitive to all turbulence, regardless of its intensity. However, when the particles grow in size following maximum supercooling, low intensity turbulence may be small enough to exhibit a shearing action on the particle and increase the rate of heat transport from the particle surface. High intensity turbulence, on the other hand, has such a large time scale that even the larger particle is carried with the turbulent fluctuations and the rate of heat loss is less than for the low intensity turbulence. Unfortunately, the very small scales of the turbulence could not be measured to quantitatively evaluate the heat transfer process.

The above analysis offers some appreciation of the general features of ice production during the period of supercooling. Additional information can be deduced by determining the variation in the number of particles, their size, and the rate of growth of these particles. This is done in the following section, where an energy budget, coupled with measured particle growth rates and the measured supercooling curves, is used to compute the production rate of frazil particles.

4.3 Nucleation and Growth of Frazil Particles

The production of frazil has two components: generation of new nuclei by heterogeneous or secondary nucleation and the subsequent growth of these nuclei. Both processes must be reflected in the supercooling curve. The mass balance equation, written in terms describing these processes, is as follows:

$$4/3\pi r_o^3(dN/dt) + N\, d(Cr^3)/dt = dV/dt \qquad (4.5)$$

where N is the number of particles, r the radius of each particle at time t, r_o is the critical radius of the newly nucleated particle given in Figure 4.1, V the volume of ice produced at time t, and C a constant which relates the volume of each particle to its characteristic radius.

The first term of equation 4.5 expresses the volume of ice being produced by nucleation; the second term expresses the rate of ice production by crystal growth; and the third term is the change in the total volume of ice, which can be computed by equation 1.1. It should be noted that the constant C is a function of the geometry of the frazil particles. Whereas the nucleation theories generally assume that the newly formed ice embryos are spherical, there is no doubt that these spheres grow into discs. These discs have a thickness which varies between 1.5% and 10% of their diameters (Table 2.6). Assuming that the ratio of the thickness to the radius has an average value of 5%, the value of C is 0.16. In comparison to spherical frazil particles, where C would have a value of 4.18, it is evident that the assumed particle shape can have a large influence on the estimated volume of ice produced by crystal growth.

From the literature and the present experiments it can be estimated that $r_o \simeq 10^{-3}$, $dN/dt \simeq 10^{-2}$ and $N \simeq 10^{0}$, $d(Cr^3)dt \simeq 10^{-1}$, and $dV/dt \simeq 10^{-1}$. This suggests that the first term contributes very little to the solution and can be neglected if the time over which the process is being observed is greater than 10 sec. Therefore, because

$$d(Cr^3)/dt = 3Cr^2 \, dr/dt$$

and from equation 2.18

$$dr/dt = B \, T^{3/2}$$

from which

$$r = B \int_0^t T^{3/2} \, dt \qquad (4.6)$$

equation 4.5 can be written as

$$N = [dV/dt]/3C\left(\int_0^t T^{3/2} dt\right)^2 B^3 \, T^{3/2} \qquad (4.7)$$

Evaluating numerically, equation 4.6 can be rewritten as

$$r_{i+1} = r_i + B[(T_{i+1}+T_i)/2]^{3/2} \, (t_{i+1}-t_i) \qquad (4.8)$$

and equation 4.7 can be rewritten as

$$N_{i+1} = -N_i + [8(V_{i+1}-V_i)/3C \, f(i)] \qquad (4.9)$$

where

$$f(i) = \{2r_i + B[(T_{i+1}-T_i)/2]^{3/2} \, (t_{i+1}-t_i)\}^2 \, [B(T_{i+} +T_i)/2]^{3/2} \cdot (t_{i+1}-t_i)$$

and where the subscript, i, indicates the start of a given period of time which ends at i+1.

It should be noted that equations 4.6 and 4.8 are based on Kallungal (1975) who suggested that the growth rate of a particle in supercooled water is best described by velocity to the one-half power, and water temperature to the three-halves power. The only difficulty in applying this relationship is that the velocity relative to the particle must be known. Unfortunately in turbulent flow, where the velocity relative to the particle is always changing, this velocity is difficult to evaluate. Therefore, equation 2.18 must be modified such that the constant coefficient and the velocity term are lumped into one heat transfer coefficient, B. The value of B then becomes a function of the turbulence intensity.

In equation 4.9 the number of frazil particles is a function of the measured time and temperature along the supercooling curve. It is also a function of B, which must be independently evaluated. This can be done by observing the changes in the size of the ice particles with time and using equation 4.8 to relate the coefficient B to the turbulence intensity.

4.3.1 Growth of Frazil Particles

Growth of frazil particles depends on the supercooling and the ability of turbulence to remove heat from the surface of the growing ice particle. In equation 4.8, given an initial particle radius r_o, the particle radius at any time can be determined. It should be noted however, that equation 4.5 allows the computation of only the largest particle size evident at any time. The average particle size depends on the nucleation rate during this period and the length of time that these previously nucleated particles have been immersed in the supercooled water.

An "a priori" evaluation of B was made by estimating the size of the observed frazil particles. This estimate was always made upon the first visual sighting and would therefore be biased towards the larger particles, or those particles which were nucleated at time, t_n. Furthermore, the first sighting always occurred near the time of maximum supercooling, t_s, and all the observed ice particles had diameters in the order of 1 to 2 mm. Hence, an approximate value of B can be determined from equation 4.5 if the initial particle size r_o, which is about 10^{-3} mm, is considered to be much smaller than the ice particle size r_s ,at time t_s. Therefore, from equation 4.8

$$B = r_s \left((T_n+T_s)/2\right)^{-3/2} (t_s-t_n)^{-1} \tag{4.10}$$

A summary of the results is shown in Table 4.2 and the variation of B with u' is illustrated in Figure 4.6. It is emphasized that the values of B shown are only as accurate as the estimate of the particle sizes. Because the particles were observed by eye and no photographic record was made,

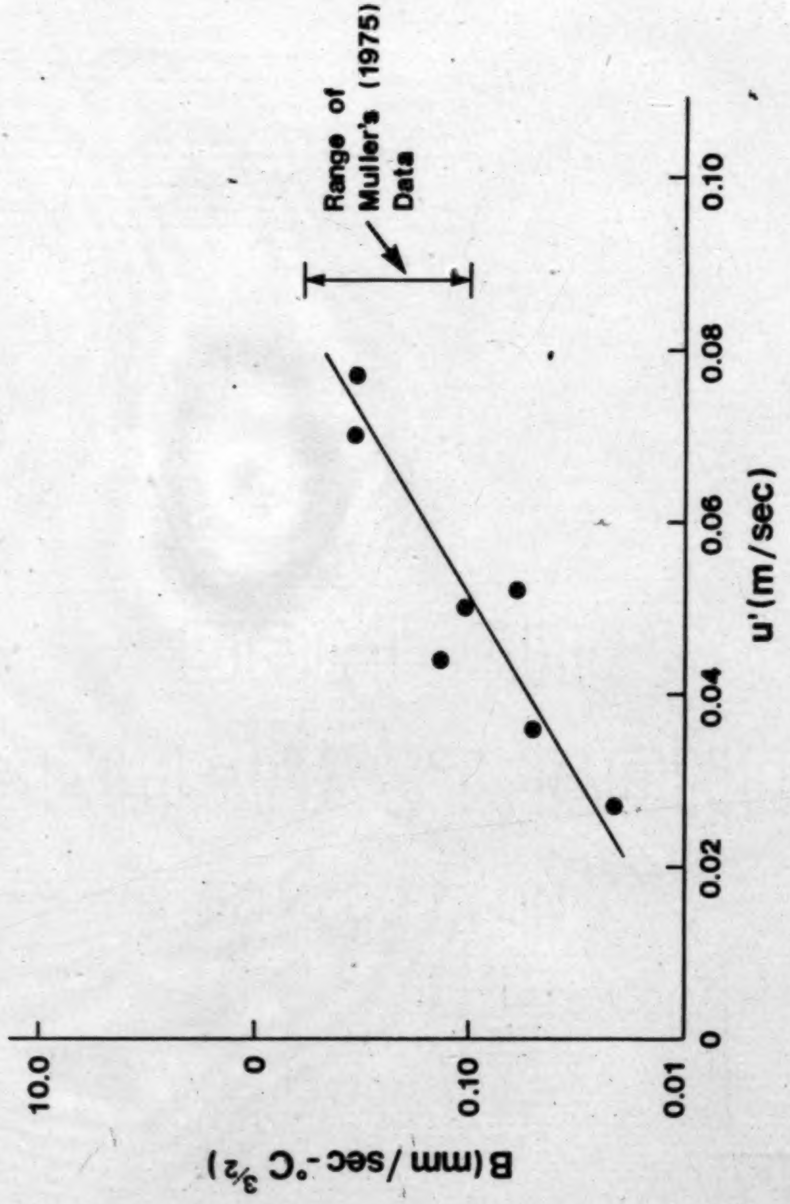

Figure 4.6 Effects of Turbulence on the Heat Transfer Coefficient

the estimate can be in error by up to 2 times. In all probability the particle sizes were underestimated. That is, the particle sizes could be up to 2 times as large as observed, but not any smaller than noted.

Therefore, the value of B shown in Table 4.2 is a minimum value and B could be up to twice as large as indicated. It is apparent, though, from Figure 4.6, that B does vary significantly with the turbulence intensity.

With the coefficient, B, determined, equation 4.8 can be used to compute the size of the largest frazil particles that should exist at any time during supercooling. It must be assumed, however, that B is constant even as the particle size is increasing. Table 4.3 summarizes the computed sizes of the largest ice particles at the characteristic times t_s and t_r. At residual supercooling the radii of the frazil particles vary within a range of 0.6 mm and 3 mm, although in run number 22 the diameter of the ice particles is about 4.5 mm. Figure 4.7, which illustrates the computed relationship between u' and r_r for various air temperatures, has considerable scatter with no obvious effects of air temperature on the maximum size of frazil particles. There is some tendency for the size of the frazil particle to increase with the turbulence, although whether this is due to the effects of u' on the duration of supercooling or the effects of u' on the growth rate is difficult to say.

Table 4.2

Computed Values of B From Estimates of Frazil Particle Sizes

Run Number	u' (m/sec)	Time Interval (sec)	Mean Supercooling (°C)	B (mm/sec•°C$^{3/2}$)
15	0.027	1425	0.11	0.021
21	0.050	600	0.06	0.11
32	0.044	600	0.05	0.15
34	0.070	114	0.09	0.35
41	0.036	540	0.11	0.05
50	0.052	1240	0.07	0.05
52	0.049	255	0.05	0.35

Table 4.3

Frazil Particle Sizes

Run Number	B (mm/sec•°C$^{3/2}$)	r_s (mm)	r_r (mm)
11	0.10	0.89	2.1
12	0.16	0.64	1.9
13	0.060	1.0	1.5
15	0.027	1.3	1.4
21	0.10	0.88	1.4
22	0.40	2.0	4.7
23	0.20	0.38	1.2
24	0.13	0.39	0.96
25	0.055	1.2	1.4
32	0.070	0.47	0.61
33	0.16	0.36	1.5
34	0.29	0.82	2.0
35	0.40	1.3	3.1
41	0.045	0.89	1.9
42	0.055	1.1	1.8
43	0.15	0.63	1.5
44	0.29	1.6	3.3
45	0.50	0.15	1.7
50	0.11	2.3	2.9
51	0.40	0.42	2.2
52	0.090	0.26	0.61
53	0.40	0.76	1.7

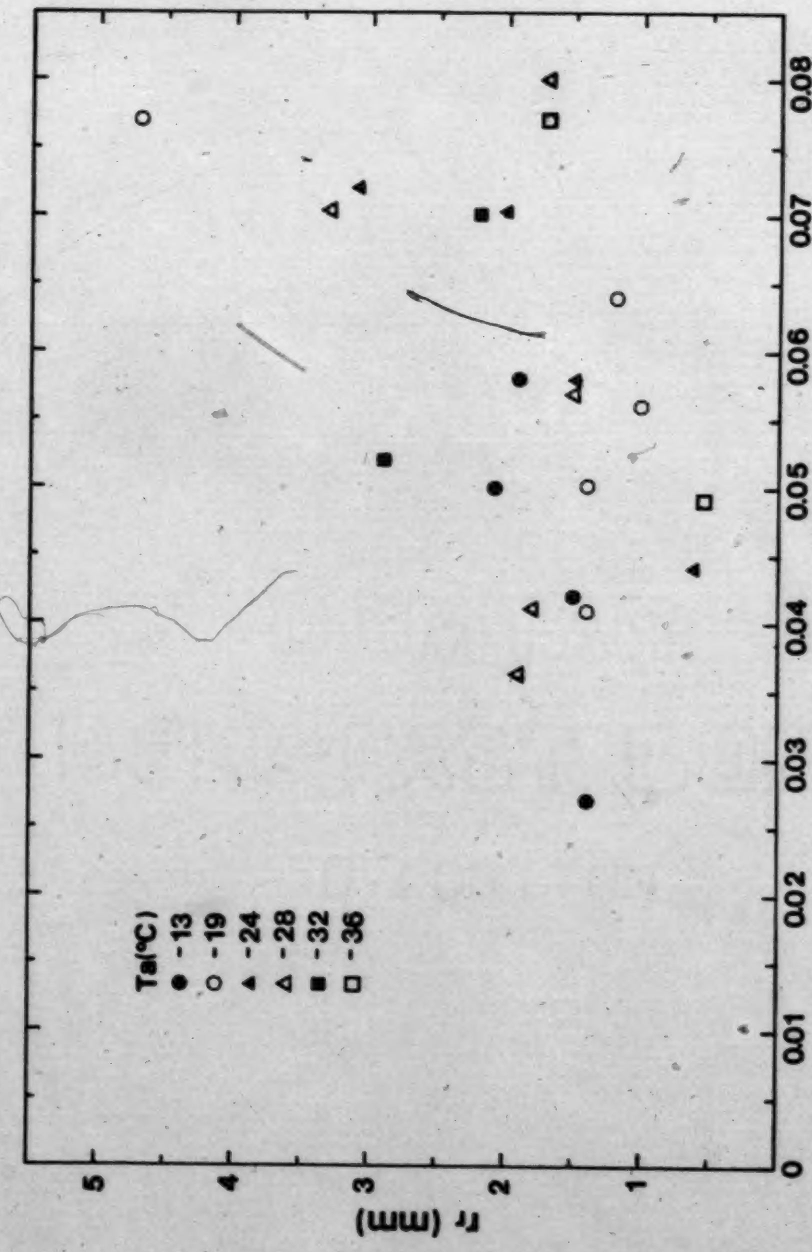

Figure 4.7 Effects of Turbulence on the Computed Frazil Particle Size

4.3.2 Nucleation Prior to Maximum Supercooling

According to Fletcher's theory of heterogeneous nucleation, numerous nucleating particles of various sizes either exist in, or are being transported into, the supercooled water. The ability of each of these to act as a nucleating agent depends upon the amount of supercooling. At the nucleation temperature determined from the supercooling curves, the largest of the nucleating particles presumably becomes active. As the temperature continues to fall to maximum supercooling, smaller nucleating particles should also become active. This results in a continuous nucleating process at least up to time t_s and small ice particles with radii in the order of 10^{-3} mm (Figure 4.1) should appear continuously.

The number of particles at time t_s can be determined from equation 4.9 if $r_i = r_o$, $N_i = 0$, and $V_i = 0$ at time t_n. Because the rate of ice production was linearized (Table 4.1) over this period and

$$2r_o\, B^{-1}\, [(T_s+T_n)/2]^{-3/2}\, (t_s-t_n)^{-1} \simeq 10^{-4}$$

equation 4.9 can be reduced to

$$N_s = \frac{16.97\, V_s}{B^3 [(T_s+T_n)/2]^{9/2}\, (t_s-t_n)^3} \qquad (4.11)$$

where N_s is the number of particles at time t_s. In reality, the value of N at time t_n is probably not zero. It has a finite value which is a function of both the air temperature and the turbulence, with N increasing as the turbulence increases and the air temperature decreases (Section 4.1). However, if it is assumed that secondary nucleation or additional heterogeneous nucleation occur at significant rates after t_n then it is a reasonable approximation to assume N_i is relatively small and approaches zero.

Table 4.4 tabulates the number of frazil particles produced at time t and the rate of production of these particles in the time period between t_n and t_s. The number of particles per cm³ of water varies between a minimum of 0.26 and a maximum of 330. From the observations made during the experimentation it was perceived, although not actually measured, that the number varied within an order of magnitude of 1.0. This suggests that in many instances the value of B was either poorly estimated or is not a constant over the period of time the changes in N were calculated. Considering the error in estimating the particle sizes could have been 200%, and that N is a function of B to the third power, the number of particles could be overestimated by a factor of eight. This could reduce the maximum concentration of particles at time t_s to about 40.

Nevertheless, assuming that the error in the computed values of N_s is the same for all experiments something can still be determined from the results. Figures 4.8 and 4.9 show the variation of N_s and $\dot{N}_{ns}$ (the nucleation rate) with the turbulence intensity respectively. Both the number of

Table 4.4
Summary of Nucleation Rates

Run No.	Ns (#/cm^3)	$\dot{N}$ns (#/cm^3•sec)	Nr (#/cm^3)	$\dot{N}$sr (#/cm^3•sec)
11	2.12	0.049	-14.5	-0.045
12	6.5	0.052	- 5.9	-0.029
13	13.1	0.016	- 6.2	-0.029
15	6.1	0.0042	47.7	0.25
21	28.8	0.048	21.6	-0.048
22	0.26	0.0016	0.20	-0.0002
23	118	1.68	- 103	-0.87
24	153	1.14	- 118	-0.90
25	20.7	0.017	2.6	-0.046
32	188	0.31	-88.6	-0.87
33	208	2.31	- 194	-0.93
34	16.9	0.15	-12.1	-0.11
35	5.3	0.034	- 3.7	-0.026
41	7.5	0.014	-0.77	-0.0085
42	9.6	0.018	0.54	-0.017
43	33.8	0.12	-21.6	-0.11
44	9.3	0.022	- 7.8	-0.037
45	248	20.6	- 240	-2.39
50	2.8	0.0023	- 1.4	-0.012
51	126	0.66	- 121	-0.44
52	330	1.29	- 159	-1.02
53	65.3	0.23	-45.9	-0.46

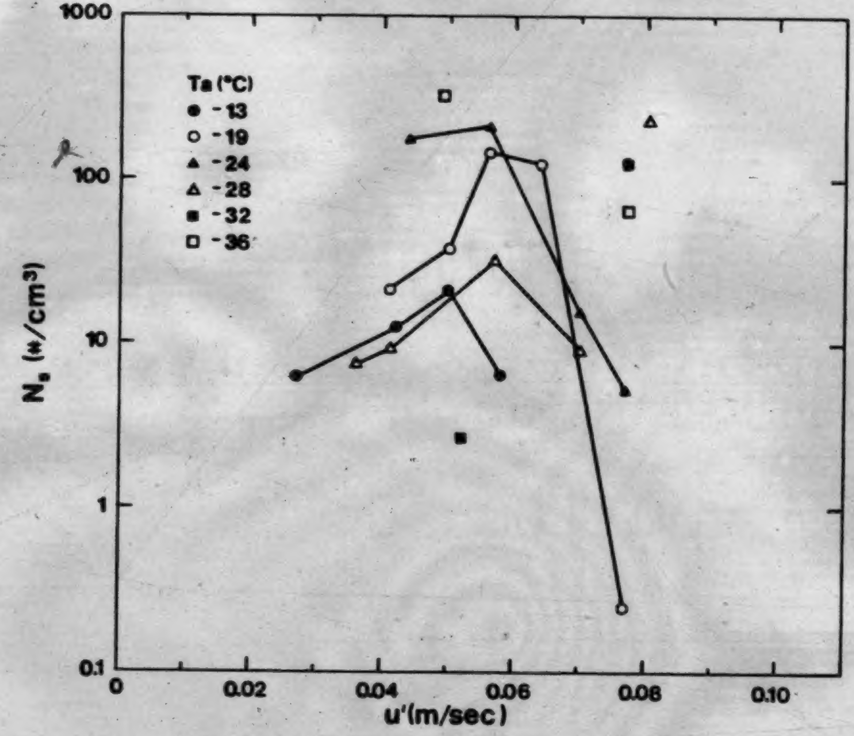

Figure 4.8 Effects of Turbulence on the Production of Frazil Particles

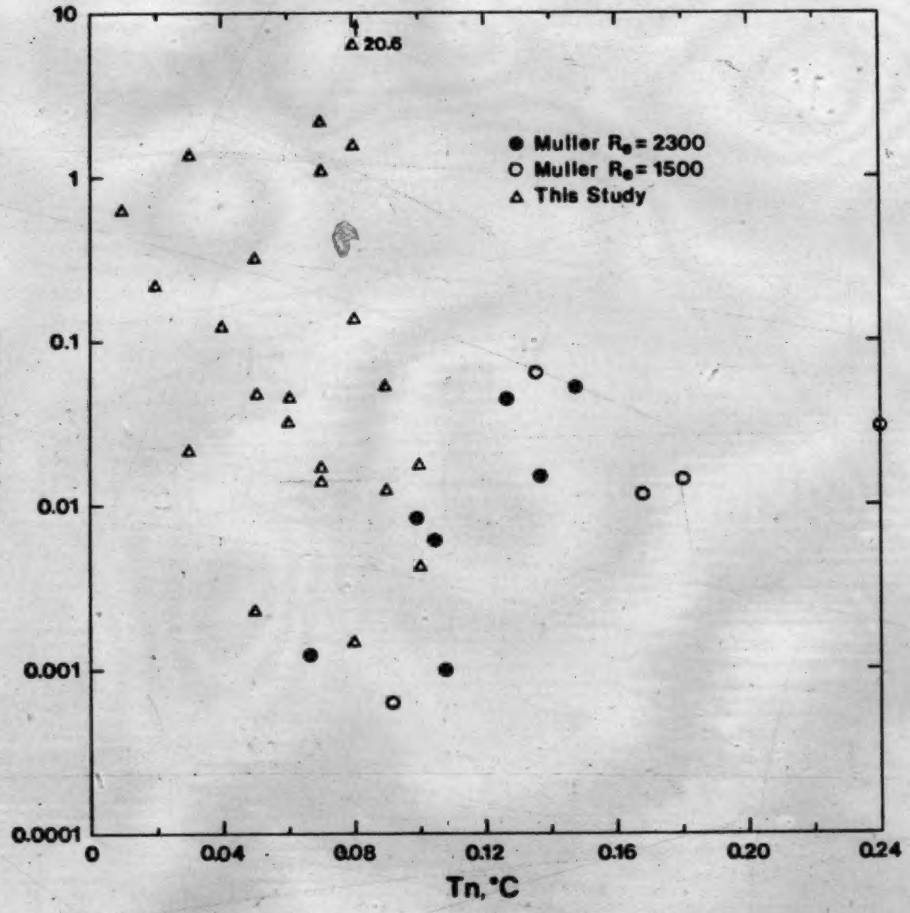

Figure 4.9 Effects of Turbulence on the Rate of Production of Frazil Particles

particles produced and the rate of nucleation is a maximum in the vicinity of u'=0.05 m/sec if the computed values are stratified on the basis of air temperature. This suggests that at low turbulent intensities less nucleation occurs, either because of a reduction in the availability of nucleating particles or the reduction in secondary nucleation. At turbulence intensities greater than about 0.05 m/sec the nucleation rate is again reduced, perhaps because more energy is going into crystal growth and nucleation is being suppressed.

There does not appear to be any relationship between the optimum turbulence intensity and the air temperature.

4.3.3 Nucleation Following Maximum Supercooling

Following maximum supercooling the major ice production processes are those of crystal growth and, perhaps, secondary nucleation. Heterogeneous nucleation may also be responsible for the appearance of additional ice particles because it is probable that the nucleating agents active prior to maximum supercooling will also be active on the rising limb of the supercooling curve, at least until the water temperature increases above the nucleating temperature.

Equations 4.8 and 4.9 can be solved for N_r at time t_r if $N_i=N_s$, $r_i=r_s$, and $V_i=V_s$. Thus:

$$N_r = \frac{16.97(V_r-V_s)}{(2a+1)^2\ B^3[(T_r+T_s)/2]^{9/2}(t_r-t_s)^3} - N_s \qquad (4.12)$$

where

$$a = \left(\frac{T_s - T_n}{T_r + T_s}\right)^{3/2} \left(\frac{t_s - t_n}{t_r - t_s}\right)$$

which arises because the initial size of the ice particles at t_s is no longer negligible with respect to the growth of the ice particle between the times t_s and t_r. The parameter "a" is an indication of the relative potential growth of an ice particle prior to and following maximum supercooling. The nucleation rate, $\dot{N}_{sr}$, can be determined by dividing equation 4.14 by $t_r - t_s$.

The computed values of N_r and $\dot{N}_{sr}$ are shown in Table 4.4 where they are compared to the nucleation rates prior to maximum supercooling. In the majority of cases the calculated values of both N_r and $\dot{N}_{sr}$ are negative. This is unexpected. Inspection of equation 4.12 reveals that $N_r<0$ only if N_s is greater than the first term on the right side of the equation. This can only occur if the value of B prior to maximum supercooling is underestimated relative to the value of B following maximum supercooling. However, because the former was determined on the basis of growth rates of the frazil particles, it is most likely that the latter must be less that that assumed.

An indication of the relative changes in B required for the number of particles to be preserved following maximum supercooling ($N_s=N_r$) can be made by assuming that B_s and B_r (the values of B prior to and following maximum supercooling) are constant over the respective time periods and $B_s \neq B_r$. Dividing equation 4.12 by equation 4.11 results in

$$(B_r/B_s)^3 + 4a\,(B_r/B_s)^2 + 4a^2\,(B_r/B_s) = [(V_r - V_s)/2V_s]\,a^3 \qquad (4.13)$$

which can be solved for the ratio of B_r/B_s. In general, it is found that $0.15 < B_r/B_s < 0.75$ and that the ratio varies significantly with the turbulence intensity as shown in Figure 4.10.

It is apparent then that when ice particles are immersed in high intensity turbulence the rate of heat loss from the particle is reduced as the particle size increases. In other words, as the ratio of the length scale of the particle to the length scale of the turbulence increases the rate of heat loss decreases. This is contrary to expectation. Figure 4.10 also indicates that the reduction in B as the particle size increases is less if the turbulence intensity is low. This suggests that at low intensity turbulence the rate of heat loss from the particle is independent of the change in the ratio of the length scales of the particle and the turbulence.

At this time it is difficult to explain the discrepancy, although assuming that the growth rate is independent of the crystal size is probably the major reason. Other sources of error could be the mathematical approximations or the assumption that the heat transfer from a particle in turbulent flow is a function of $T^{3/2}$. Because

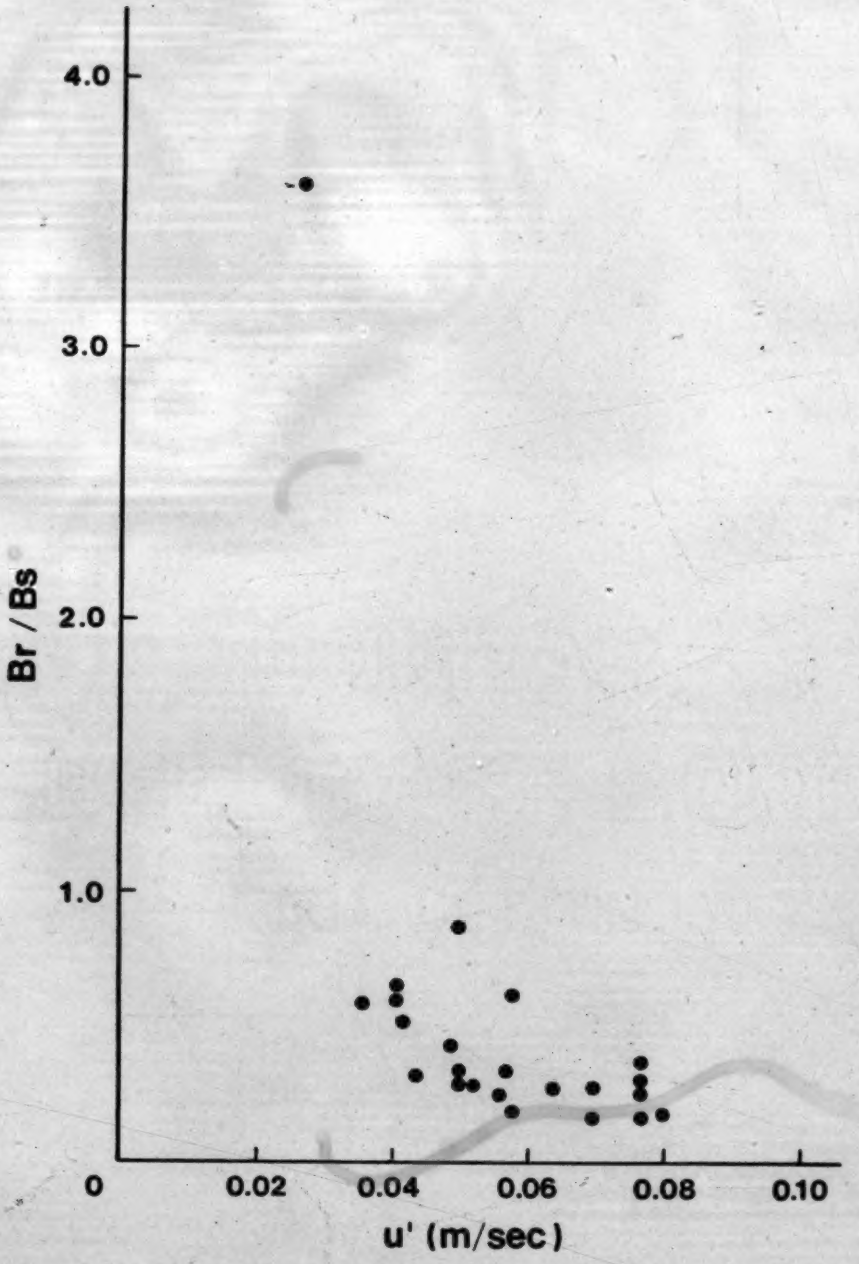

Figure 4.10 Variation of B_r/B_s with Turbulence Intensity

this relationship was borrowed from the growth rate theory of stationary ice crystals in steady, supercooled flow, this is not improbable.

Nevertheless, because the value of N_s was overestimated in equation 4.11, it is impossible to get an appreciation of secondary nucleaton.

4.4 Comparison with Muller's Data

A summary of Muller's data pertaining to nucleation and growth of the frazil particles is tabulated in Table 4.5.

As described in Section 2.4, Muller cooled a sample of filtered water in a small refrigerated container open to above-zero air temperatures. Either because of the absence of the supercooled layer at the surface or the lack of ice transported across the air-water interface, nucleation did not occur until initiated artificially. Muller did this by injecting a single particle of ice into the supercooled water at a chosen supercooled temperature. He then measured the change in water temperature and counted the number of ice particles produced during the first 40% or 50% of the duration of supercooling. In some experiments the number of particles was so great that single particles could not be differentiated in the photographs. The total volume of ice produced was computed from the increase in water temperature, taking into consideration heat transport across the boundaries of the water sample. Knowing the total volume of ice produced and the number of particles (from photographs) at any time following nucleation it was possible to compute the average size of the ice particles. Although Muller could have independently estimated the size of the ice particles by photography, he chose not to. This is unfortunate because it does not allow an independent assessment of the rate of particle growth.

Muller's experimental technique differed considerably from that employed in the present experiments. Firstly, Muller did not produce a supercooling curve similar to that found in natural situations. In most of his experiments no maximum supercooling was evident following nucleation. This is because of the extremely low cooling rates, which were completely dwarfed by high ice production at lower nucleation temperatures than generally occur naturally. Secondly, in each experiment the initial nucleation always occurred in the same manner. That is, one ice particle was always placed into the supercooled water. This did not allow for the variation in the number of nucleating particles which can normally be found in nature. A graphical representation of the change with time of temperature, number of particles, and particle size in one of Muller's experiments is shown in Figure 4.11.

A comparison of the sizes of the frazil particles produced in this study and Muller's study can be made by considering Table 4.3 and Table 4.5. Firstly, it should be noted that the particle sizes in Table 4.3 are the largest

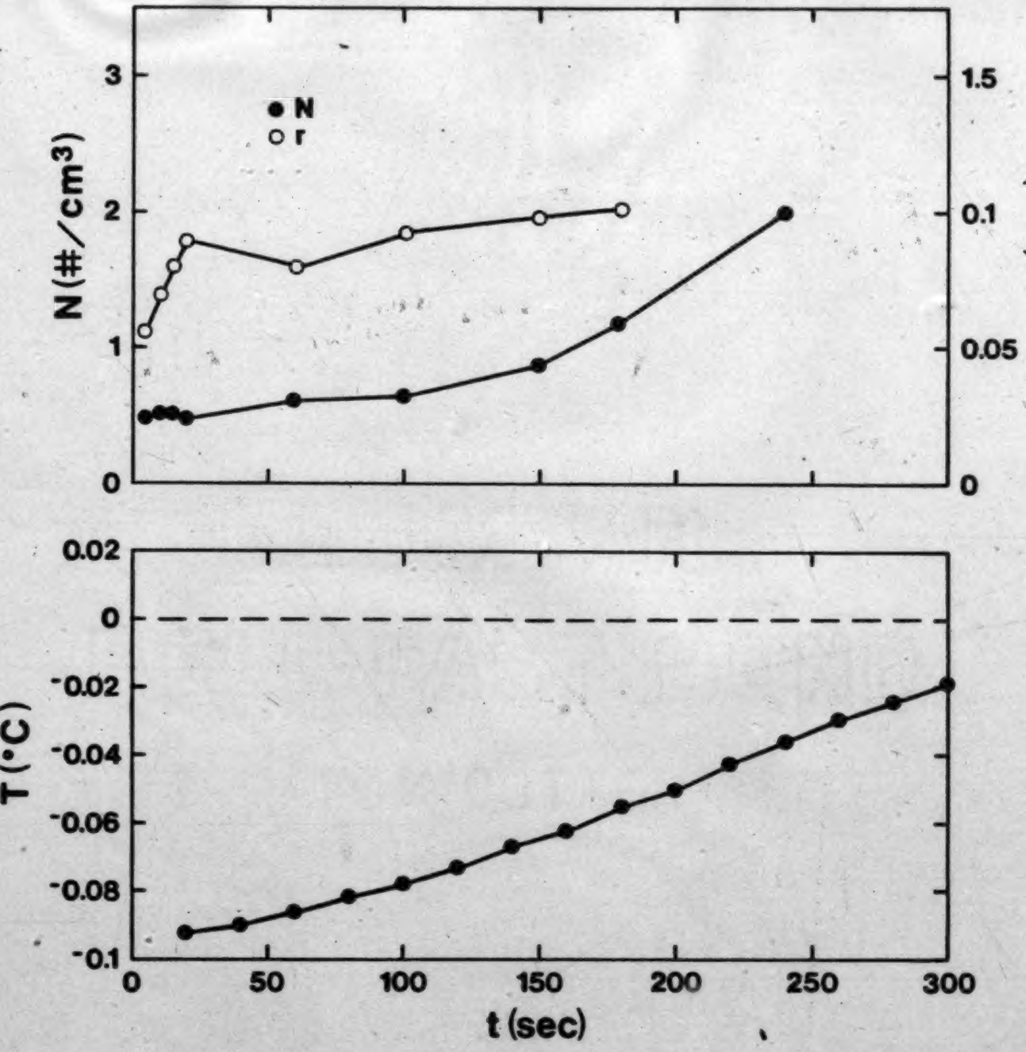

Figure 4.11 Results of a Typical Experiment by Muller (1978)

of any given size distribution at one time, while those of Muller are the mean size. Secondly, Muller assumed that the particles were spheres and the resulting sizes (Table 2.1) are considerably smaller. To be consistent with the estimates from this study, the reported radii were recalculated on the assumption that the spheres were in fact discs with a volume of $0.16\ r^3$. It is these results which appear in Table 4.5. The observed and calculated sizes in both experiments are consistent with those observed in rivers. However, because Muller operated at considerably larger supercooling the sizes of his frazil particles tend to be larger, even though the duration of growth is less.

The estimated average size of the frazil particles also allows the determination of the coefficient B and its variation with respect to the differences in turbulence. These values of B are also shown in Table 4.5 and their range is compared to the values of B determined in this study in Figure 4.6. Again, it must be noted that the evaluation of B from Muller's data was made on the basis of the mean particle size. This results in a low estimate. If B was computed from the largest particle size, considerably higher values of B than estimated in this study would have been evident. This may be either because Muller ran his experiments at considerably higher turbulent intensities or the value of B in this study is underestimated. Unfortunately a detailed comparison is difficult because of the absence of a common representation of turbulence.

Table 4.5

Summary of Muller's (1975) Nucleation Data

Run No.	V (mm^3/cm^3)	T (°C)	N (#/cm^3)	t (sec)	r' (mm)	B (mm/sec•°$C^{1/2}$)	N/Δt (#/cm^3•sec)
E3	0.26	0.117	2.64	60	0.86	0.36	0.044
E5	0.99	0.098	2.83	180	1.31	0.24	0.016
E6	0.48	0.075	0.54	540	1.78	0.16	0.0010
E7	0.76	0.261	2.70	90	1.21	0.10	0.030
E8	1.45	0.127	2.55	150	1.54	0.23	0.017
E9	1.18	0.088	1.33	240	1.78	0.28	0.055
E11	0.50	0.140	2.08	180	1.15	0.12	0.012
E12	0.24	0.080	0.11	180	2.4	0.58	0.00061
E13	0.45	0.127	3.72	90	0.91	0.22	0.041
E14[1]	-	-	0.34	270	-	-	0.0013
E15[1]	-	0.071	1.79	300	-	-	0.0060
E16	0.297	0.068	1.98	240	0.99	0.23	0.0083

[1] particles assumed discoidal with C=0.16

One point of interest with respect to B in Muller's data is that it does not vary significantly for the two turbulence levels. The mean values of B for his representative Reynold's numbers of 2300 and 1500 are 0.26 and 0.24 respectively. The larger variation in B found in this study suggests that a much larger range of turbulence intensity was utilized in this study.

A comparison of the nucleation rate and the number of frazil particles produced at the end of the supercooling period in both studies is very difficult. The method used in computing the number of particles produced in this study could not be applied over the whole range of supercooling (Section 4.3.3). Also, the experimental procedure and the defined independent variables in both sets of experiments are not consistent enough to allow a representative comparison. However, some comparison can be made on the basis of the nucleation temperature if it is accepted that the number of computed particles at time t_s in this study and the number of particles reported by Muller is representative of the number of particles produced. The relationship between N and T_n is shown in Figure 4.12. It is obvious that Muller's data appears to behave well, if stratified on the basis of the turbulence intensity. His data also plots below the data from this study, even though nucleation in his experiments occurred at much greater supercooling. Again, it must be emphasized that in some instances Muller could not count the maximum number of

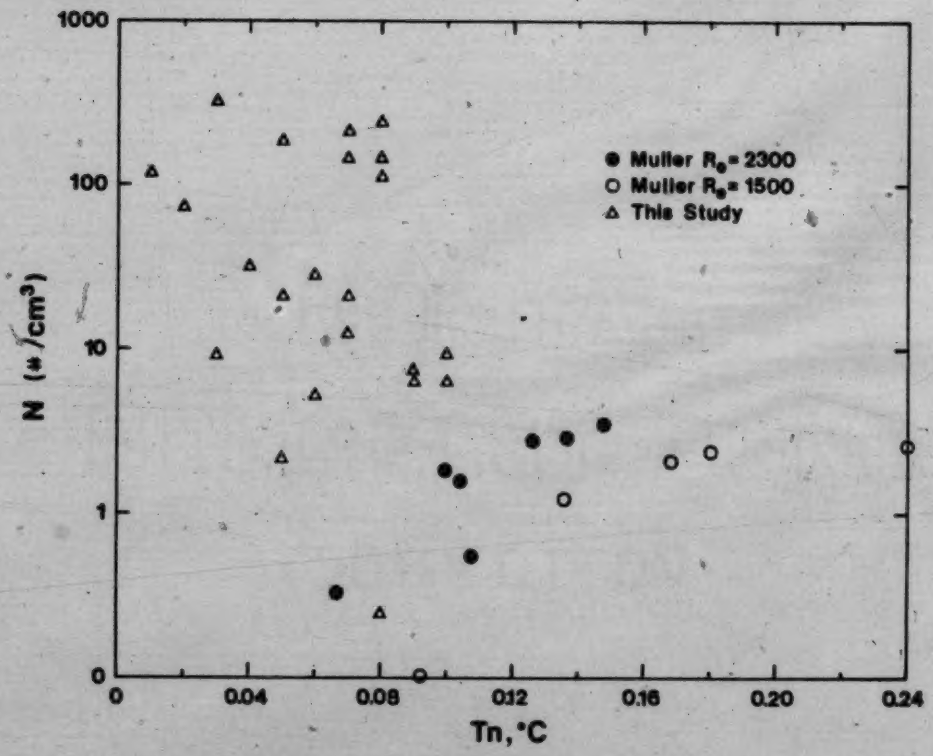

Figure 4.12 Effects of the Nucleation Temperature on the Number of Frazil Particles Produced

particles because their numbers were so great they could not be resolved photographically. There is no obvious trend in the data from this study. Because B in this study can be in error by a factor of 2, the value of N could be reduced by a factor of 8, thus placing the bulk of the data close to that of Muller.

Figure 4.13 compares the nucleation rates in both studies and the trends from both studies are similar to those in Figure 4.12.

4.5 Residual Supercooling

Following the return to residual supercooling, only the heat loss from the boundary of the water, H_o, is responsible for the continued growth of ice. During this period of residual supercooling, if it is unlikely that significant heterogeneous or secondary nucleation is occurring, all the heat loss must result in the production of ice by the growth of the existing frazil particles. The growth of these particles can only occur if there is a difference between the temperature of the ice particle and the water. This can only be possible if a certain amount of supercooling is maintained.

The behavior of this residual temperature can be determined from the equation which relates the change in particle size to the amount of ice produced:

$$N_r \, 3 \, C \, r^2 \, dr/dt = H_o \qquad (4.14)$$

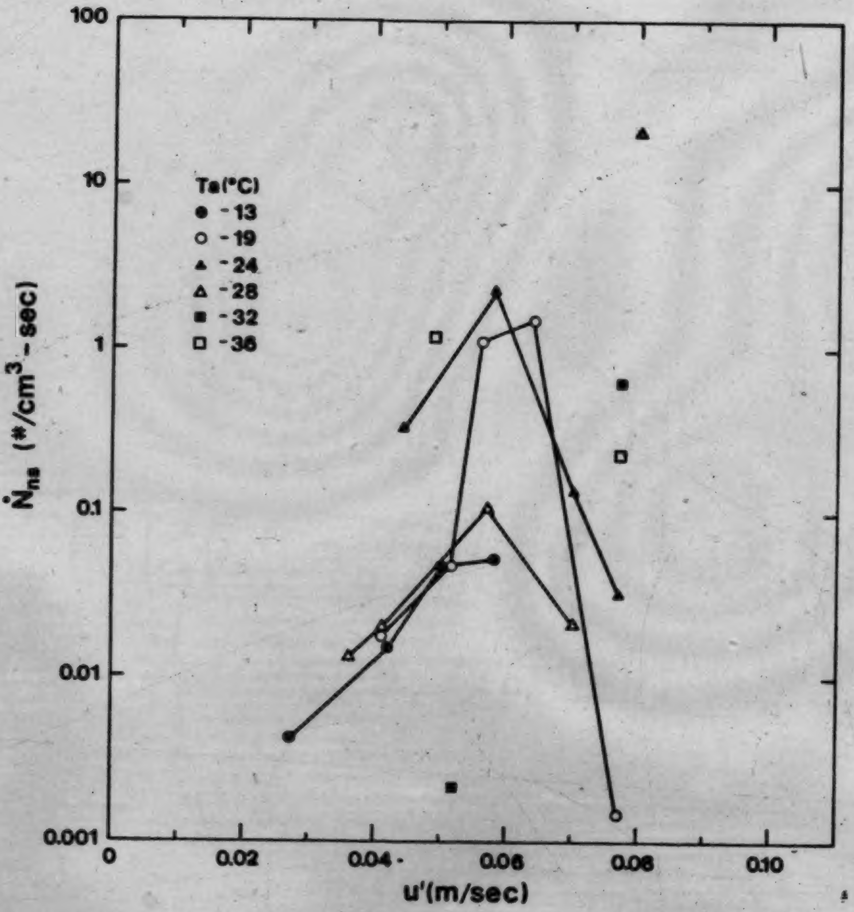

Figure 4.13 The Effects of the Nucleation Temperature on the Nucleation Rate of Frazil Particles

where N_r is the number of particles at the beginning of the residual supercooling phase. Now

$$dr/dt = B\ T^{3/2} \qquad (4.15)$$

so that

$$T = [H_o/N_r\ 3Cr^2 B]^{2/3} \qquad (4.16)$$

Because r is constantly increasing, at an ever-decreasing rate (the greater the particle size the larger the rate of ice produced for any given radius increase) T must approach the melting temperature asymptotically.

Carstens (1966), in his classification of the different phases of supercooling identified a time following the supercooling period when the water temperature appeared to remain constant. This residual supercooling has been debated considerably and, in fact, even measurements have not shown conclusively if such a condition actually exists.

However, a residual supercooling temperature T_r, can be defined at time t_r and its value can be calculated by equation 4.16. In this study the difficulty in computing an increase in the number of frazil particles being produced following maximum supercooling makes it necessary to make some assumptions in order to solve for T_r. If it is assumed that N_s=N_r, B_r/B_s has values as illustrated in Figure 4.10, and the heat transfer coefficient B for the period following residual supercooling is equal to B_r, then equations 4.8 and 4.12 can be combined with equation 4.16 to give

$$T_r = \left[0.25\left(\frac{H_o}{V_r - V_s}\right)\left(\frac{T_r + T_s}{2}\right)^{3/2} \frac{(t_r - t_s)}{f(a,B)}\right]^{2/3} \qquad (4.17)$$

where

$$f(a,B) = [((B_r/B_s)a+1)/((2(B_r/B_s)a) + 1)]^2$$

if C=0.16. This shows that, for a given air temperature (which determines H_o), the amount of required supercooling depends on the characteristics of the supercooling curve. If there was a long duration of supercooling then a limited amount of residual supercooling is required. However, if the supercooling period is short and the number and size of the frazil particles are small, then more residual supercooling is required to balance the heat loss to the air.

Table 4.6 summarizes the computed necessary residual supercooling. These are compared to the measured residual supercoolings in Figure 4.14. The aggreement is reasonable, considering that the resolution of measurement was only 0.01°C. In most instances the computed values of T_r are greater than the measured values. This would suggest that either the number or the size of the particles is overestimated by the calculations in Section 4.3. Probably, even though N_r was constrained to always equal N_s, the number of particles was overestimated and the size of the particles was underestimated, given the observed concentrations of frazil particles. Nevertheless, a certain amount of supercooling must be established following every supercooling phase if frazil is generated. This residual supercooling can vary between almost nil and at least 0.04°C.

Table 4.6
Comparison of Measured and Calculated Residual Temperatures

Run No.	Tr (°C) Measured	Calculated
11	0.02	0.039
12	0.03	0.029
13	0.03	0.028
15	0.01	0.009
21	0.01	0.014
22	0.02	0.025
23	0.03	0.034
24	0.03	0.035
25	0.01	0.021
32	0.02	0.021
33	0.03	0.032
34	0.03	0.035
35	0.02	0.035
41	0.03	0.039
42	0.04	0.028
43	0.02	0.030
44	0.03	0.043
45	0.03	0.025
50	0.04	0.039
51	0.02	0.028
52	0.01	0.022
53	0.01	0.022

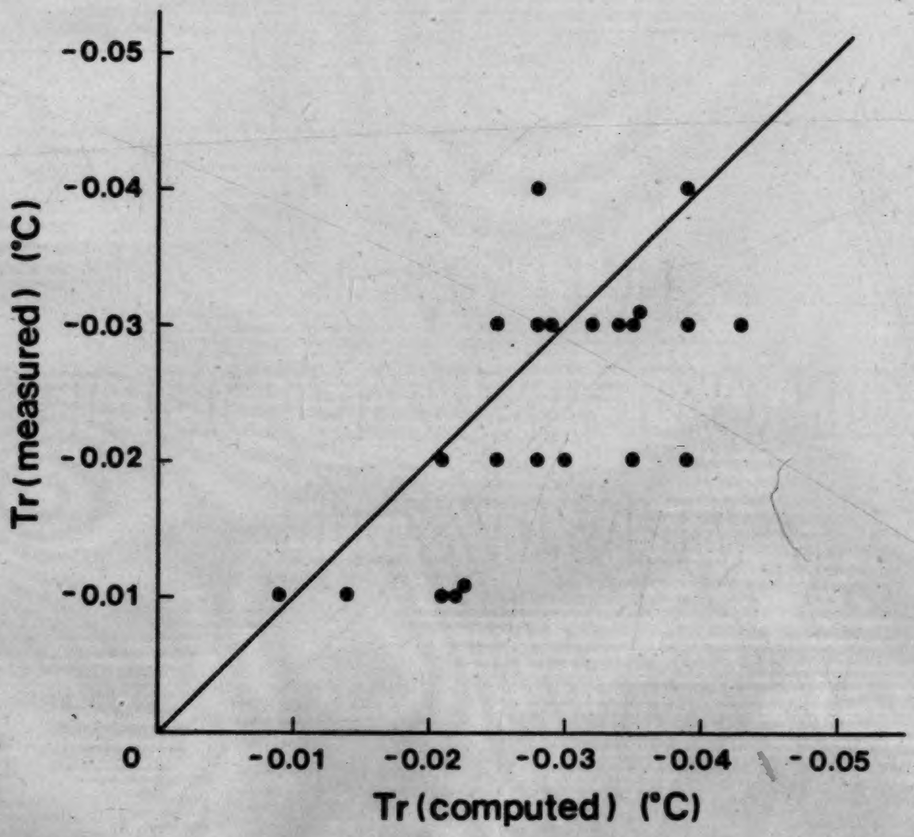

Figure 4.14 Comparison of Measured and Calculated Residual Supercooling

5. CONCLUSIONS AND RECOMMENDATIONS

A laboratory model was constructed to observe the generation of frazil for various combinations of air temperature and turbulence typical of a small stream during winter. Temperatures were measured to within 0.01°C by calibrated thermistor probes and the turbulence was characterized by the rms of the velocity fluctuations which were measured using a laser anemometer. Qualitative observations of the formation of surface ice, nucleation, and the growth of frazil particles were made. Nucleation rates were calculated from the measured supercooling curves. The differentiation between the ice produced by crystal growth and by nucleation was based on an expression for crystal growth taken from the literature.

5.1 Conclusions

5.1.1 Surface Cover Development and Nucleation Temperatures

The experimental evidence suggests that formation of a surface cover and frazil generation are the same process - heterogeneous nucleation. Although surface ice growth occurred outwards from the boundaries of the water surface by heat conduction through the ice and the vessel, its extent was limited to the boundaries by the turbulence, or degree of agitation of the water surface. However a surface cover could still form by surface nucleation well away from the boundaries. The formation of this type of ice cover was related to the air temperature and to the turbulence intensity. For any air temperatures of -10°C and -30°C the likelihood for this type of surface cover to form was small for turbulence intensities of 0.005 m/sec and 0.02 m/sec respectively.

The actual time and temperature of nucleation could not be observed, but was inferred from the shape of the supercooling curve. These nucleation temperatures, always greater than -0.10°C, suggest that nucleation is initiated by small ice particles acting as nucleating agents. If the turbulence intensity was large enough to cause entrainment of the small ice particles which nucleated on the surface, they were transported into the flow. This occurred in conjunction with the measurement of relatively higher nucleation temperatures. On the other hand, if the turbulence intensity was low and the surface particles could not be entrained, a surface cover developed and a much lower nucleation temperature was recorded.

The recorded nucleation temperatures can be related to the air temperature and turbulence. Although the relationship shows considerable scatter there is a trend which shows that extremely cold air and high turbulence intensity result in higher nucleation temperatures than for warmer air and lower turbulence, or even warmer air and high turbulence.

The source of the ice particles which initiate nucleation was deduced to be the air above the water surface. These particles, probably formed by water vapour condensation and freezing, deposit on the surface and initiate both the development of a surface cover and frazil generation. The presence of a strongly supercooled layer of water at the surface accelerates both of these processes.

The accepted nucleation theories are inadequate for defining the nucleation temperatures because their application depends on impossible 'a priori' estimates of the nature and size of the active nucleating agents. At best, a known nucleation temperature can be used to determine the characteristics of these particles.

5.1.2 Ice Production During Supercooling

The amount and rate of ice produced during supercooling was determined from the shape of measured supercooling curves. In general, regardless of the air temperature, when the turbulence intensity was low, the portion of the curve prior to maximum supercooling (when heterogeneous nucleation could occur) was long and drawn-out. During this period considerable ice could be produced, but at a slow rate. If the turbulence intensity was large, the curve was shorter, exhibiting a higher rate of ice production but not necessarily producing more ice because of the shorter production time.

In all cases, the highest rate of ice production occurred after maximum supercooling and varied between two and four times that produced prior to maximum supercooling.

The ratio of the mean frazil production rate during the supercooling period to that following supercooling varied between 1.0 and 2.0. This ratio was a function of the nucleation temperature and an increase in this ratio was evident when the supercooling at nucleation became greater than 0.05°C. Any effect of turbulence intensity on the ratio could not be determined from the data.

5.1.3 The Shape and Growth of Frazil Particles

All the observed frazil particles were discoidal in shape, with estimated diameters varying between 1 and 2 mm. This shape and size is compatible with that predicted by the differential growth rates of ice crystals along the a- and c-axes, and also similar to that observed by other experimenters in laboratory and natural conditions.

The growth rates inferred from the observed crystal sizes were also compatible with those of other investigators. However, there is a large discrepancy in reported growth rates, with order of magnitude differences being not uncommon. It was found that improperly assumed shapes of the frazil particle can lead to large errors in growth rate estimates if only one characteristic dimension is used to describe the particle.

5.1.4 Nucleation of Frazil Particles

Other than the appearance of visible ice particles, the actual nucleation process could not be observed because of its microscopic nature. This prevented an independent confirmation of the nucleation temperature and the rates of nucleation inferred from the supercooling curves. It also prevented any distinction being made between the so-called secondary nucleation and heterogeneous nucleation.

However, an equation which distinguished the volume of ice produced by nucleation from that produced by the growth of the ice particles gives estimates of the number of particles, and the rate of production of these particles, that are within an order of magnitude of those observed by others in laboratory studies. These estimates of 0.3 to 300 particles per cm^3, produced prior to maximum supercooling, were found to be extremely sensitive to the measured growth rates of the ice particles. Errors in the estimates of these growth rates could reduce the number of particles by an order of magnitude.

The computed values of both the number of particles produced and the rate of their production by primarily heterogeneous nucleation prior to maximum supercooling, for each of the measured supercooling curves, was independent of the nucleation temperature (contrary to previous investigators) but highly dependent on the turbulence intensity. The number of particles produced and the rate of production was maximized at turbulence intensities of 0.05

m/sec. At lower turbulence intensities the limited transport of nucleating agents from the surface was the most likely cause of the low nucleation rate. At higher turbulence intensities, the reason for lower production rates is more difficult to determine.

An interesting phenomena was observed when the effects of nucleation were made visible by altering an equilibrium condition between the growth of a surface cover and the supercooled condition by breaking the surface cover. Numerous frazil particles became evident. This suggests that water molecules can liberate latent heat by adopting an internal ice-like structure which cannot be differentiated from the surrounding water. Then, with some disturbance, these ice-like structures suddenly become visible, perhaps by a minor alteration of their structure.

The secondary nucleation process, which most likely predominates after maximum supercooling, could not be identified because a realistic solution of the nucleation equation could not be found for that portion of the supercooling curve. The assumption, for any given turbulence intensity, that the size of the ice particle does not alter the rate of its growth, was the most likely source of error.

5.1.5 Residual Temperature

It was shown that a residual supercooling exists following the supercooling phase. The amount of supercooling is a function of the rate of heat loss from the water, the number of particles present, and their size. The predicted residual supercooling was close to that measured in the experiments and was found to vary between almost nil and -0.04°C.

Some practical conclusions from the experimentation and analysis are apparant. The nucleation of frazil generally results in particle concentrations of 1 to 10/cm^3. During the supercooling period these particles can grow to a size of 4 to 10 mm in diameter. The rate of ice production during the supercooling curve is strongly dependent on the nucleation temperature and because this temperature is weakly a function of turbulence it appears that the relative effects of the supercooling are less important for highly turbulent conditions. The experiments suggest that, for the lowest possible nucleation temperature, the rate of frazil generation never exceeded twice the rate one would expect if equilibrium conditions prevailed. Considering the short length of time that supercooling was evident, the increased ice produced because of the supercooling phenomena is relatively small. The most significant aspect of the supercooling condition is the creation of ice particles which can then grow in size. The total amount of ice produced in this manner is far greater than by nucleation and is a function of the rate of heat loss from the boundaries of the water and the duration of time over which this heat loss is allowed to continue.

5.2 Recommendations

The goals of the experimental investigation were to study the effects of air temperature and turbulence on frazil generation in natural streams. Unfortunately the processes of frazil formation are microscopic and the large scale of apparatus allowed only the gathering of data that inferred these processes. This resulted in conclusions which had to be supported from numerous sources in the literature and could not be confirmed by direct observation.

Further study of the frazil generation phenomenon requires that the basic processes identified in this study be considered separately, on a small scale where all the variables can be controlled and microscale measurements made.

It is recommended that:

1. The existence and deposition of atmospheric ice particles be confirmed by microscopic, high speed photography over a body of water subjected to various air temperatures and where the existence of any other forms of ice (border ice) is prevented.
2. The abilities of turbulence to entrain small ice-like structures from the surface be explored from a theoretical basis and also through experiment.
3. The mechanisms of secondary nucleation must be observed directly, so that the effects of turbulence on this process can be determined.
4. Considering the fact that considerable theoretical work

has been done on the heat transfer rate from bodies within a turbulent flow field, further experimentation is required to measure that heat loss from very small, almost non-buoyant, discoidal shaped particles suspended in a turbulent flow field. One of the fundamental requirements of such a study is precise determination of the structure of the turbulence.

With the current stage of knowledge of frazil generation, particularly in the aspects of nucleation, serious field measurements will not provide additional insight. At this time, it would be more fruitful to measure the fundamental variables such as climate (air temperature, humidity) and turbulence to ensure that they are being reproduced in the laboratory. Also, it is necessary to at least verify that the classical supercooling curves are being produced in natural streams, and that they exist over a large enough volume so that an estimate of the amount of ice being produced can be made from easily measured variables such as discharge, flow area, velocity, and air temperature.

Of course, the nucleation problem is only one small unknown. Other problems, such as adhesive and cohesive tendencies of frazil, also require research. It is more likely that these problems can be studied in natural streams.

Since the earliest studies and theories of frazil production produced by Henshaw, tremendous advances in instrumentation and measurement have been made. These advances must be utilized in direct observation of frazil production process because, at this time, an engineering solution to the frazil generation problem will not come from theoretical physics or thermodynamics.

6. LIST OF REFERENCES

Acres Ltd., Review of Current Ice Technology and Evaluation of Research Priorities. Canada Department of the Environment, Inland Waters Branch, Ottawa, 1971.

Altberg, W.J., Twenty Years of Work in the Domain of Underwater Ice Formation (1915-1935), Bulletin No. 23, International Association of Scientific Hydrology, 1936, pp. 373-407.

Arakawa, K., Experimental Studies on Freezing of Water, International Union of Geodesy aand Geophysics, International Association of Scientific Hydrology, 1954, pp. 474-477.

Arden, R.S., and Wigle, T.E., Dynamics of Ice Formation in the Upper Niagara River, Proceedings of the Banff Symposia: The Role of Snow and Ice in Hydrology, UNESCO-World Meteorology Organization-IAHR, 1972.

Barnes, H.T., Ice Engineering, Renouf Publishing Co., Montreal, Quebec, Canada, 1928.

Beltaos, S. and Dean, A., Field Investigations of a Hanging Ice Dam, International Symposium on Ice, Internation Association for Hydraulic Research, Quebec City, 1981.

Calkins, D.J., Accelerated Ice Growth in Rivers, U.S. Army Corps of Engineers, Cold Regions Research and Engineering Laboratory, Hanover, 1979.

Carstens, T., Heat Exchanges and Frazil Formation, Proceedings of the Symposium on Ice and its Action on Hydraulic Structures, International Association for

Hydraulic Research, Reykjavik, 1970.

Carstens T., Experiments with Supercooling and Ice Formation in Open Water, Geofysiske, Publikasjoner, Vol. 26, No. 9, 1966 pp. 1-18.

Chalmers, B. and Williamson, R.B., Crystal Multiplication without Nucleation, Science, Vol. 148, No. 3676, 1965, pp. 1717-1718.

Devik, O., Supercooling and Ice Formation in Open Waters, International Association of Scientific Hydrology, Vol. 2, 1948, pp. 380-389.

Dorsey, N.E., The Freezing of Supercooled Water, Transactions of the American Philosophical Society, Vol. 38, Part 3, 1948, pp. 247-328.

Fletcher, N.H., Size Effects in Heterogeneous Nucleation, The Journal of Chemical Physics, Vol. 29, No. 3, 1958, pp. 572-576.

Fletcher, N.H., Nucleation by Crystalline Particles, The Journal of Chemical Physics, Vol. 38, No. 1, 1965, pp. 237-241.

Fletcher, N.H., Entropy Effects in Ice Crystal Nucleation, The Journal of Chemical Physics, Vol. 30, No. 6, 1959, pp. 1476-1482.

Fletcher, N.H., The Chemical Physics of Ice, University Press, Cambridge, 1970.

Frank, H.S., Structural Models, Water: A Comprehensive Treatise, Plenum Press, New York, 1972.

Franks, F., The Properties of Ice, Water: A Comprehensive

Treatise, Plenum Press, New York, 1972.

Freysteinsson, S., Calculation of Frazil Ice Production, International Association of Hydraulic Research, Reykjavik, 1970.

Gilfilian, R.E., Kline, W.L., Osterkamp, T.E., and Benson, C.E, Ice Formation in a Small Sub-arctic Alaskan Stream, Proceedings of the Banff Symposia: The Role of Snow and Ice in Hydrology, UNESCO-World Meteorology Organization-IAHR, 1972.

Gilpin, R.R., The Effect of Cooling Rate on the Formation of Dendritic Ice in a Pipe With No Main Flow, Journal of Heat Transfer, Vol. 99, No. 3, 1977, pp. 419-424.

Gilpin, R.R., A Study of Factors Affecting the Ice Nucleation Temperature in a Domestic Water Supply, The Canadian Journal of Chemical Engineering, Vol. 56, 1978.

Gold, L.W., and Williams, G.P., An Unusual Ice Formation on the Ottawa River, Journal of Glaciology, Vol. 4, No. 35, 1963, pp. 569-573.

Hanley, T.O'D. and Michel B., Laboratory Formation of Border Ice and Frazil Slush, Canadian Journal of Civil Engineering, Vol. 4, No. 2, 1977, pp. 153-160.

Henshaw, G.H., Frazil Ice: On its Nature, and the Prevention of Its Action in Causing Floods, Canadian Society of Civil Engineers, Vol. I, 1887, pp. 1-23.

Hobbs, P.V., Ice Physics, Clarendon Press, Oxford, 1974.

Jackson, K.A., Interface Structure, Proceedings of the International Conference on Crystal Growth, Cooperstown, New York, 1958.

Kallungal, J.P., _The Growth of Single Ice Crystals Parallel to the A-axis in Subcooled Quiescent and Flowing Water_, Ph.D. Thesis, Syracuse University, 1975.

Kumai, M., and Itagaki, K., Cinematographic Study of Ice Crystal Formation in Water, International Union of Geodesy and Geophysics, International Association of Scientific Hydrology, 1954, pp. 463-467.

Kuuskoski, M.V., On Frazil Ice Measurements in the Kemi River, International Association of Hydraulic Research, Leningrad, 1972.

Lindenmeyer, C.S., and Chalmers, B., Morphology of Ice Dendrites, Journal of Chemical Physics, Vol. 45, No. 8, 1966, pp. 2804-2806.

Mason, B.J., The Supercooling and Nucleation of Water, Advances in Physics, Vol. 27, No. 26, 1958, pp. 221-234.

Mellor, M., _Snow and Ice on the Earth's Surface_, Report Number II-C1, U.S. Army Corps of Engineers, Cold Regions Research and Engineering Laboratory, Hanover, 1964.

Michel, B., Theory of Formation and Deposition of Frazil Ice, Proceedings of the Eastern Snow Conference, 1963.

Michel, B., From the Nucleation of Ice Crystals in Clouds to the Formation of Frazil Ice in Rivers, Proceedings of the International Conference on Low Temperature Sciences, Hokkaido University, Japan, Vol. I, 1967.

Michel, B., _Winter Regime of Rivers and Lakes_, Report Number III-B1a, U.S. Army Corps of Engineers, Cold Regions

Research and Engineering Laboratory, Hanover, 1971.

Muller, A., Frazil Ice Formation in Turbulent Flow, Report Number 214, Iowa Institute of Hydraulic Research, The University of Iowa, Iowa City, 1978.

Nanten, A.H. and Levy, H.A., Liquid Water: Scattering of X-Rays, Water: A Comprehensive Treatise, Plenum Press, New York, 1972.

Nemethy, G., and Scheraga, H.A. Structure of Water and Hydrophopic Bonding in Proteins. I. A Model for the Thermodynamic Properties of Liquid Water, The Journal of Chemical Physics, Vol. 36, No. 1962, pp. 3382-3400.

Osterkamp, T.E., Gilfilian, R.E., and Benson, C.S., Observations of Stage, Discharge, pH, and Electrical Conductivity During Periods of Ice Formation in a Small Subarctic Stream, Water Resources Research, Vol. 2, No. 2, 1975, pp. 268-272.

Osterkamp, T.E., Frazil Ice Nucleation by Mass Exchange Processes at the Air-Water Interface, Journal of Glaciology, Vol. 19, No. 81, 1977, pp. 619-625.

Peterson, A.W. and Howells, R.F., Users Manual for HYPOL, Department of Civil Engineering, University of Alberta, 1972.

Rao, C.N.R., Theory of Hydrogen Bonding in Water, Water: A Comprehensive Treatise, Plenum Press, New York, 1972.

Sampson, F., The Ice Regime of the Peace River in the Vicinity of Portage Mountain Development, Prior to and During Diversion, NRC Technical Memorandum No. 1077, 1973.

Schaefer, V.J., The Formation of Frazil and Anchor Ice in Cold Water, Transactions of the American Geophysical Union, Vol. 31, No. 6, 1950, pp. 885-893.

Stakle, P. "Frazil and Anchor Ice in the Rivers of Latvia", Bulletin No. 23, International Association of Scientific Hydrology, 1936, pp. 351-366.

Suzuki, S. and Kuroiwa, J., Grain Boundary Energy and Grain Boundary Grove Angles in Ice, Journal of Glaciology, Vol. 11, No. 62, 1972, pp. 265-277.

Tesaker, E., Accumulation of Frazil Ice In An Intake Reservoir, Proceedings of the Third International Symposium on Ice Problems, International Association of Hydraulic Research, Hanover, 1975.

Tsang, G., Change of Velocity Distribution in a Cross-section of a Freezing River and the Effects of Frazil Ice Loading on Velocity Distribution, Proceedings of the Symposium on Ice and its Action on Hydraulic Structures, International Association for Hydraulic Research, Reykjavik, 1970.

Tsang, G., Resistance of the Beauharnois Canal in Winter, Proceedings of the Workshop on Hydraulic Resistance of River Ice, National Water Research Institute, Environment Canada, 1980.

Turnball, D., and Fisher, J.C., Rate of Nucleation in Condensed Systems, The Journal of Chemical Physics, Vol. 17, No. 1, 1949, pp. 71-73.

Van Hook, A., Crystallization: Theory and Practice, Reinhold Publishing Corporation, New York, 1961.

Walrafen, G.E., Raman and Infrared Spectral Investigations of Water Structure, Water: A Comprehensive Treatise, Plenum Press, New York, 1972.

Walley, E., Structure Problems of Ice, Proceedings of the International Symposium on the Physics of Ice, Munich, 1948, pp. 19-43.

Willey, C.K., Some Aspects of the Design of Ice Passage Facilities for the Burfell Hydroelectric Project, International Association of Hydraulic Research, Reykjavik, 1970.

Williams, G.P., Adhesion of Frazil Ice to Underwater Structures, Proceedings of the Eastern Snow Conference, Vol. 24, 1967.

Williams, G.P., Frazil Ice During Spring Break-up, International Association of Hydraulic Research, Leningrad, 1972.

APPENDIX A

MEASURED SUPERCOOLING CURVES

The following figures, from which the data in Table 3.5 was synthesized, represent the temperature measurements as plotted by the plotlib plotting routine on the Calcomp plotter. The recorded temperature from each of the five probes is plotted for each experiment. In some instances, when the probe positioned near the water surface was immersed in ice, the temperature departed from the expected supercooling curve. It should be noted that the scales of both the ordinate and the absisca are not always constant when comparing the various experiments.

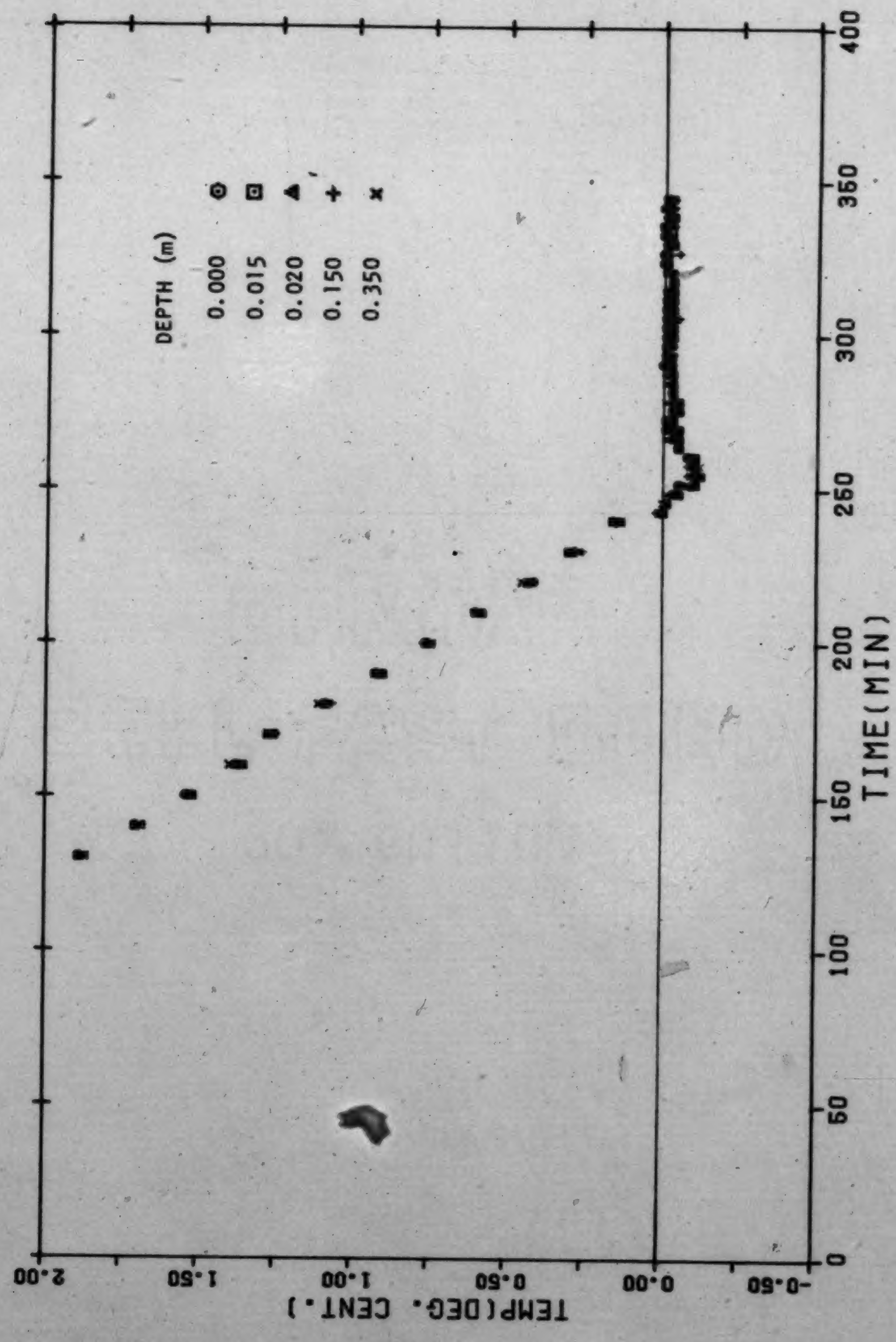

RUN #11-TEMP. VS. TIME FOR VARIOUS DEPTHS

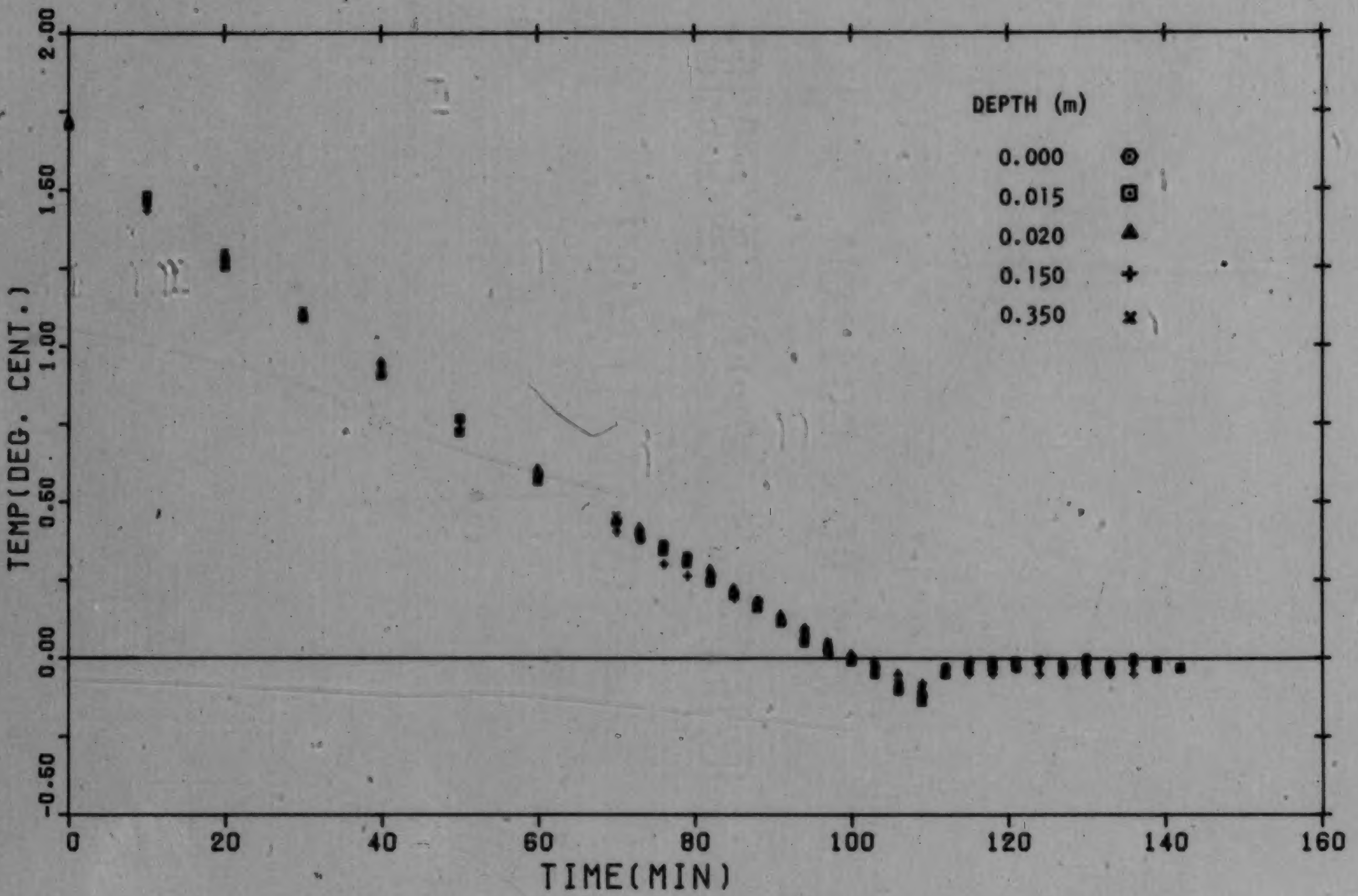

RUN #12-TEMP. VS. TIME FOR VARIOUS DEPTHS

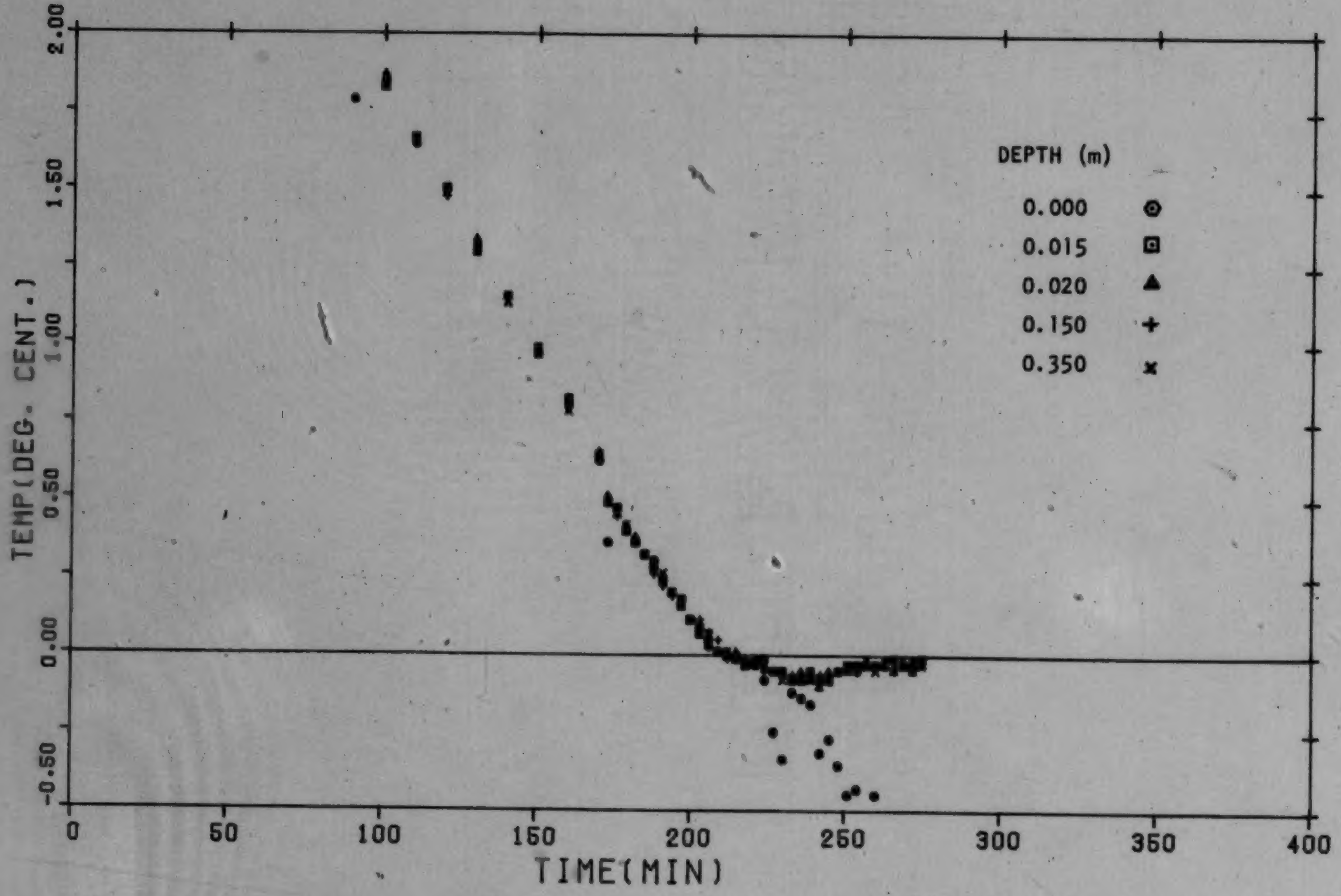

RUN #13-TEMP. VS. TIME FOR VARIOUS DEPTHS

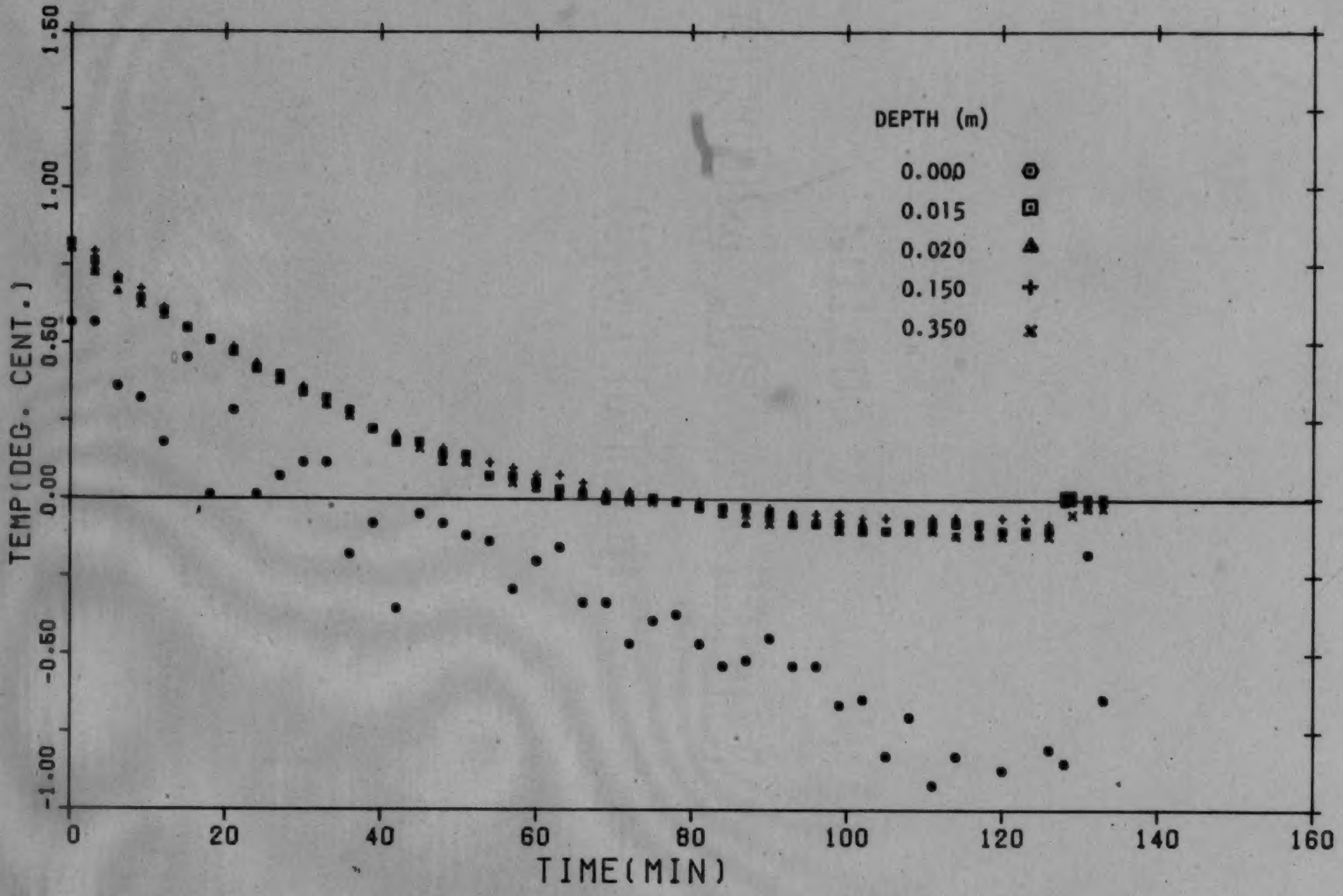

RUN #15-TEMP. VS. TIME FOR VARIOUS DEPTHS

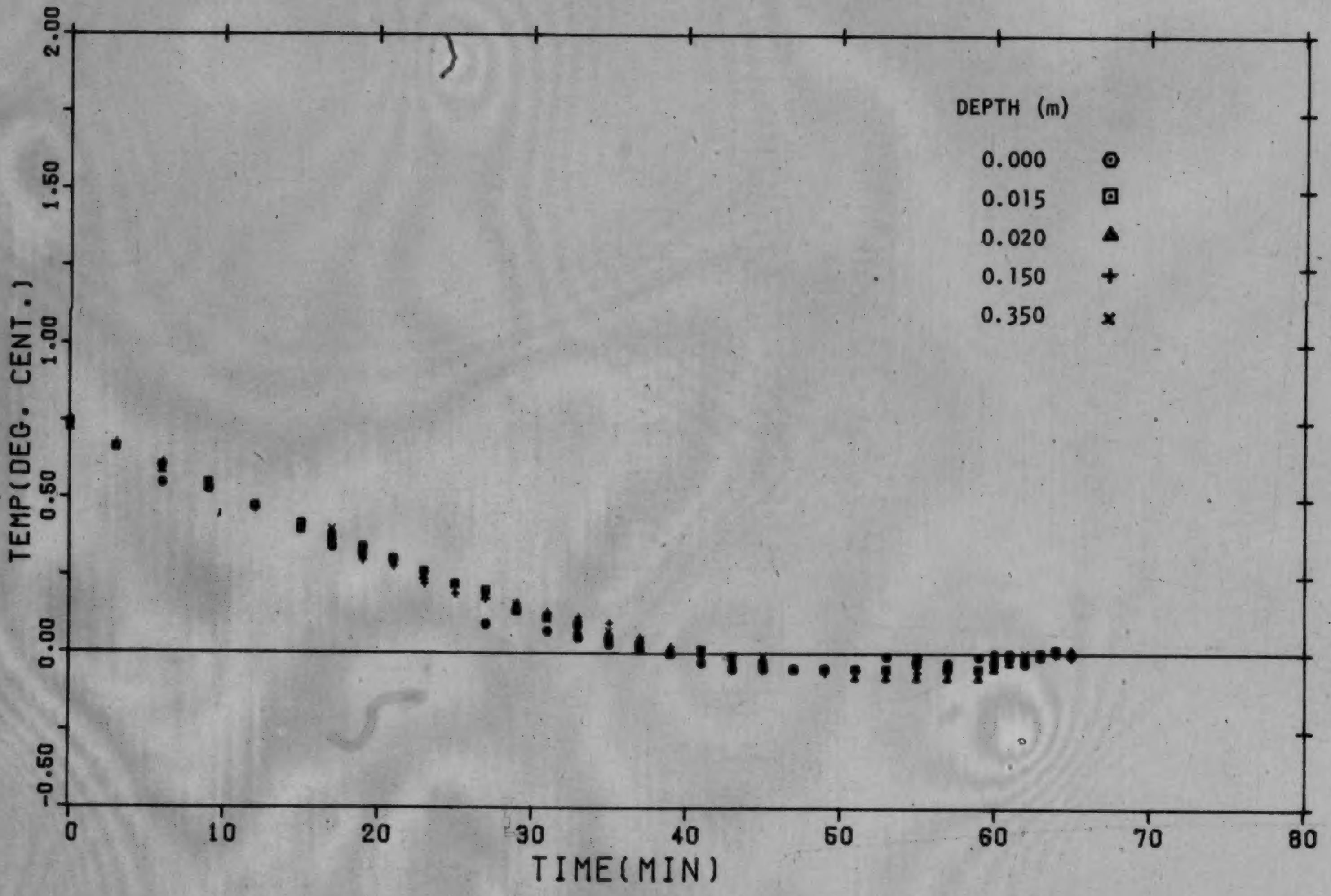

RUN #21-TEMP. VS. TIME FOR VARIOUS DEPTHS

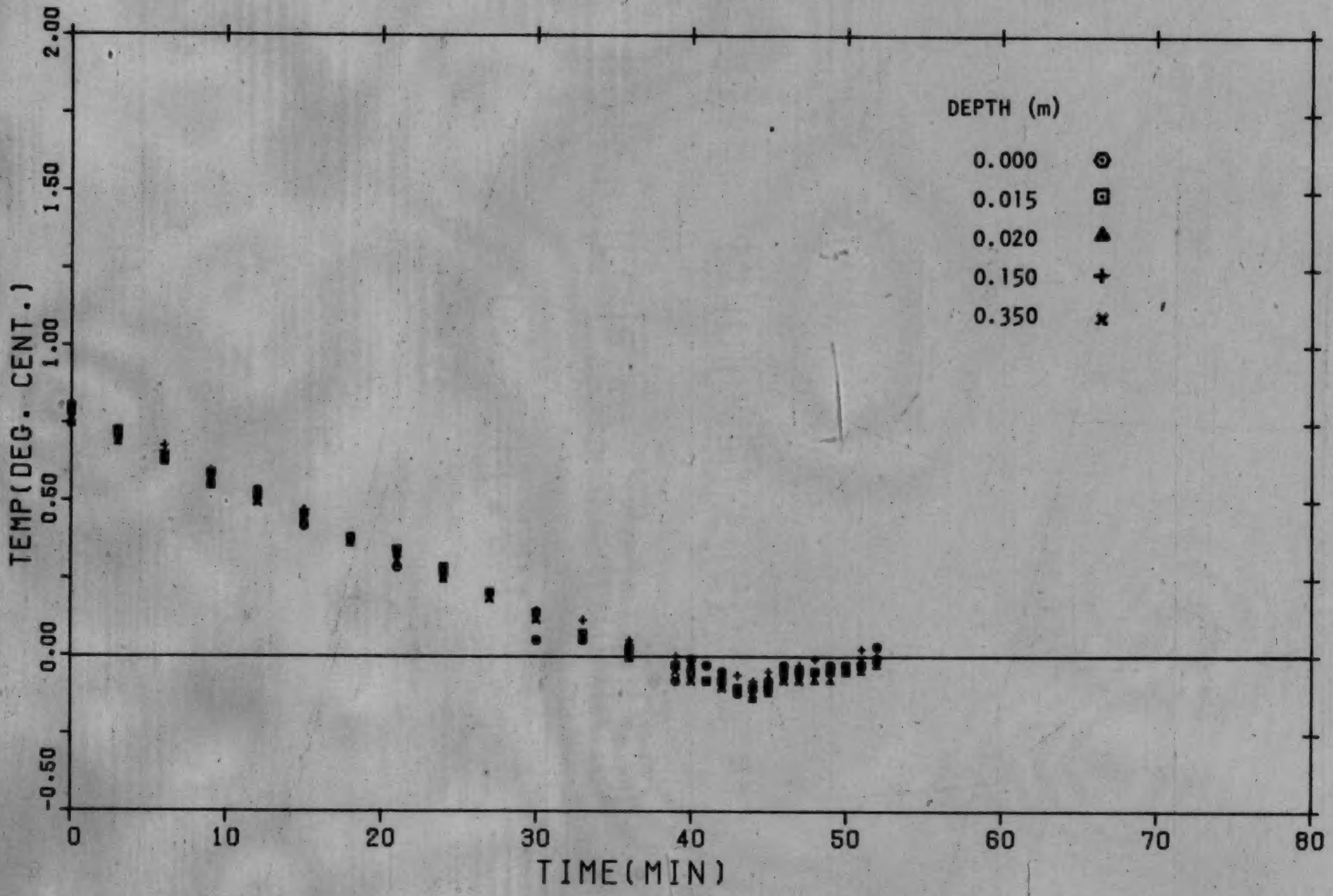

RUN #22-TEMP. VS. TIME FOR VARIOUS DEPTHS

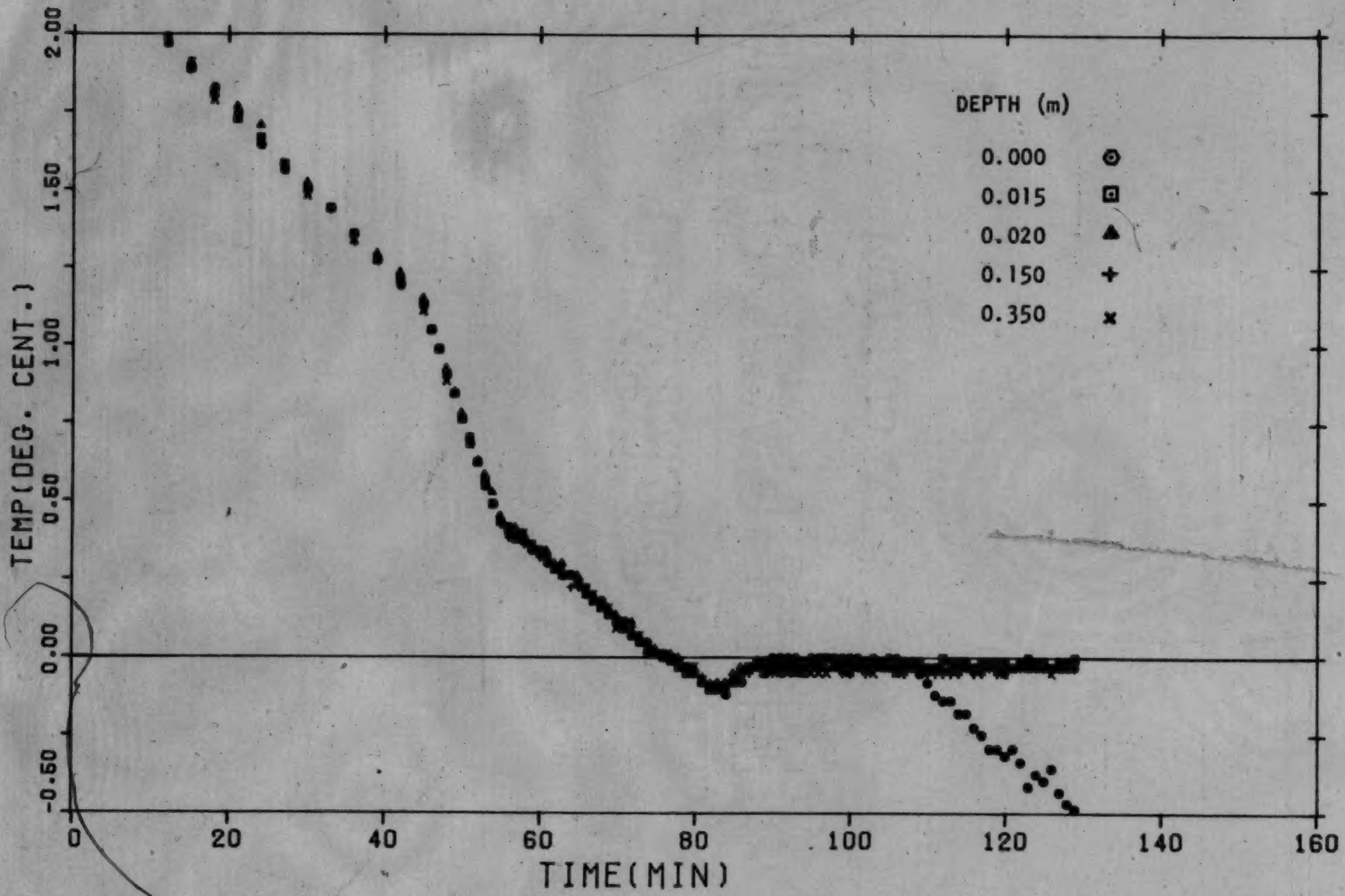

RUN #23-TEMP. VS. TIME FOR VARIOUS DEPTHS

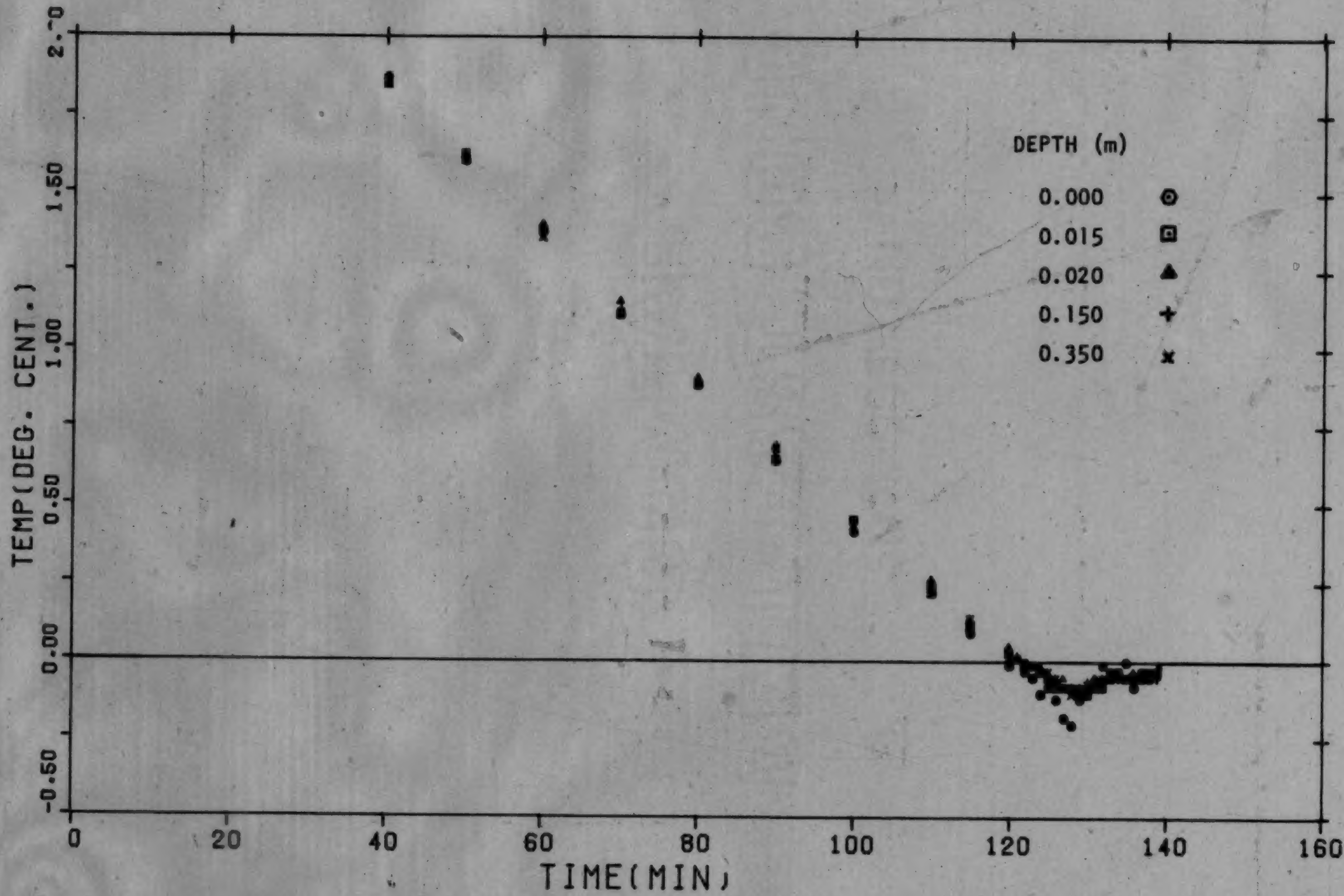

RUN #24-TEMP. VS. TIME FOR VARICUS DEPTHS

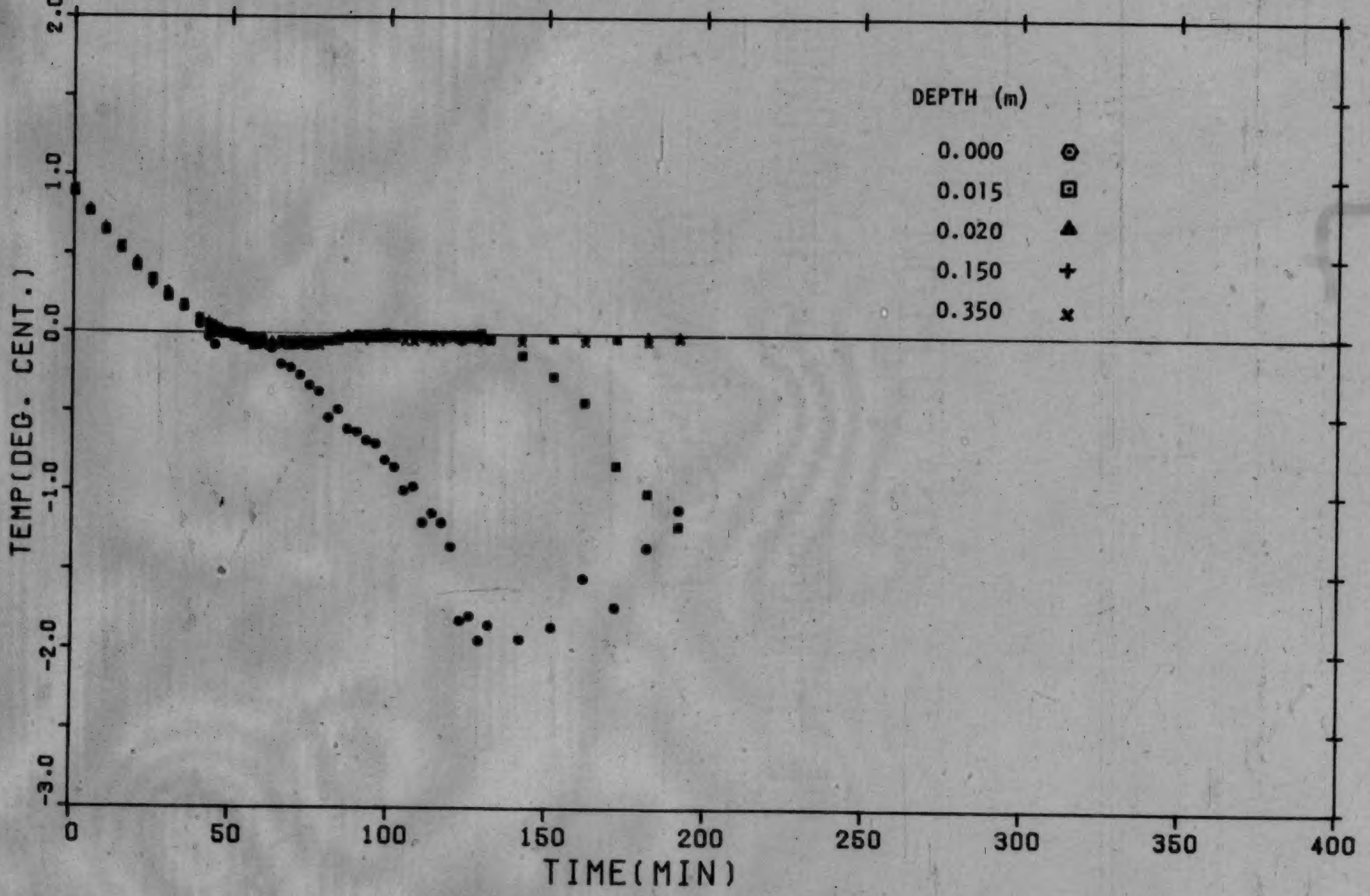

RUN #25-TEMP. VS. TIME FOR VARIOUS DEPTHS

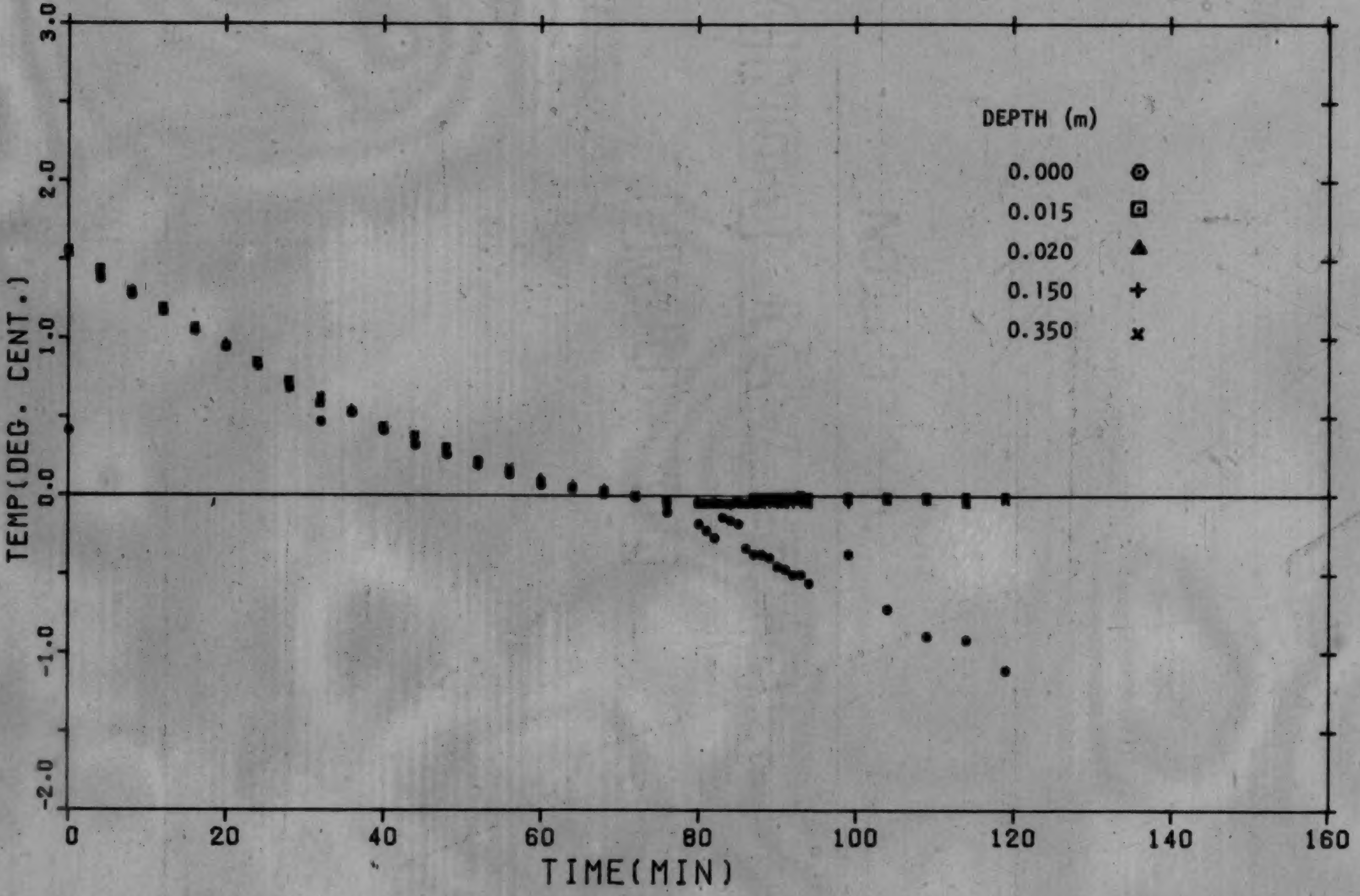

RUN #32-TEMP. VS. TIME FOR VARIOUS DEPTHS

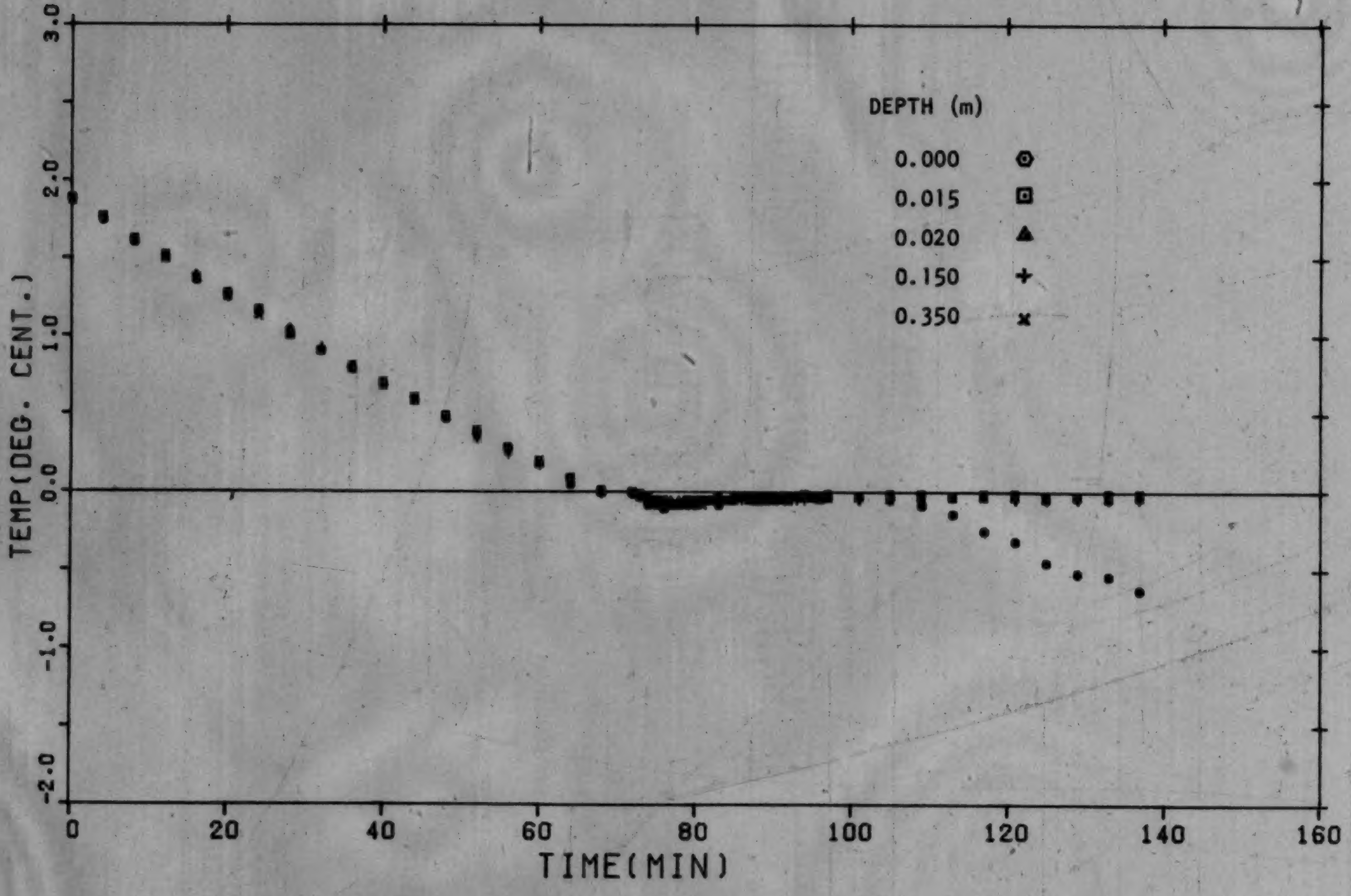

RUN #33-TEMP. VS. TIME FOR VARIOUS DEPTHS

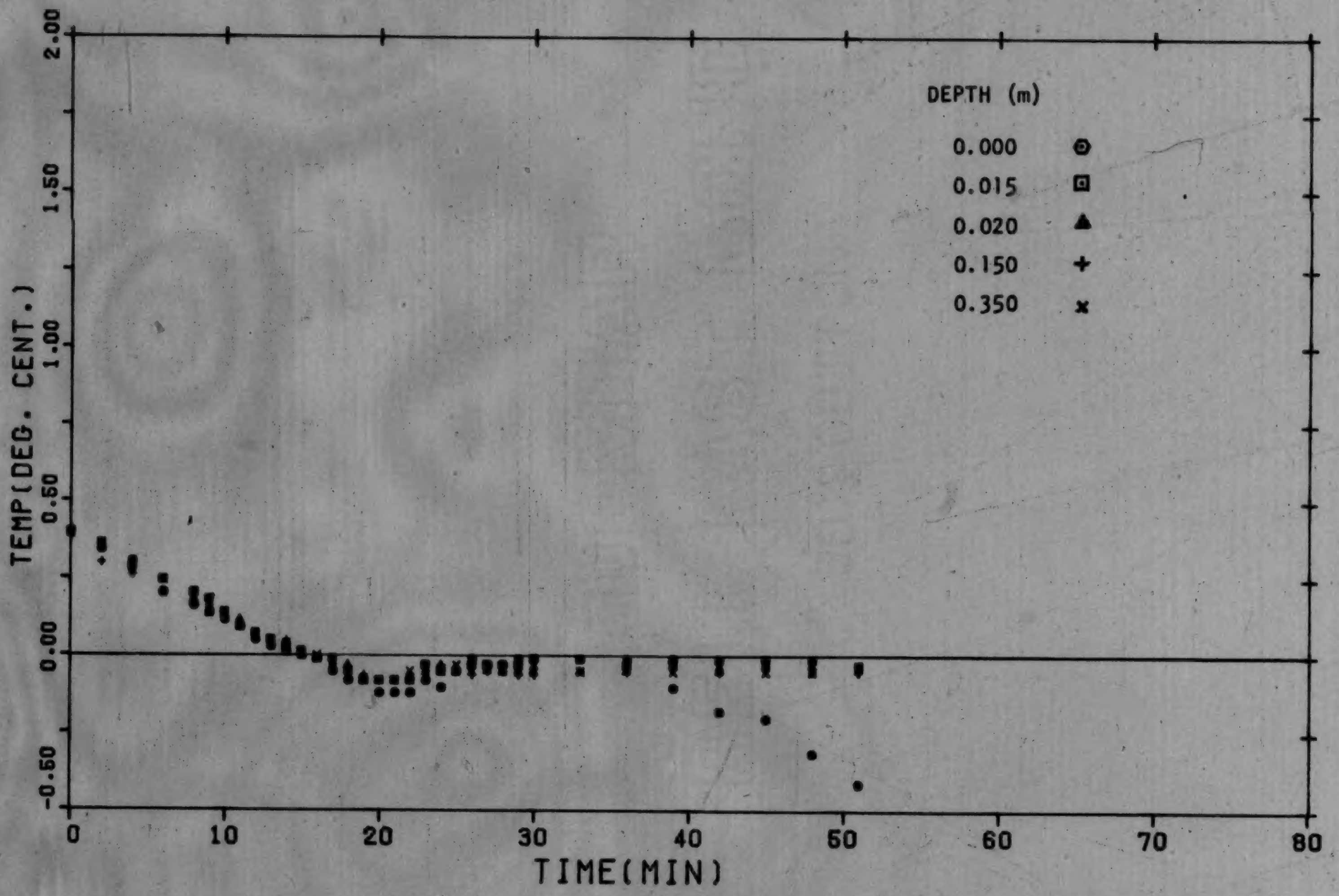

RUN #34-TEMP. VS. TIME FOR VARIOUS DEPTHS

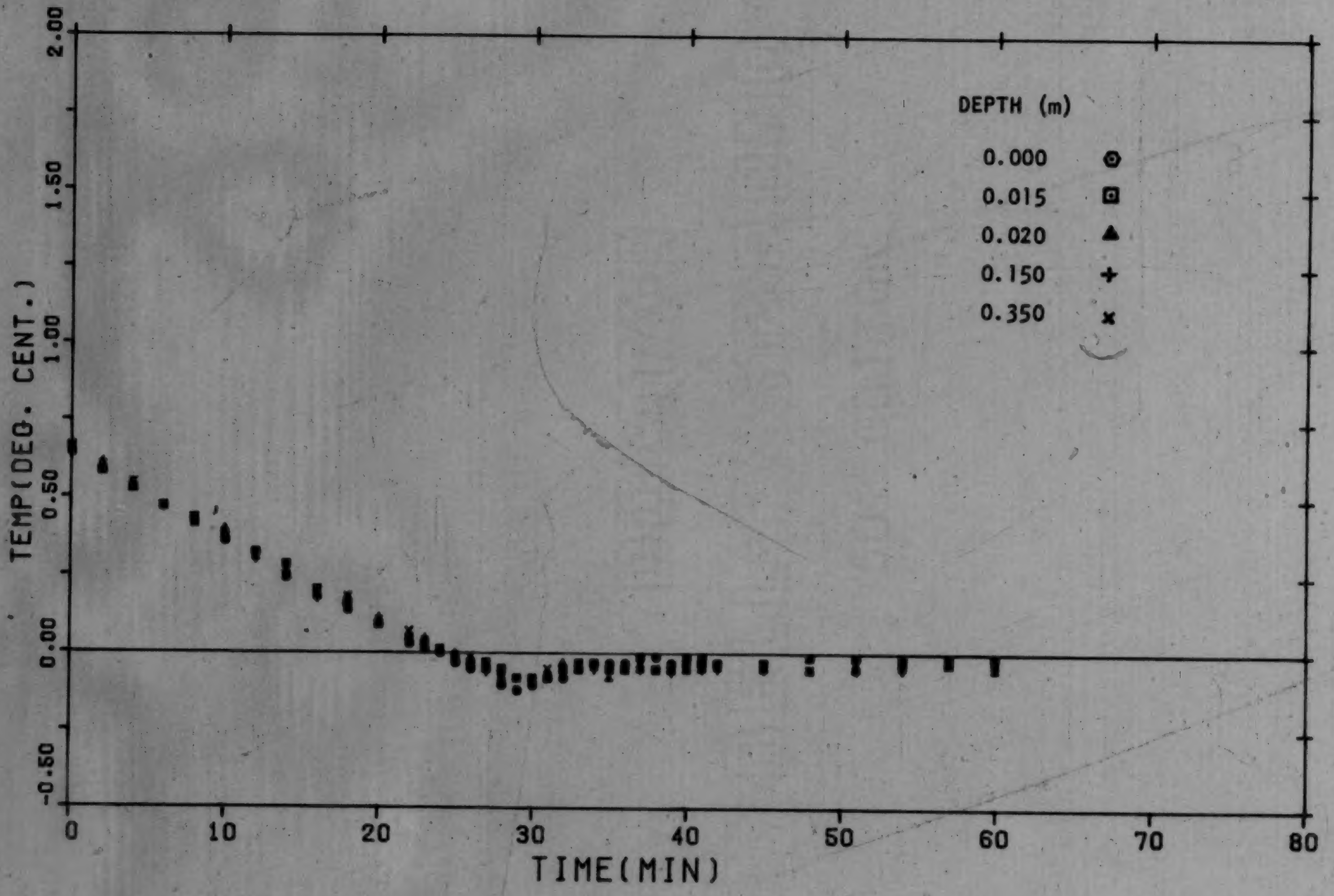

RUN #35-TEMP. VS. TIME FOR VARIOUS DEPTHS

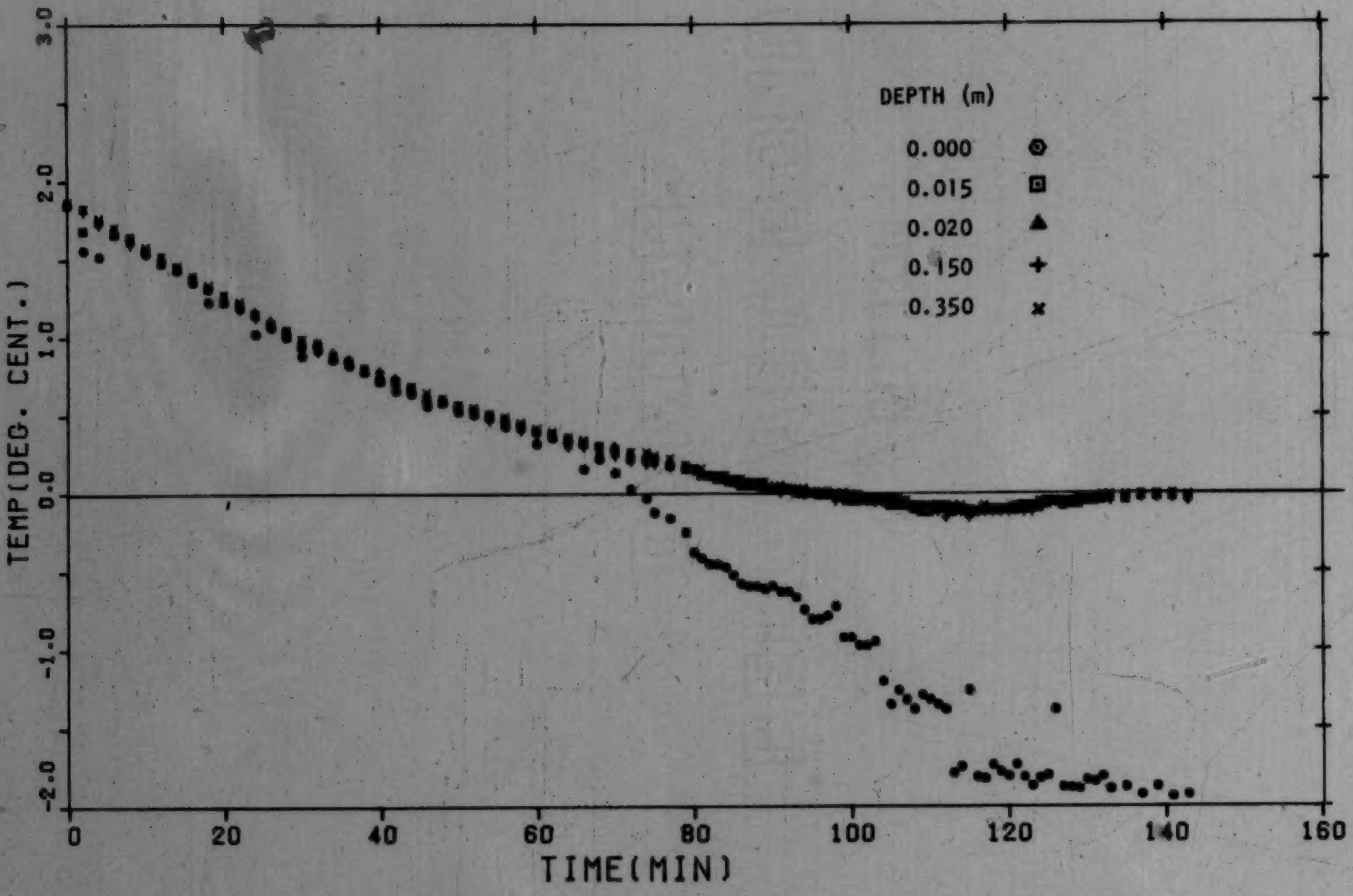

RUN #41-TEMP. VS. TIME FOR VARIOUS DEPTHS

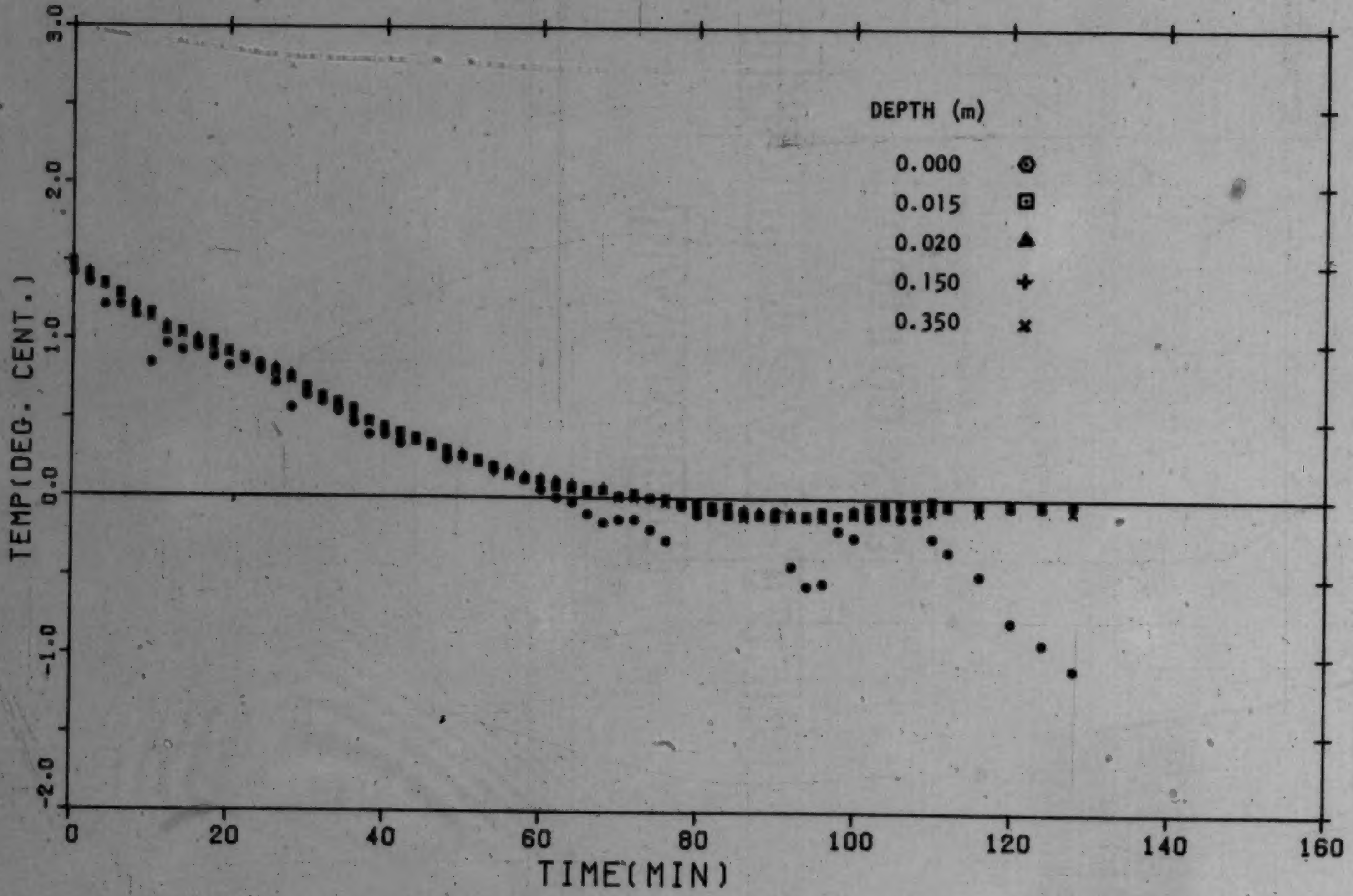

RUN #42-TEMP. VS. TIME FOR VARIOUS DEPTHS

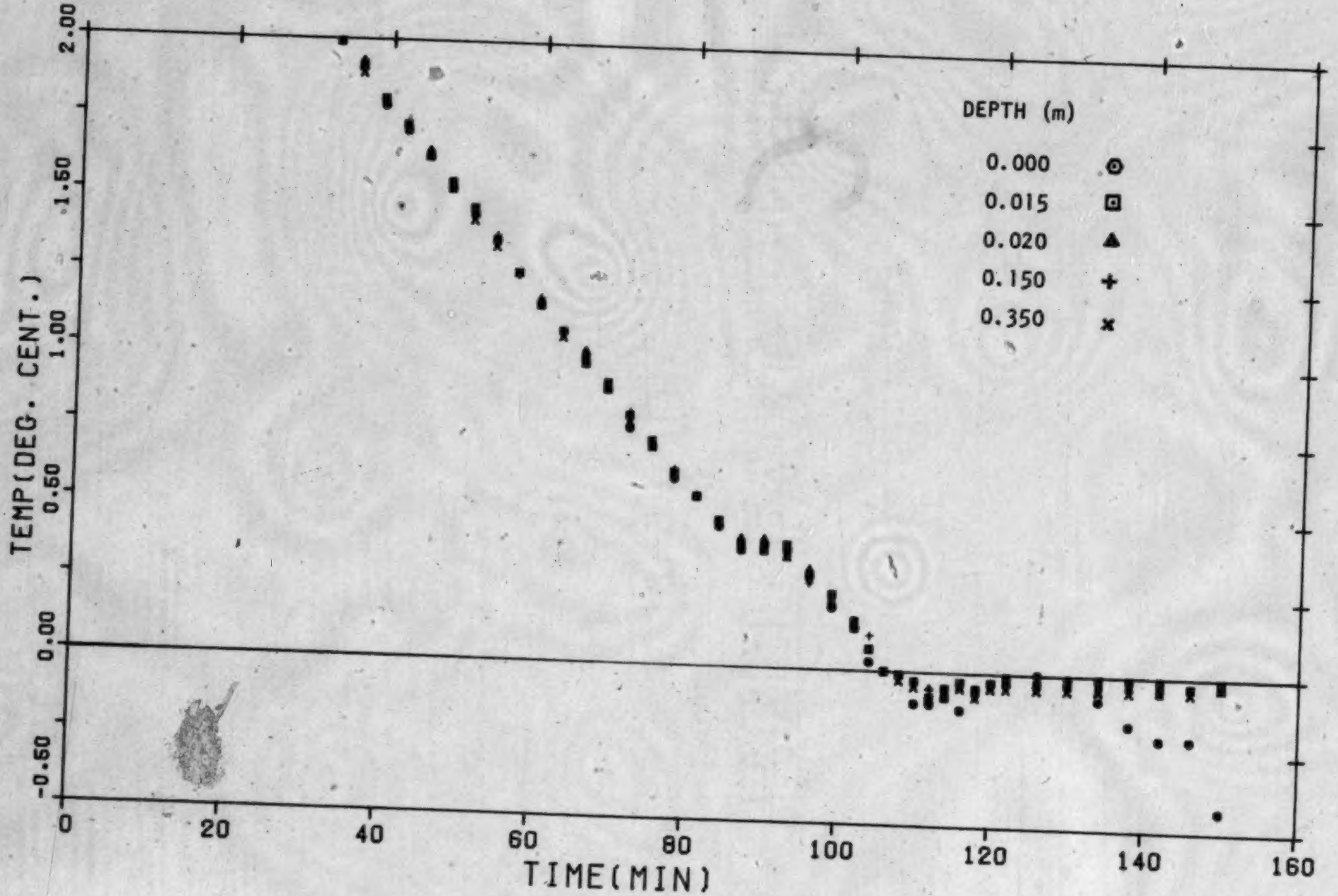

RUN #43-TEMP. VS. TIME FOR VARIOUS DEPTHS

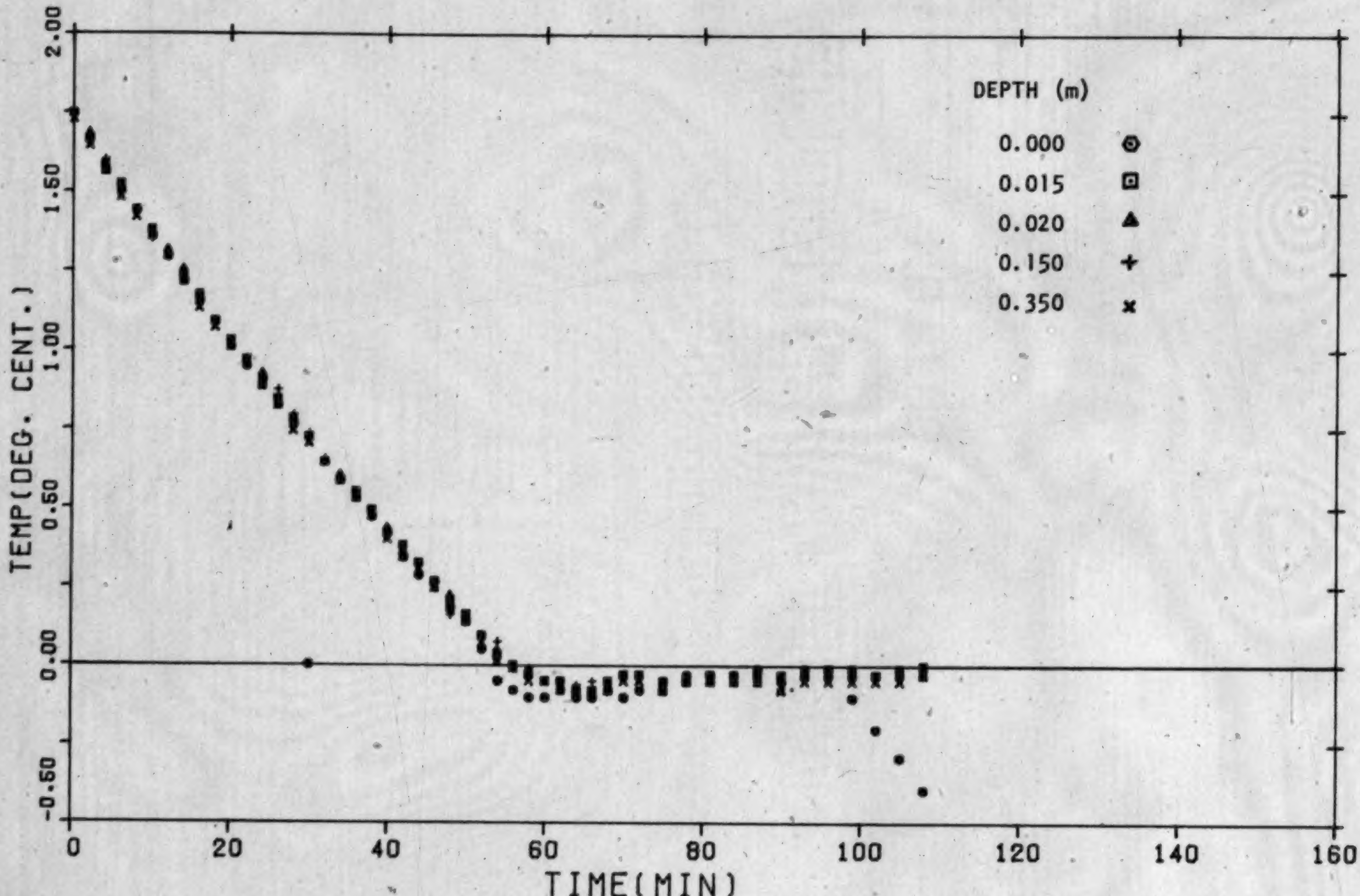

RUN #44-TEMP. VS. TIME FOR VARIOUS DEPTHS

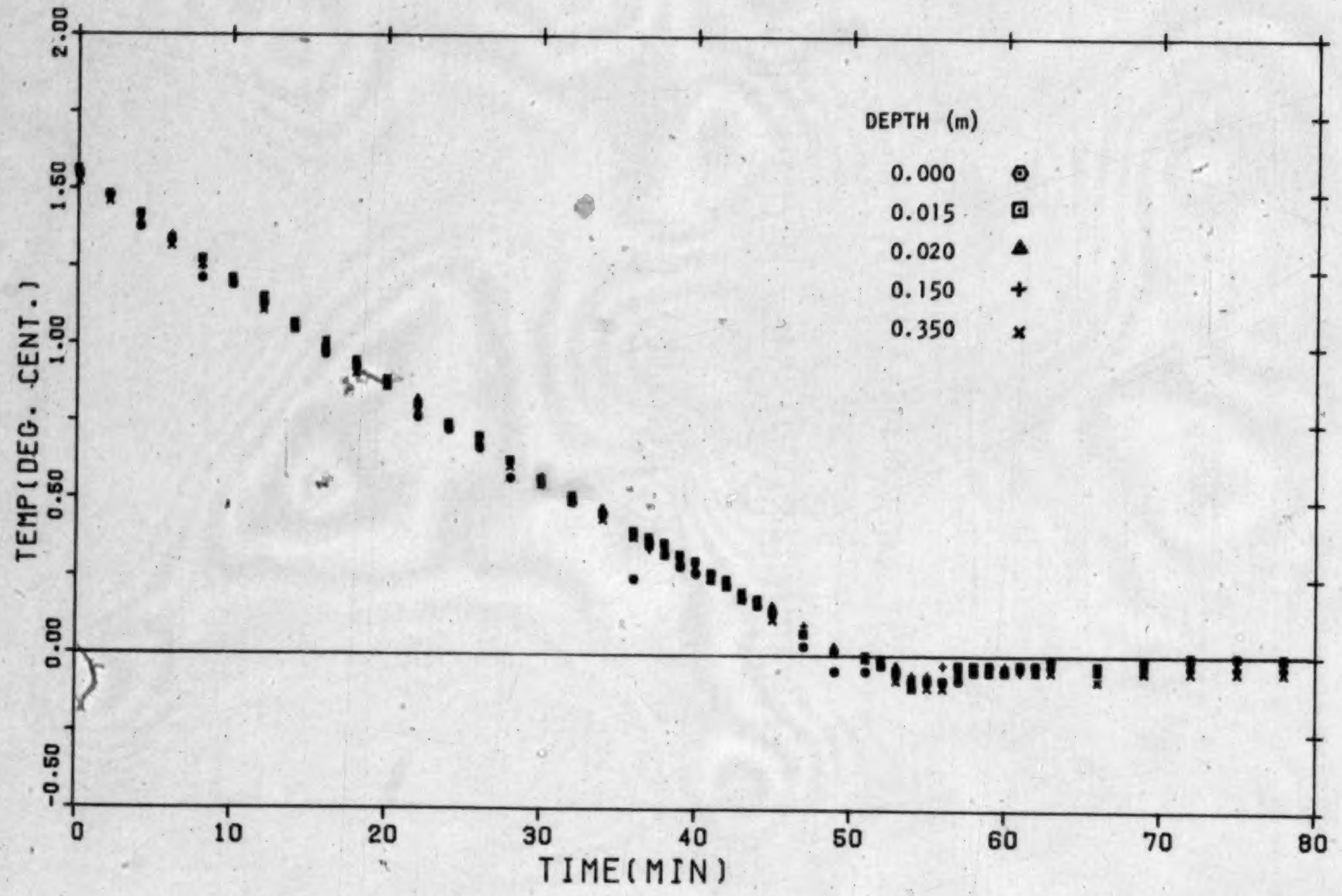

RUN #45-TEMP. VS. TIME FOR VARIOUS DEPTHS

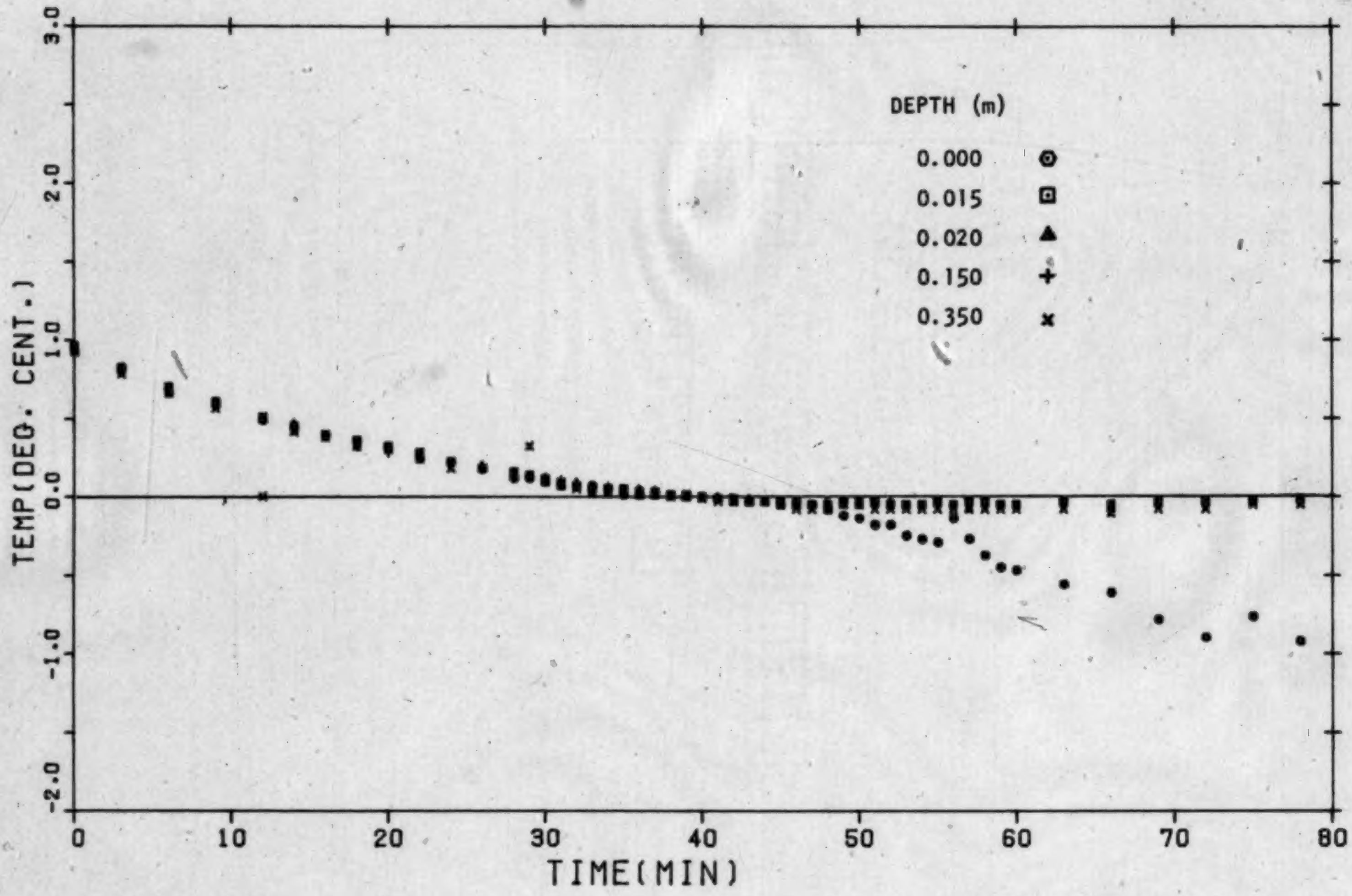

RUN #50-TEMP. VS. TIME FOR VARIOUS DEPTHS

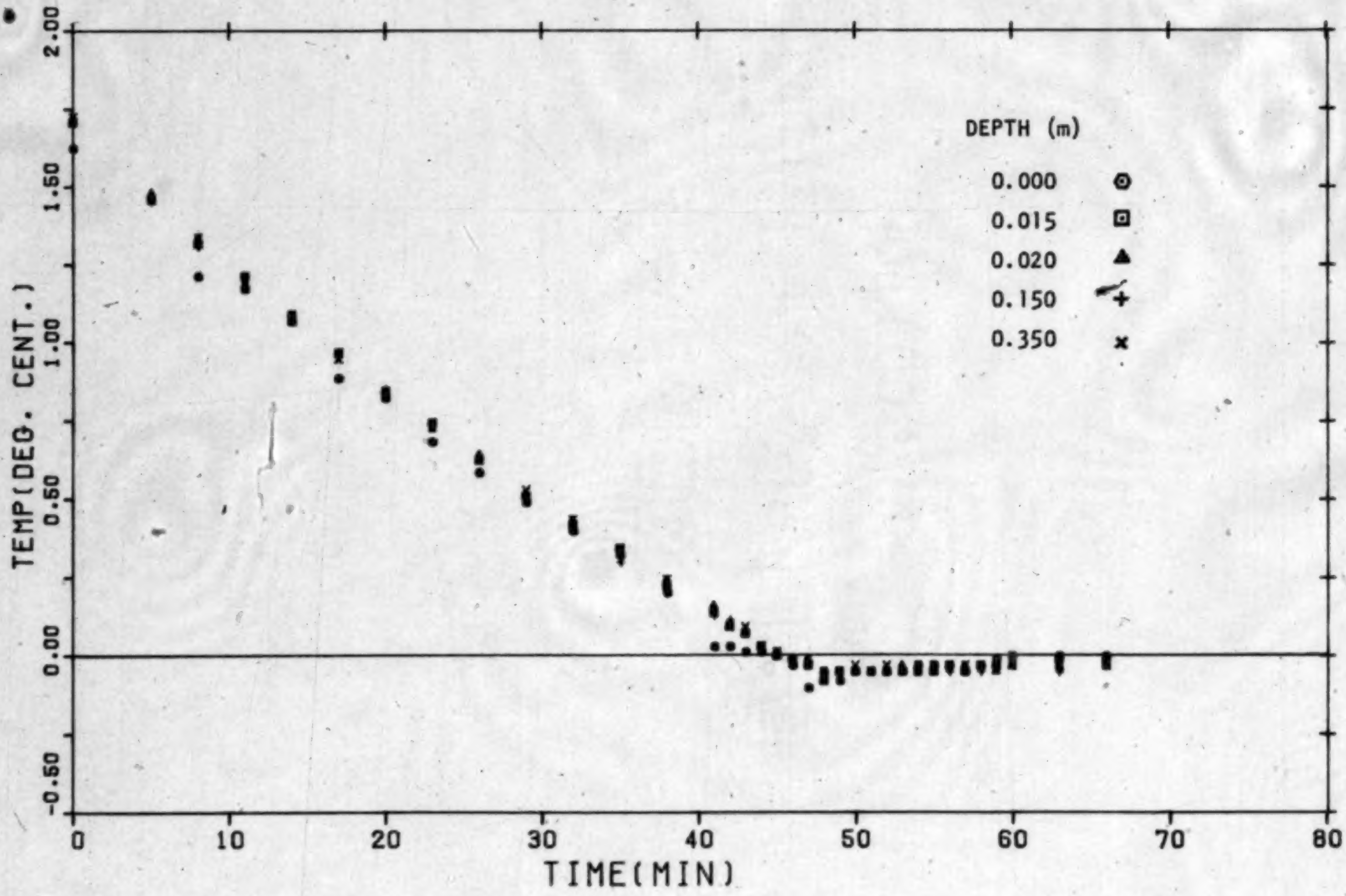

RUN #51-TEMP. VS. TIME FOR VARIOUS DEPTHS

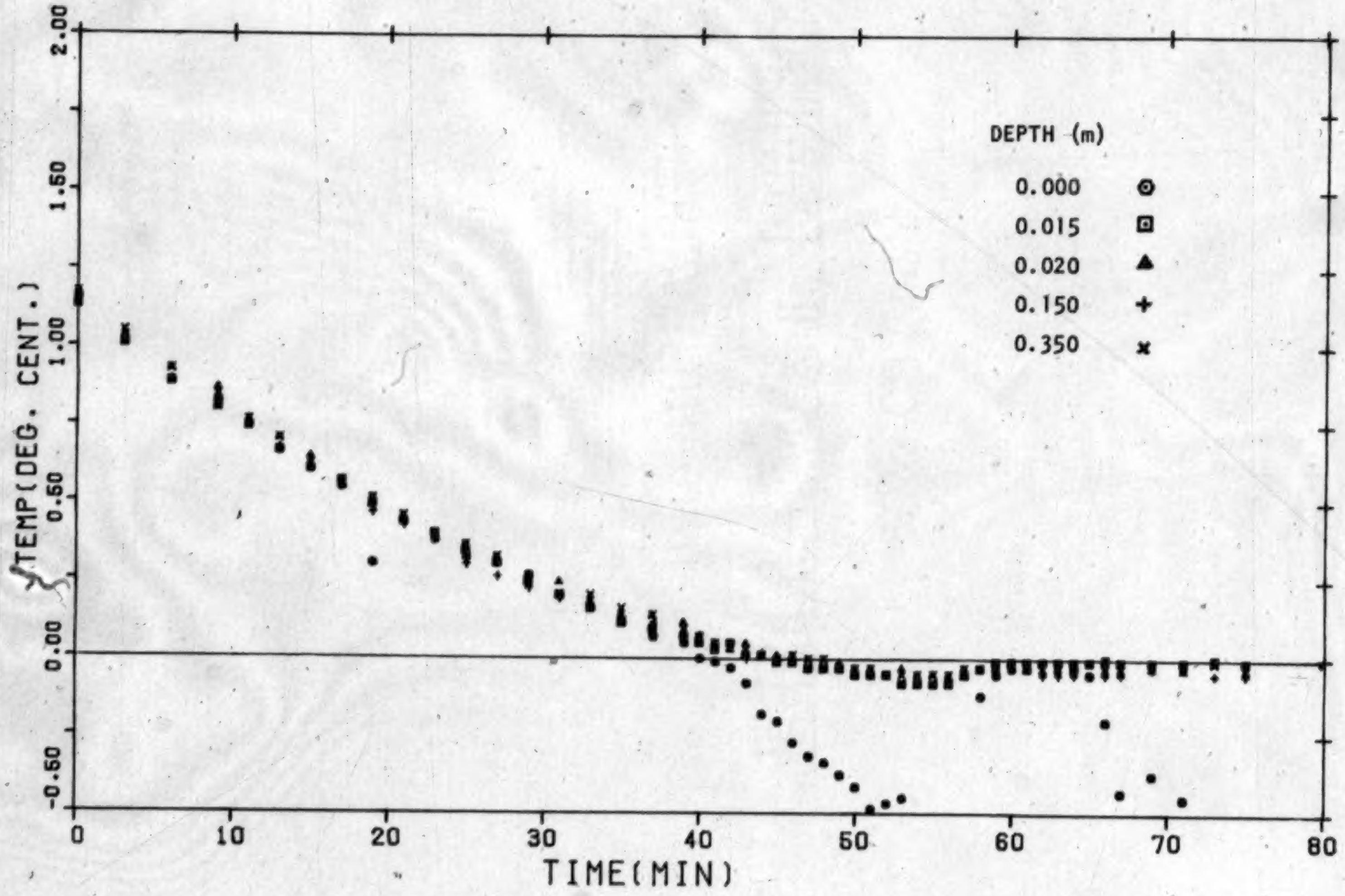

RUN #52-TEMP. VS. TIME FOR VARIOUS DEPTHS